

### **Journal Information**

*Maejo International Journal of Science and Technology* (ISSN 1905-7873 © 2011), the international journal for preliminary communications in Science and Technology is the first peerrefereed scientific journal of Maejo University ([www.mju.ac.th](http://www.mju.ac.th)). Intended as a medium for communication, discussion, and rapid dissemination of important issues in Science and Technology, articles are initially published online in an open access format, which thereby gives authors the chance to communicate with a wide range of readers in an international community.

### **Publication Information**

MIJST is published triannually. Articles are available online and can be accessed free of charge at <http://www.mijst.mju.ac.th>. Printed and bound copies of each volume are produced and distributed to authors and selected groups or individuals. This journal and the individual contributions contained in it are protected under the copyright by Maejo University.

### **Abstracting/Indexing Information**

MIJST is covered and cited by Science Citation Index Expanded, SCOPUS, Journal Citation Reports/Science Edition, Zoological Record, Chemical Abstracts Service (CAS), SciFinder Scholar, Directory of Open Access Journals (DOAJ) and Google Scholar.

### **Contact Information**

Editorial office: Maejo International Journal of Science and Technology (MIJST), 1st floor, Orchid Building, Maejo University, San Sai, Chiang Mai 50290, Thailand

Tel: +66-53-87-3880

E-mails: [duang@mju.ac.th](mailto:duang@mju.ac.th)



## MAEJO INTERNATIONAL JOURNAL OF SCIENCE AND TECHNOLOGY

### Editor

Duang Buddhasukh, Maejo University, Thailand.

### Associate Editors

Jatuphong Varith, Maejo University, Thailand.

Wasin Charerntantanakul, Maejo University, Thailand.

Morakot Sukchotiratana, Chiang Mai University, Thailand.

Nakorn Tippayawong, Chiang Mai University, Thailand.

### Editorial Assistants

James F. Maxwell, Chiang Mai University, Thailand.

Jirawan Banditpuritat, Maejo University, Thailand.

### Editorial Board

Prof. Dallas E. Alston	University of Puerto Rico, USA.
Dr. Pei-Yi Chu	Changhua Christian Hospital, Taiwan, R.O.C.
Asst. Prof. Ekachai Chukeatirote	Mae Fah Luang University, Thailand.
Prof. Richard L. Deming	California State University Fullerton, Fullerton CA
Prof. Cynthia C. Divina	Central Luzon State University, Philippines.
Prof. Mary Garson	The University of Queensland, Australia.
Prof. Kate Grudpan	Chiang Mai University, Thailand.
Assoc. Prof. Duangrat Inthorn	Mahidol University, Thailand.
Prof. Minoru Isobe	Nagoya University, Japan.
Prof. Kunimitsu Kaya	Tohoku University, Japan.
Assoc. Prof. Margaret E. Kerr	Worcester State College, Worcester, MA
Dr. Ignacy Kitowski	University of Maria-Curie Sklodowska, Poland.
Asst. Prof. Andrzej Komosa	University of Maria-Curie Sklodowska, Poland.
Asst. Prof. Pradeep Kumar	Jaypee University of Information Technology, India.
Asst. Prof. Ma. Elizabeth C. Leoveras	Central Luzon State University, Philippines.
Dr. Subhash C. Mandal	Jadavpur University, India.
Prof. Amarendra N. Misra	Fakir Mohan University, Orissa, India.
Dr. Robert Molloy	Chiang Mai University, Thailand.
Prof. Mohammad A. Mottaleb	Northwest Missouri State University, USA.
Prof. Stephen G. Pyne	University of Wollongong, Australia.
Prof. Renato G. Reyes	Central Luzon State University, Philippines.
Dr. Waya Sengpracha	Silpakorn University, Thailand.
Dr. Settha Siripin	Maejo University, Thailand.
Prof. Paisarn Sithigorngul	Srinakharinwirot University, Thailand.
Prof. Anupam Srivastav	College of Engineering and Technology, India.
Prof. Maitree Suttajit	Naresuan University (Payao Campus), Thailand.
Assoc. Prof. Chatchai Tayapiwatana	Chiang Mai University, Thailand.
Emeritus Prof. Bela Ternai	La Trobe University, Australia.
Asst. Prof. Narin Tongwittaya	Maejo University, Thailand.
Asst. Prof. Jatuphong Varith	Maejo University, Thailand.
Assoc. Prof. Niwoot Whangchai	Maejo University, Thailand.

### Consultants

Asst. Prof. Chamnian Yosraj, Ph.D., President of Maejo University

Assoc. Prof. Thep Phongparnich, Ed. D., Former President of Maejo University

Assoc. Prof. Chalermchai Panyadee, Ph.D., Vice-President in Research of Maejo University

# **MAEJO INTERNATIONAL JOURNAL OF SCIENCE AND TECHNOLOGY**

*The International Journal for the Rapid Publication of Preliminary  
Communications in Science and Technology*





## MAEJO INTERNATIONAL JOURNAL OF SCIENCE AND TECHNOLOGY

Volume 5, Issue 2 (May – August 2011)

### CONTENTS

	<b>Page</b>
Combining a differential global positioning system and double electric compass to improve multi-path error correction for a high-precision agricultural robotic vehicle <i>Choatpong Kanjanaphachaoat, Kuen-Chang Hsieh, Chung-Teh Cheng* and Hwang Mins-Shi</i> .....	169-180
Changes in essential oil content and composition of leaf and leaf powder of <i>Rosmarinus officinalis</i> cv. CIM-Hariyali during storage <i>Ram S. Verma*, Laiq ur Rahman, Sunita Mishra, Rajesh K. Verma, Amit Chauhan and Anand Singh</i> .....	181-190
A comparative study of sequencing batch reactor and movingbed sequencing batch reactor for piggery wastewater treatment <i>Kwannate Sombatsompop*, Anusak Songpim, Sillapa Reabroo and Prapatpong Inkong-ngam</i> .....	191-203
LDPC concatenated space-time block coded system in multipath fading environment: Analysis and evaluation <i>Surbhi Sharma* and Rajesh Khanna</i> .....	204-214
Agentless robust load sharing strategy for utilising heterogeneous resources over wide area network <i>Natthakrit Sanguandikul* and Natawut Nupairoj</i> .....	215-230
Utilisation of vegetable oils in the production of lovastatin by <i>Aspergillus terreus</i> ATCC 20542 in submerged cultivation <i>Pattana Sripalakit*, Janya Riunkesorn and Aurasorn Saraphanchotiwitthaya</i> .....	231-240
Effects of forest road clearings on understory diversity beneath <i>Alnus subcordata</i> L. stands in Iran <i>Seyed A. Hosseini *, Hamid Jalilvand, Mohammad R. Pourmajidian and Aidin Parsakhoo</i> .....	241-251
Dynamic changes in enzyme activities and phenolic content during in vitro rooting of tree peony ( <i>Paeonia suffruticosa</i> Andr.) plantlets <i>Zhenzhu Fu, Panpan Xu, Songlin He*, Jaime A. Teixeira da Silva and Michio Tanaka</i> .....	252-265
A one-mode-for-all predictor for text messaging <i>Vimala Balakrishnan*, Sim Foo Guan and Ram Gopal Raj</i> .....	266-278
The production and shelf life of high-iron, pre-cooked rice porridge with ferrous sulphate and other high-iron materials <i>Chowladda Teangpook* and Urai Paosangtong</i> .....	279-291

# **MAEJO INTERNATIONAL JOURNAL OF SCIENCE AND TECHNOLOGY**

*Volume 5, Issue 2 (May – August 2011)*

## **Author Index**

<b>Author</b>	<b>Page</b>	<b>Author</b>	<b>Page</b>
Balakrishnan V.	266	Raj R. G.	266
Chauhan A.	181	Reabroo S.	191
Cheng C.-T.	169	Riunkesorn J.	231
Fu Z.	252	Sanguandikul N.	215
Guan S. F.	266	Saraphanchotiwitthaya A.	231
He S.	252	Sharma S.	204
Hosseini S. A.	241	Singh A.	181
Hsieh K.-C.	169	Sombatsompop K.	191
Inkong-ngam P.	191	Songpim A.	191
Jalilvand H.	241	Sripalakit P.	231
Kanjanaphachaoat C.	169	Tanaka M.	252
Khanna R.	204	Teangpook C.	279
Mins-Shi H.	169	Teixeira da Silva J. A.	252
Mishra S.	181	Verma R. K.	181
Nupairoj N.	215	Verma R. S.	181
Paosangtong U.	279	Xu P.	252
Parsakhoo A.	241		
Pourmajidian M. R.	241		
Rahman L.	181		

## **Instructions for Authors**

A proper introductory e-mail page containing the title of the submitted article and certifying its originality should be sent to the editor (Duang Buddhasukh, e-mail : duang@mju.ac.th). The manuscript proper together with a list of suggested referees should be attached in separate files. The list should contain at least 3 referees (one or more non-native) with appropriate expertise. Each referee's academic/professional position, scientific expertise, affiliation and e-mail address must be given. The referees should not be affiliated to the same university/institution as any of the authors, nor should any two referees come from the same university/institution.

Failure to conform to the above instructions will result in non-consideration of the submission.

Please also ensure that English and style is properly edited before submission. Authors who would like to consult a professional service can visit [www.journalexperts.com](http://www.journalexperts.com), [www.proof-reading-service.com](http://www.proof-reading-service.com), [www.editage.com](http://www.editage.com), [www.enago.com](http://www.enago.com), [www.bioedit.co.uk](http://www.bioedit.co.uk) (bioscience and medical papers), [www.bioscienceeditingsolutions.com](http://www.bioscienceeditingsolutions.com), [www.scribendi.com](http://www.scribendi.com), or [www.letpub.com](http://www.letpub.com).

**Important : Manuscript with substandard English and style will not be considered.**

**Warning :** Plagiarism (including self-plagiarism) may be checked for at *the last* stage of processing and, if detected, will result in a rejection and blacklisting.

## **Manuscript Preparation**

Manuscripts should be prepared in English using a word processor. MS Word for Macintosh or Windows, and .doc or .rtf files are preferred. Manuscripts may be prepared with other software provided that the full document (with figures, schemes and tables inserted into the text) is exported to a MS Word format for submission. Times or Times New Roman font is preferred. The font size should be 12 pt and the line spacing 'at least 17 pt'. A4 paper size is used and margins must be 1.5 cm on top, 2.0 cm at the bottom and 2.0 cm on both left and right sides of the paper. Although our final output is in .pdf format, authors are asked NOT to send manuscripts in this format as editing them is much more complicated. Under the above settings, a manuscript submitted should not be longer than **15 pages** for a full paper or **20 pages** for a review paper.

A template file may be downloaded from the *Maejo Int. J. Sci. Technol.* homepage. ([DOWNLOAD HERE](#))

Authors' full mailing addresses, homepage addresses, phone and fax numbers, and e-mail addresses homepages can be included in the title page and these will be published in the manuscripts and the Table of Contents. The corresponding author should be clearly identified. It is the corresponding author's responsibility to ensure that all co-authors are aware of and approve of the contents of a submitted manuscript.

A brief (200 word maximum) Abstract should be provided. The use in the Abstract of numbers to identify compounds should be avoided unless these compounds are also identified by names.

A list of three to five keywords must be given and placed after the Abstract. Keywords may be single words or very short phrases.

Although variations in accord with contents of a manuscript are permissible, in general all papers should have the following sections: Introduction, Materials and Methods, Results and Discussion, Conclusions, Acknowledgments (if applicable) and References.

Authors are encouraged to prepare Figures and Schemes in colour. Full colour graphics will be published free of charge.

Tables and Figures should be inserted into the main text, and numbers and titles supplied for all Tables and Figures. All table columns should have an explanatory heading. To facilitate layout of large tables, smaller fonts may be used, but in no case should these be less than 10 pt in size. Authors should use the Table option of MS Word to create tables, rather than tabs, as tab-delimited columns are often difficult to format in .pdf for final output.

Figures, tables and schemes should also be placed in numerical order in the appropriate place within the main text. Numbers, titles and legends should be provided for all tables, schemes and figures. Chemical structures and reaction schemes should be drawn using an appropriate software package designed for this purpose. As a guideline, these should be drawn to a scale such that all the details and text are clearly legible when placed in the manuscript (i.e. text should be no smaller than 8-9 pt).

For bibliographic citations, the reference numbers should be placed in square brackets, i.e. [ ], and placed before the punctuation, for example [4] or [1-3], and all the references should be listed separately and as the last section at the end of the manuscript

## **Format for References**

### **Journal :**

1. D. Buddhasukh, J. R. Cannon, B. W. Metcalf and A. J. Power, "Synthesis of 5-n-alkylresorcinol dimethyl ethers and related compounds via substituted thiophens", *Aust. J. Chem.*, **1971**, *24*, 2655-2664.

### **Text :**

2. A. I. Vogel, "A Textbook of Practical Organic Chemistry", 3rd Edn., Longmans, London, **1956**, pp. 130-132.

### **Chapter in an edited text :**

3. W. Leistritz, "Methods of bacterial reduction in spices ", in "Spices: Flavor Chemistry and Antioxidant Properties" (Ed. S. J. Risch and C-T. Ito), American Chemical Society, Washington, DC, **1997**, Ch. 2.

### **Thesis / Dissertation :**

4. W. phutdhawong, "Isolation of glycosides by electrolytic decolourisation and synthesis of pentinomycin", *PhD. Thesis*, **2002**, Chiang Mai University, Thailand.

### **Patent :**

5. K. Miwa, S. Maeda and Y. Murata, "Purification of stevioside by electrolysis", *Jpn. Kokai Tokkyo Koho* **79 89,066 (1979)**.

### **Proceedings :**

6. P. M. Sears, J. Peele, M. Lassauzet and P. Blackburn, "Use of antimicrobial proteins in the treatment of bovine mastitis", Proceedings of the 3rd International Mastitis Seminars, **1995**, Tel-Aviv, Israel, pp. 17-18.

***Maejo International  
Journal of Science and Technology***

ISSN 1905-7873  
Available online at [www.mijst.mju.ac.th](http://www.mijst.mju.ac.th)

*Full Paper*

**Combining a differential global positioning system and double electric compass to improve multi-path error correction for a high-precision agricultural robotic vehicle**

**Choatpong Kanjanaphachao<sup>1</sup>, Kuen-Chang Hsieh<sup>2</sup>, Chung-Teh Cheng<sup>1,\*</sup> and Hwang Mins-Shi<sup>2</sup>**

<sup>1</sup> Department of Bio-Industrial Mechatronics Engineering, The College of Agriculture and Natural Resources, National Chung Hsing University, 250 KuoKuang Road, Taichung, Taiwan 402, the R.O.C.

<sup>2</sup> Charden Electronic Co., Ltd., 103 Guozhong Road, Taichung, Taiwan 402, the R.O.C.

\* Corresponding author, e-mail: ctsheng@dragon.nchu.edu.tw

*Received: 11 November 2010/Accepted: 20 May 2011/Published: 23 May 2011*

---

**Abstract:** This work has addressed the improving of the multi-path error in positioning systems by coupling a differential global positioning system (DGPS) and double electric compass (DEC) in the navigation system of an orchard robotic vehicle. A novel corrective algorithm model was applied to predicting the positioning coordinates during vehicle movement. The model manipulates a combination of data from both the DEC and the DGPS when the DGPS receiver is in problematic conditions in which the horizontal dilution of precision (HDOP) is higher than three and the number of satellites is fewer than six. The constructed corrective algorithm model, the DEC and the DGPS together form a combined DGPS-DEC system that is inexpensive and of high-precision fitting for a vehicle-guiding instrument. In a field test in an outdoor environment with sections of tree shade in the guiding path, the combined DGPS-DEC positioning system effectively improved the reliability of positioning by correcting the DGPS multi-path error precisely to within 20 cm. By applying a mini-sprayer, further agricultural applications were feasible. In summary, the combined DGPS-DEC positioning system can obtain the correct position of a vehicle in real time for agricultural applications.

**Keywords:** positioning systems, differential global positioning system (DGPS), double electric compass (DEC), multi-path error, agricultural robotic vehicle

---

## INTRODUCTION

Application of the global positioning system (GPS) to detect and track an object on the earth has been widely developed and applied in several fields such as transportation, surveying, agriculture, natural resources and the environment. In agricultural tasks, GPS is very useful for several applications, especially precision farming in which an autonomous vehicle is navigated and guided [1-7]. The application of GPS in agriculture can improve production because an autonomous system is applied instead of human labour. However, the current application of GPS in an orchard farm is limited by the shading effects of natural obstructions such as trees, which can lead to loss of satellite signals from the sky. Current studies on positioning systems for orchard fields are rare and despite the many applications of GPS for outdoor localisation within an accuracy of 5-10 m during travel, this level of accuracy is not adequate for navigation in an orchard.

Recently, differential GPS (DGPS) has made localisation possible in an outdoor environment (open field) within centimetres. However, current papers addressing movement measurements by DGPS have demonstrated the loss of signal due to shading effects from tree canopies [2, 8-10]. The range in error measurement by DGPS tends to be larger if the location of the receiver is near a building or under trees [10-11]. In fact, DGPS signals are biased and corrupted when the signals from satellites in the field of view are not adequate, which causes multi-path error. If fewer than six satellites are available because the rest are obscured by buildings or trees, the error is greater than 30 cm, which is the limitation of DGPS [9]. In other words, the number of fewer than six satellites leads to greater bias, which causes data to fluctuate from the trend line.

In our preliminary experiment, a Trimble DSM 232-DGPS device, a DSM 232 receiver and an antenna-GPS/Beacon DSM132 were used to measure the position of a mini-sprayer vehicle passing through tree bushes on the roadside at low speed (0.24 km/hr) (Figure 1a). The DGPS reported irregular measured positions over its route with errors greater than one metre when six satellites or fewer were in the field of view. With fewer than five available satellites, the positioning data became corrupted (Figure 1b), which is a major problem for positioning systems in autonomous agricultural vehicles. To overcome this problem, this research develops a double electric compass (DEC) with a low-cost sensor to estimate the vehicle's heading angle and the position measured by DGPS. The output from the developed DEC is used to estimate the vehicle's position when DGPS cannot measure it. Measurement errors caused by sensitivity to external interferences from a magnetic field are studied using an external interference field, a calibration algorithm and a predictive algorithm, the key concept for the resolution as proposed by Lee et.al. [12] and Li et.al.[13] being the presumption that the interference to the DEC occurs in the same direction This development reduces the error often found in DGPS measurement as the trajectory is continuously estimated for a vehicle that moves along a path under tree shade.



**Figure 1.** (a) DGPS observation data for a moving route test with tree bushes; (b) lack of data (outage) and corrupted positioning data from an inadequate number of satellites in view

## MATERIALS AND METHODS

### Differential GPS (DGPS)

DGPS was developed by combining a Trimble DSM 232-DGPS device, a DSM 232 receiver and an antenna-GPS/Beacon DSM132 (Trimble companies, USA) to act as the positioning sensors. The DGPS vehicle position was determined in real time with high accuracy. The DPGS error was less than 25 cm at the best-performing condition, as corrected by the satellite-based augmentation systems (SBAS), when more than six available satellites and a horizontal dilution of precision (HDOP) of less than three occurred. The data from the positioning sensor (DGPS) were obtained from the satellites as NMEA-0183 messages (National Marine Electronic Association), which received real-time corrections of positional data from the Tianda Shan station or Zhenhai Jiao station in Fujian, China. The data consisted of the latitude, longitude and ground speed with respect to a WGS-84 geographic coordinate system and were presented in GGA messages (GPS fix data), and velocity true ground (VTG) messages were presented as NMEA-0183. The DGPS functioned as the primary error eliminator for errors caused by shade from bushes. The signal error was further reduced by the custom-designed DSM 132 receiver. However, the multi-path error remained due to reflection from the environmental obstructions, which could be corrected using the proposed algorithm to determine the position.

### Heading System

The use of DEC sensors developed by Compass Point V2Xe (Parallax, Inc., Taiwan) to construct a compass system to determine the direction of the heading angle of a vehicle was performed by referring to the horizontal x-axis as the direction of the magnetic northern pole and the horizontal y-axis as the east. The DEC signals experienced interference from both the static magnetic field generated by operating the instrument and the environmental magnetic field as well as time interferences caused by sensor offset, scale mismatch and misalignment. These errors were corrected by centring the coordinate origin using one-turn rotation (OTR) scheme [14]. The scheme is a

traditional method used to compensate for magnetic interference which originates from changes in the radius and shifts in the centre of the magnetism circle, depending on the ambient environment of the sensor [12-13, 15-16]. The heading system also experienced time-varying errors caused by dynamic external interference including terrain road slope and tilt as well as movement during driving. Among the various external interferences, high-frequency interferences could be eliminated by a predictive calibration algorithm proposed by Lee et al. and Li et al [12-13]. Figure 2 shows a module containing the designed DEC. Two electric compasses were installed parallel to each other 19 cm apart. Output of the double electric compass was transmitted to a receiver board at a rate of 19200 bps using a frequency of 10 Hz. The external interference field and calibration algorithm were further processed using Microsoft Visual Basic 2008®.

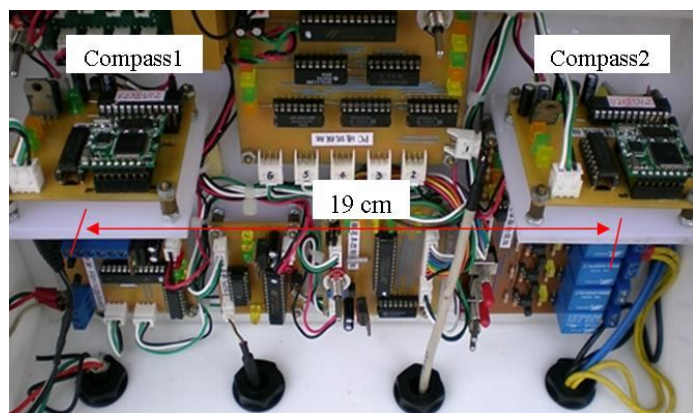


**Figure 2.** Double electric compass

### Vehicle Platform and Location of Experiment

The tested vehicle was a mini-four-wheel sprayer designed for an outdoor orchard and shown in Figure 3. The vehicle was controlled by a hydraulic system (a) through joysticks (b). The heading sensor was mounted in a box in front of the sprayer (c) and the DGPS receiver was mounted above a box (d). An antenna was placed on the vehicle 250 cm above ground level and offset from the centre of the sprayer on the x-axis at 30 cm and y-axis at 60 cm (e). The main electronic-circuit receiver board and the controller board were also mounted in the box in front of the sprayer. All output data from the DGPS and heading sensor were sampled and transmitted at 10 Hz to the receiver board and sent to a laptop computer (f) at a rate of 19200 bps via an RS232 port.

The experiment was performed on our campus, which has buildings (5-25 m high) and tall trees (2-7 m) that simulate multi-path problems. The tests consisted of straight-line, U-turn, right-turn and left-turn movements and those on sloping and tilting roads.

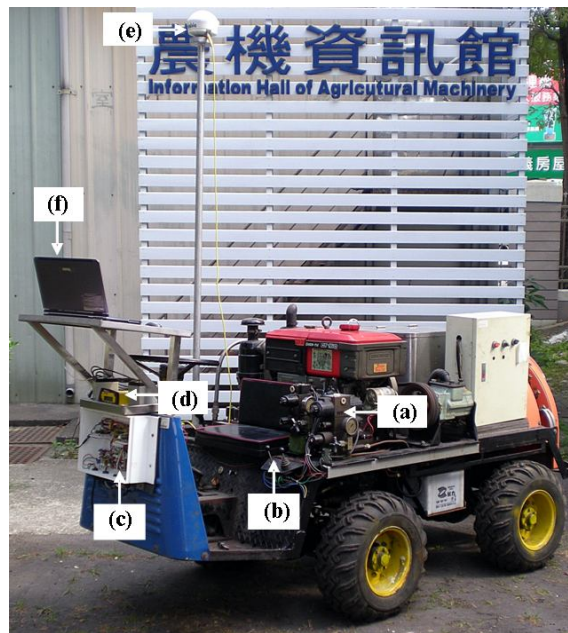


**Figure 3.** Mini-four-wheel sprayer: (a) vehicle hydraulic control system; (b) joysticks; (c) heading sensor and receiver board; (d) DGPS receiver; (e) DGPS antenna; and (f) laptop computer

### Positioning System

Figure 4 illustrates the integrated positioning system algorithm using the coupled DGPS-DEC to calculate real-time vehicle positions. The DGPS-DEC receiver obtains positional data (latitude, longitude, speed, number of satellites, HDOP) and magnetic field values and sends them to a computer. The positioning software converts the positional coordinates in latitude and longitude into the universal transverse Mercator (UTM) coordinate system as proposed by Snyder [17]. Our system automatically uses the predictive algorithm to estimate the vehicle position, even under inappropriate conditions as the DGPS is working, or multi-path error detected by the DGPS. Thus, it can estimate the current position of a vehicle in real time.

### Position Predictive Algorithm

A predictive algorithm is a dynamic model used to solve problems in multi-path error situations when the DGPS receiver is working in problematic conditions, as for instance, when the number of signals from satellites is less than six or the value of HDOP is greater than three. The principle of the predictive algorithm is to use both the heading angle values obtained from a DEC and the latest vehicle velocity values from the DGPS receiver to estimate the new position. The estimated data replace the measurement of the positional error in real time. Figure 5 represents a predictive platform flow diagram. The input is  $x_{GPS}$  and  $y_{GPS}$  for the current x and y coordinates on the operation field, and  $\theta_{compass}$  for the heading angle obtained from DEC at time  $t$ . Two algorithm conditions are applied: (1) the number of the satellites is required to be greater than six; and (2) HDOP is required to be less than three. If both conditions are satisfied, the input values will be

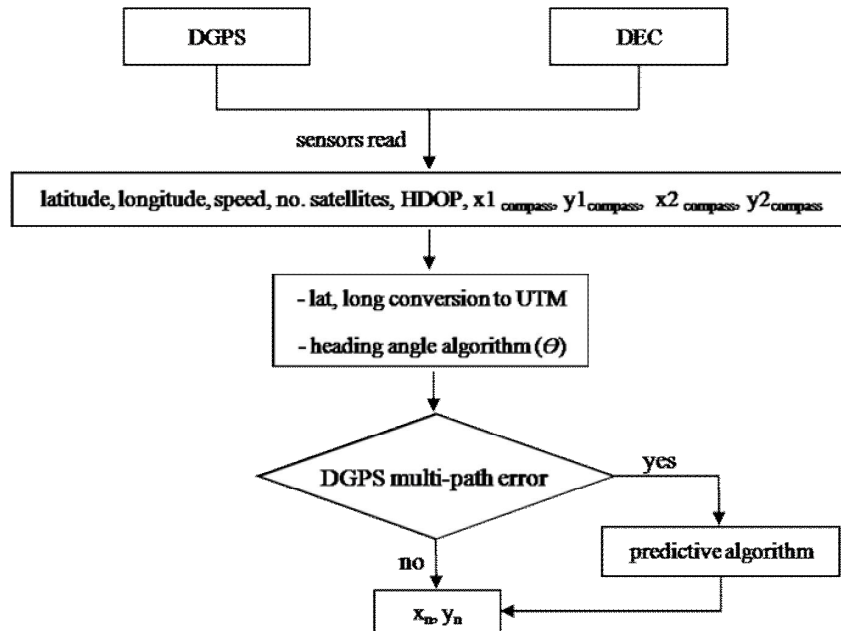


**Figure 4.** Overall structure of the positioning system

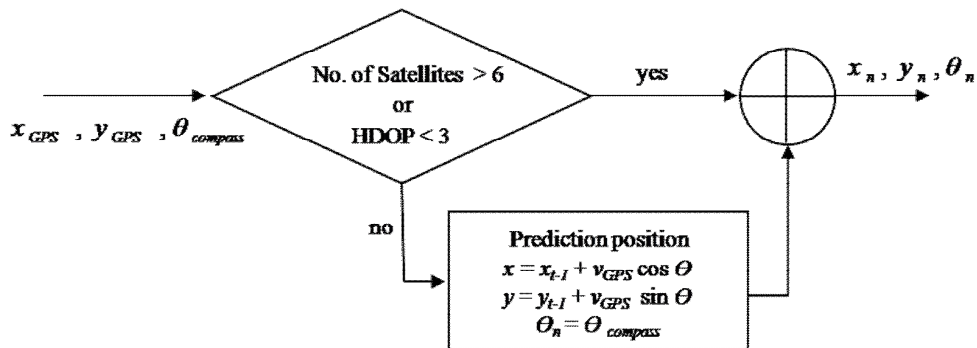


**Figure 5.** Predictive platform box diagram

accepted as the correct position coordinates for the current time  $t$ . Otherwise, they will be applied to the position predicting equations to obtain the final correct position coordinates. For the position predicting equations, the  $x_{t-1}$  and  $y_{t-1}$  values are the latest vehicle position coordinates detected by the receiver,  $v_{GPS}$  is a vector that describes the most recent vehicle ground speed (m/s) obtained from the receiver (GGA message), and  $x_n$ ,  $y_n$  and  $\theta_n$  describe the estimated position of the vehicle at time  $t$ .

### **One-turn Rotation (OTR) Scheme**

The OTR scheme is a method widely used to compensate the magnetic interferences. Two types of magnetic interferences are: (1) the time invariant originating from change in the radius of the magnetism circle, and (2) the time varying caused by shifts in the centre of the magnetism circle, depending on the ambient environment of the sensor [12-15]. For the OTR scheme, the high-frequency interference technique is employed to overcome the effects of road slope and tilt.

The OTR scheme for the DEC sensor was rotated by 360° (full turn) on the horizontal plane without any interference. Following the guidelines suggested by Lenz [14], the sensor output was recorded as a reference magnetism circle and was referred by a reference radius ( $V_{ref}$ ). The sprayer was then rotated by 360° after the sensor installation. The coefficients  $V_{x,max}$ ,  $V_{x,min}$ ,  $V_{y,max}$  and  $V_{y,min}$  were measured and used to calculate the coefficients  $V_r$ ,  $V_{x,sf}$ ,  $V_{y,sf}$ ,  $V_{x,off}$  and  $V_{y,off}$ . The threshold value for the magnetism-circle error ( $\varepsilon$ ), that for the azimuth angle error ( $\gamma$ ) and that for slope and tilt ( $\delta$ ) were estimated by considering the environment and error tolerance range for a specific application, which can be optimally adjusted through experiments.

### **Softwares**

All of the algorithms developed were implemented with Microsoft Visual Basic 2008 under Windows XP. The real-time positioning software was developed specifically for an agricultural vehicle working in an orchard environment. For the experimental procedure in the software, the necessary input data were obtained from DGPS and DEC. The software was run by following the algorithm as shown in Figure 4. The calculation of the vehicle's coordinates under the terms of DGPS multi-path error was then executed. The calculating function for the vehicle positions worked automatically in real time.

## **RESULTS AND DISCUSSION**

### **Elimination of Electric Compass Interference**

A number of tests were performed to verify the performance of the OTR scheme with respect to compensation for the magnetic interference (time invariant) while the radius changes and shifts of the centre of the magnetism circle depended on the sensor location. The interference caused by the slope and tilt was compensated for by measuring the external interference field and using the calibration algorithm proposed by Lee et al [12]. These methods were used to find the appropriate coefficient values for our sensor, which included the threshold value for the magnetism-circle error ( $\varepsilon$ ), that for the azimuth angle error ( $\gamma$ ) and that for slope and tilt ( $\delta$ ). The results of the OTR compensation and coefficient setting are shown in Table 1, which shows all the essential coefficients used for measuring the external interference field and for calibrating electrical compasses 1 and 2.

**Table 1.** OTR results and coefficients of compasses 1 and 2

Item	Compass 1	Compass 2	Value
$V_{x,\max}$	-33	4	Maximum value of x-axis sensor output; mG
$V_{x,\min}$	-162	-120	Minimum value of x-axis sensor output; mG
$V_{y,\max}$	350	206	Maximum value of y-axis sensor output; mG
$V_{y,\min}$	138	3	Minimum value of y-axis sensor output; mG
$V_r$	105.9993	101.5002	Error of radius of magnetism circle; mG
$V_{x,sf}$	1.6434	1.6371	x-Axis output ratio between compass 1 and 2
$V_{y,sf}$	1.0000	1.0000	y-Axis output ratio between compass 1 and 2
$V_{x,off}$	160.2326	94.9516	Centre offset of x-axis sensor; mG
$V_{y,off}$	-244.0	-104.5	Centre offset of y-axis sensor; mG
$\varepsilon$	10	10	Threshold value for magnetism-circle error; mG
$\gamma$	30	30	Threshold value for azimuth angle error; mG
$\delta$	17	17	Threshold value for slope and tilt; mG
FIFO	100	100	Size of FIFO (first in first out) queue

Note: mG = milligauss

The calibration of our DEC installed on the vehicle was completed to confirm the heading and heading angle error (Figure 6). Figure 6(a) shows a practical magnetism circle obtained from the DEC as it is rotated by 360 degrees. The dark blue circle and the red circle represent the raw data (magnetism values) measured by electric compasses 1 and 2 respectively. Both circles are shifted and shrunk because of the effects of the vehicle body. The pink and blue plots show the estimated magnetism values; the circles are shifted to the origin and are also modified to compensate for the interference caused by the slope and tilt. Figure 6(b) illustrates the results of the heading angle measured by electric compasses 1 and 2 with an external interference model for the DEC [12].

The combinations of the heading angle errors in the two compasses in the DEC at the external interference nearly matched the linear cycles with very small disturbance. Figure 6(c) is a plot of the errors in our heading estimation when the vehicle was driven from east to west. It shows that the heading error is always within  $\pm 0.3$  degree. Lee et al. [12] reported heading errors within  $\pm 0.5$  degree.

### Vehicle Position Estimated by the Positioning System

Figure 7 shows the tracks of the vehicle: the green square plot illustrates the position measured by the DGPS with errors while the red plot illustrates the estimated and corrected position using our positioning algorithm. The circled portions in Figure 7 demonstrate that while DGPS working was not in the optimal conditions, our system correctly estimated the vehicle position by using the latest vehicle velocity values and the heading angle at that moment to calculate the new position. Both input values were apparently more reliable than the values obtained by DGPS and gave a smoother track without outage, bias or corruption errors.

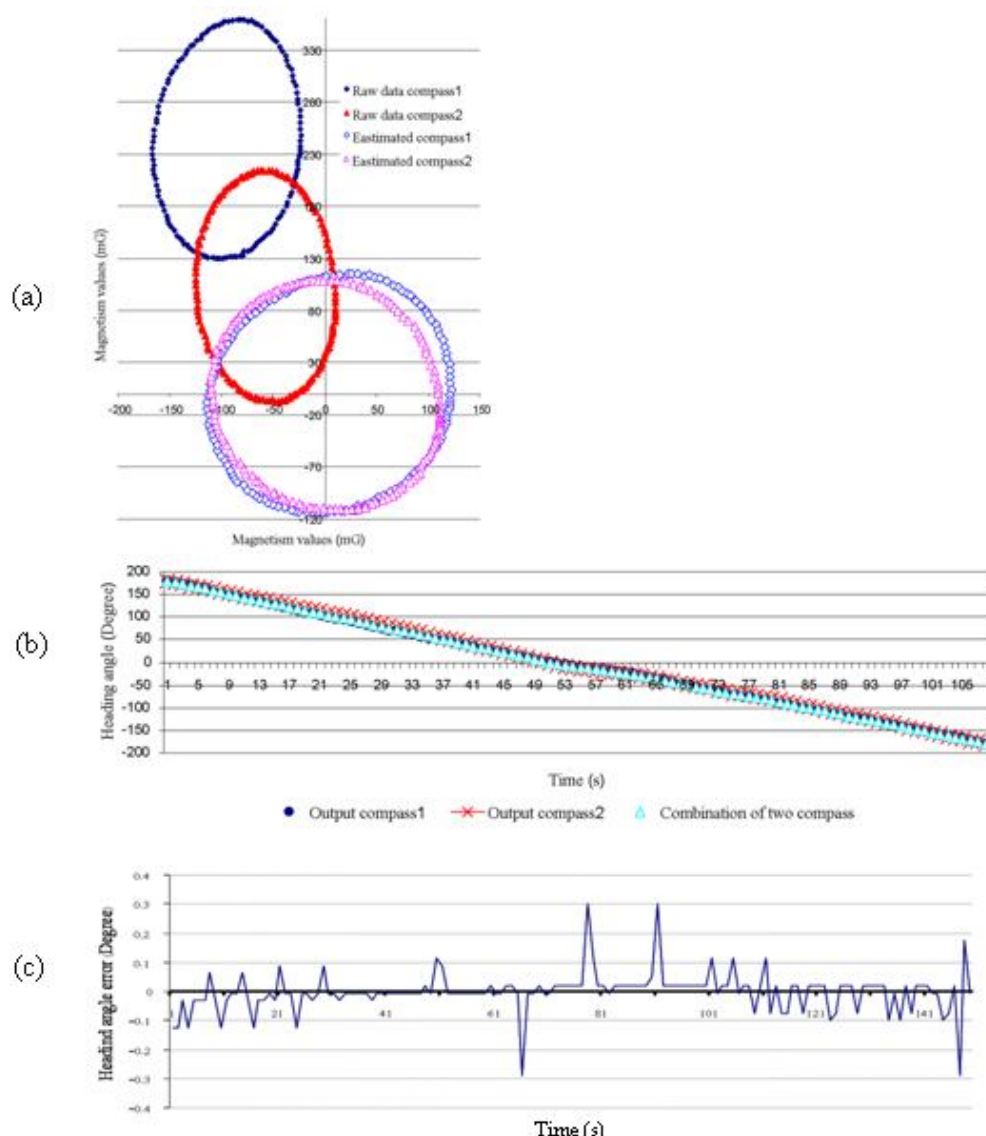


**Figure 6.** Measurement results: (a) angle measurement of external interference field and calibration function; (b) heading angles; and (c) heading angle errors on path

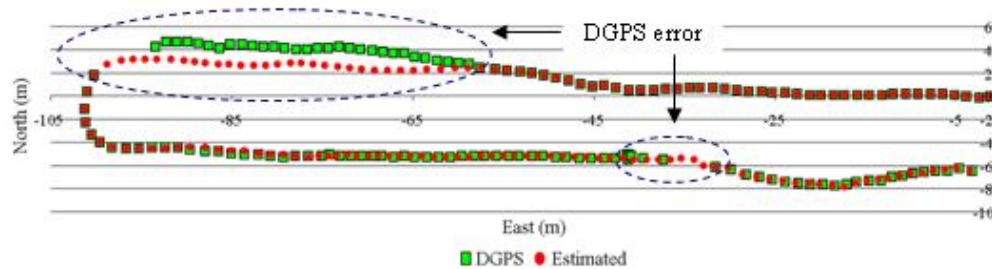


**Figure 7.** Difference between vehicle track determined by DGPS and that estimated by DGPS-DEC positioning system

Figures 8(a) and 8(b) show the position plots on the x-axis and y-axis vs. time respectively, while Figure 8(c) compares the number of satellites used and the HDOP values vs. time. Since the vehicle was driven at low speed (0.24 km/hr), the positioning error was expected to be small or insignificant. The error mainly stemmed from the inadequate number of satellites and the high value of HDOP. Significant errors can be observed at 230-370 seconds and 620-660 seconds consistently in Figures 9(a) and 9(b). The DGPS error increased when fewer than six satellites were used and the HDOP value was greater than three. Nevertheless, our estimation using the latest corrected DGPS system was capable of keeping track on the right position for the vehicle.

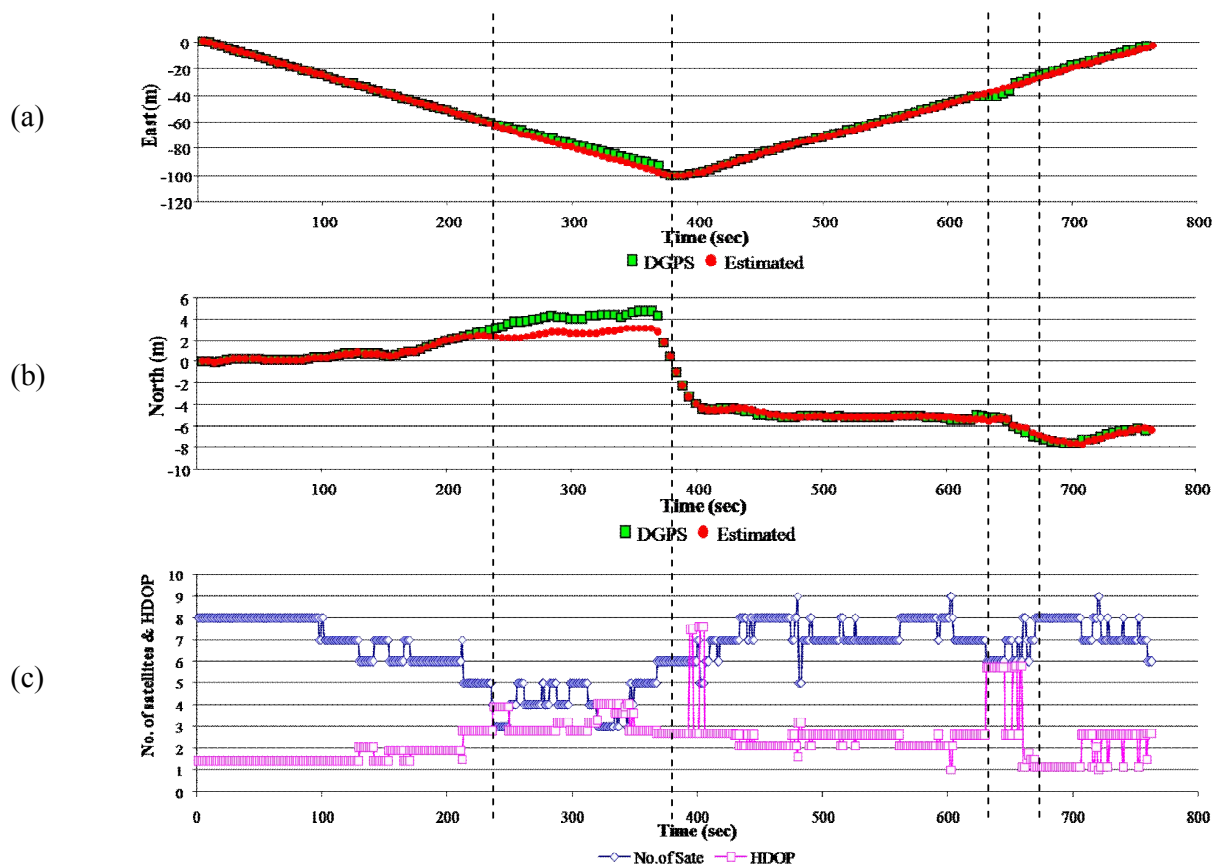


**Figure 8.** Plot of coordinate positions by DGPS (green squares) and combined DGPS-DEC positioning system (red circles) on the x-axis (a) and the y-axis (b), and number of satellites used (blue strip) and HDOP value (pink strip) (c)

To confirm the reliability of our system, an experiment was conducted in which the vehicle was driven along the same path 9 times. The total distance driven was about 20 m for each run, and the radius of the U-turn was 5 m. The number of satellites in use was 4 to 8 satellites, and the HDOP value ranged from 1.1 to 3.1. The positions measured while collecting the position coordinates every second in every path motion were used to calculate the standard deviation (SD) of the distance error. The results are shown in Table 2, which indicates that for straight line path, the positioning system

had an average SD of 20.7 cm and an average distance error of 17.5 cm. For the U-turn path, the figures were 9.5 cm and 22.3 cm respectively. The reason for a narrower SD obtained in the case of the U-turn was probably due to is the shorter distance in the experiment, hence a smaller number of observed data, providing more chance of higher accuracy. For the case of the straight route with much longer observed distance, more variation of data was expected, resulting in a higher SD value.

**Table 2.** Results of distance errors

Order no. of path tracing	Distance error (m)			
	Straight line		U-turn	
	Mean	SD	Mean	SD
1	0.243	0.286	0.413	0.205
2	0.544	0.633	0.171	0.046
3	0.396	0.467	0.394	0.200
4	0.077	0.101	0.205	0.102
5	0.037	0.045	0.202	0.090
6	0.033	0.040	0.132	0.033
7	0.088	0.100	0.139	0.042
8	0.119	0.138	0.111	0.045
9	0.039	0.052	0.236	0.091
Average	0.175	0.207	0.223	0.095

## CONCLUSIONS

A positioning system that corrects the multi-path error to improve the performance of an orchard vehicle has been developed. In particular, the shading effects of natural obstructors and the effects of fewer than 6 satellites and of HDOP value being greater than 3 were addressed. By combining data from both the DGPS and the DEC to predict the position coordinates during movement in real time, we could overcome the problems of DGPS multi-path error using our predictive algorithm. Results have shown that our system has the ability to continue to estimate the vehicle position in real time smoothly (stably) and reliably. Our positioning system should thus be suitable for further development into a guidance control system for autonomous orchard vehicles.

## ACKNOWLEDGEMENTS

This work was financially supported by the Agriculture and Food Agency, Council of Agriculture, Executive Yuan of Taiwan and Taiwan scholarship.

## REFERENCES

1. O. C. Barawid Jr., A. Mizushima, K. Ishii and N. Noguchi, "Development of an autonomous navigation system using a two-dimensional laser scanner in an orchard application", *Biosyst. Eng.*, **2007**, 96, 139-149.
2. J. N. Wilson, "Guidance of agricultural vehicles-a historical perspective", *Comp. Electron. Agric.*, **2000**, 25, 3-9.
3. T. Bell, "Automatic tractor guidance using carrier-phase differential GPS", *Comp. Electron. Agric.*, **2000**, 25, 53-66.
4. T. Torii, "Research in autonomous agriculture vehicles in Japan", *Comp. Electron. Agric.*, **2000**, 25, 133-153.
5. J. F. Reid, Q. Zhang, N. Noguchi and M. Dickson, "Agricultural automatic guidance research in north America", *Comp. Electron. Agric.*, **2000**, 25, 155-167.
6. R. Keicher and H. Seufert, "Automatic guidance for agricultural vehicles in Europe", *Comp. Electron. Agric.*, **2000**, 25, 169-194.
7. J. Yosida, "A study on the automatic farm machine system for rice", *Comp. Electron. Agric.*, **2000**, 25, 133-153.
8. Y. Morales and T. Tsubouchi, "DGPS, RTK-GPS and StarFire DGPS performance under tree shading environments", Proceedings of IEEE International Conference on Integration Technology, **2007**, Shenzhen, China, pp.519-524.
9. S. Rezaei and R. Sengupta, "Kalman filter-based integration of DGPS and vehicle sensor for localization", *Trans. Control Syst. Technol.*, **2007**, 15, 1080-1088.
10. K. Ohno, T. Tsubouchi, B. Shigematsu, S. Maeyama and S. Yuta, "Outdoor navigation of a mobile robot between buildings based on DGPS and odometry data fusion", Proceedings of the International Conference on Robotics and Automation, **2003**, Taipei, Taiwan, pp.1978-1984.
11. K. Ohno, T. Tsubouchi and S. Yuta, "Outdoor map building based on odometry and RTK-GPS positioning fusion", Proceedings of the International Conference on Robotics and Automation, **2004**, New Orleans, LA, USA, pp.684-690.
12. K. M. Lee, Y. H. Kim, J. M. Yun and J. M. Lee, "Magnetic-interference-free dual-electric compass", *Sens. Actuators A*, **2005**, 120, 441-450.
13. X. Li, Q. Zhou., S. Lu and H. Lu, "A new method of double electric compass for localization in automobile navigation", Proceedings of the IEEE International Conference on Mechatronics and Automation, **2006**, Luoyang, China, pp.514-519.
14. J. E. Lenz, "A review of magnetic sensor", Proceedings of IEEE, **1990**, Dayton, OH, USA, pp.973-989.
15. M. J. Caruso, "Applications of magnetoresistive sensor in navigation system", *Sens. Actuators SAE* **1997**, SP-1220, 15-21.
16. L. Ojeda and J. Borenstein, "Experimental results with the KVHC-100 fluxgate compass in mobile robots", Proceedings of the IASTED International Conference on Robotics and Applications, **2000**, Honolulu, Hawaii, USA, pp.1-7.
17. J. P. Snyder, "Map Projection-A Working Manual", Paper1395, U.S. Geological Survey (USGS) Professional, Washington, DC, **1987**, p.383.

## **Changes in essential oil content and composition of leaf and leaf powder of *Rosmarinus officinalis* cv. CIM-Hariyali during storage**

**Ram S. Verma<sup>1,\*</sup>, Laiq ur Rahman<sup>2</sup>, Sunita Mishra<sup>3</sup>, Rajesh K. Verma<sup>2</sup>, Amit Chauhan<sup>1</sup> and Anand Singh<sup>3</sup>**

<sup>1</sup> Central Institute of Medicinal and Aromatic Plants (CSIR), Research Centre, Pantnagar, PO-Dairy Farm Nagla, Udhampur, Jammu and Kashmir-180011, India

<sup>2</sup> Central Institute of Medicinal and Aromatic Plants (CSIR), PO-CIMAP, Lucknow-226015, India

<sup>3</sup> Central Institute of Medicinal and Aromatic Plants (CSIR), Research Centre, Purara, PO-Gagrihole, Bageshwar, Uttarakhand-263688, India

\* Corresponding author: Tel. +91 5944 234445; Fax +91 5944 234712;  
E-mail: [rswaroop1979@yahoo.com](mailto:rswaroop1979@yahoo.com)

Received: 25 April 2010 / Accepted: 4 June 2011 / Published: 6 June 2011

**Abstract:** To see the changes in the essential oil content and composition of rosemary (*Rosmarinus officinalis* L. cv. CIM-Hariyali) during postharvest storage, freshly harvested leaves were kept under sun and shade conditions for one month and one year respectively. In addition to this, since most of the spices are marketed also in powdered form, leaves powder of rosemary was also kept for nine months. The essential oil content was found to vary non-significantly in stored leaves (from 1.05% to 1.3%; fresh weight basis). In contrast, leaves stored in the powdered form for nine months showed sharp decrease in essential oil content (from 2.7% to 1.1%; dry weight basis). GC and GC-MS analysis of the oils revealed the presence of camphor (23.1-35.8%), 1,8-cineole (21.4-31.6%) and  $\alpha$ -pinene (6.7-15.6%) as major constituents. The leaves stored in powdered form contained higher percentages of oxygenated monoterpenoids (71.7-83.7%) compared to those in leaves that were kept in the shade (63.3-70.5%) and in the sun (65.7-67.4%). The study suggested that rosemary leaves should be dried in the shade and stored as such for better yield of quality essential oil.

**Keywords:** essential oil, rosemary, *Rosmarinus officinalis* cv. CIM-Hariyali

## INTRODUCTION

Rosemary (*Rosmarinus officinalis* L.; Lamiaceae) is a spice and medicinal herb widely used around the world. It is mainly produced in Italy, Dalmatia, Spain, Greece, Turkey, Egypt, France, Portugal and North Africa [1]. Rosemary is used since antiquity in food, cosmetics, medicinal and pharmaceutical products [2]. The leaves of rosemary are used in foodstuffs, especially for the control of microbial infections [3-5]. The leaves are also reported to be an antioxidant due to the presence of rosmarinic acid, carnosol, carnosic acid and caffeic acid [6-8]. Of the natural antioxidants, rosemary has been widely accepted as one of the spices with the highest antioxidant activity [9]. The essential oil of rosemary has been reported to be a tonic stimulant and is used as a pulmonary antiseptic, a choleric, a colagogic, and also shows stomachic, antidiarrhoeal and antirheumatic properties [10].

Several studies on the chemical composition of the essential oils of *R. officinalis* L. from different geographic origins have been performed. A survey of the literature reveals that there are mainly three chemotypes: a 1,8-cineole chemotype from France, Greece, Italy and Tunisia; a camphor-borneol chemotype from Spain; and a  $\alpha$ -pinene and verbenone chemotype from Corsica and Algeria [10-13]. The Indian rosemary oil is characterised by relative high amounts of 1,8- cineole, camphor and  $\alpha$ -pinene [14]. The chemical composition of a plant essential oil generally depends on a number of factors such as heredity, part and age of plant, isolation method, environmental condition, collecting season, dehydration procedure and storage condition under which the collected plant is kept until the essential oil is extracted [11,15-20].

A literature survey revealed that the essential oil composition of rosemary has been investigated in India at few occasions [14, 21-23], but there were no reports on postharvest storage from any part of the country. The aim of this work is therefore to observe the changes that occur in the yield and composition of the essential oil of *R. officinalis* (cv. CIM-Hariyali) leaves and leaf powder during storage.

## MATERIALS AND METHODS

### Plant Material

The fresh leaves of *R. officinalis* cv. CIM-Hariyali [24] for study was collected from the experimental farm of Central Institute of Medicinal and Aromatic Plants Research Centre, Purara, Uttarakhand, India in the month of May, 2008. The site is located between the coordinates 28° 60' to 31° 29' and 77° 49' to 80° 60' E at an altitude of 1250m in Kattyur valley. Climatologically, the site falls in the temperate zone of western Himalaya, with the monsoon usually breaking in June and continuing up to September. A total 60 random samples, weighing 100 g each (fresh weight basis) were divided in to 20 batches of three samples/batch. The first batch was distilled on the day of harvesting. Ten batches were kept in shade and the rest were kept under the sun. Observations, viz. moisture loss, oil yield, oil composition, etc., were taken for up to 30 days for under-sun (open) samples and up to one year for under-shade samples. In addition to this, shade-dried leaves were powdered with an electric grinder and stored under shade at room temperature and observations pertaining to oil yield and composition were taken at regular intervals for up to 270 days.

### **Isolation of Essential Oil**

The essential oil was isolated by hydro-distillation for 3 hours using a Clevenger type apparatus. The oil content (% v/w) of leaves and leaf powder was estimated on the fresh weight basis and dry weight basis respectively. The oil samples obtained were dehydrated over anhydrous sodium sulphate and kept in a cool and dark place before analysis.

### **GC and GC-MS**

The gas chromatographic analysis of the oil samples was carried out on a Nucon gas chromatograph model 5765 equipped with FID and BP-20 (30m×0.25mm; film thickness 0.25 µm) fused silica capillary column, and on a Perkin-Elmer Auto XL GC equipped with FID and PE-5 (60m×0.32mm; film thickness 0.25 µm) fused silica capillary column. Hydrogen was the carrier gas at 1.0 mL/min. Temperature programming was 70-230°C at 4°C/min with initial and final hold time of 2 min (for BP-20) and 70-250°C at 3°C/min (for PE-5). Split ratio was 1:30. The injector and detector temperatures were 200°C and 230°C on BP-20 column, and 220°C and 300°C on PE-5 column respectively. GC-MS was performed on a Perkin Elmer Auto System XL GC and Turbo mass spectrometer fitted with a PE-5 fused silica capillary column (50 m x 0.32 mm; film thickness 0.25 µm). The column temperature programme was 100-280°C at 3°C/min, using helium as carrier gas at a constant pressure of 10 psi. MS conditions were: EI mode 70 eV, ion source temperature 250°C.

### **Identification of Compounds**

Compounds identification was done on the basis of retention time, retention indices, MS library search (NIST & WILEY), *n*-alkane (C<sub>9</sub>-C<sub>22</sub>) hydrocarbons pattern (Nile, Italy) and by comparing mass spectra with the MS literature data [25-26]. The relative amounts of individual components were calculated based on GC peak areas without using correction factors.

### **Statistical Analysis**

The data of oil content were subjected to statistical analysis following analysis of variance (ANOVA) technique as applicable to randomised block design [27]. The significance of treatments variance was tested with variance (F) ratio at 5.0% probability level.

## **RESULTS AND DISCUSSION**

### **Essential Oil Content**

The changes in moisture level, essential oil content and chemical composition during post harvest storage of rosemary leaves and leaves powder are given in Tables 1-4. The essential oil content of the unpowdered leaves was not affected significantly by postharvest storage. It was found to vary from 1.2% to 1.05% and 1.12% to 1.1% in leaves stored under shade and sun respectively, while the essential oil content in fresh leaves was 1.3 %. Maximum oil loss was noticed on the second day (48 hours) under shade (15.4% loss) and on the first day (24 hours) under sun (15.4 % loss). Thereafter the oil content (1.1%) was virtually unchanged under both conditions. The leaves stored for up to 1 year under shade recorded 19.2% oil loss. On the other hand, the leaves stored in powdered form showed a substantial oil loss (about 59% after 270 days).

**Table 1.** Changes in essential oil content of rosemary (*Rosmarinus officinalis*) during storage

Storage period (no. of days)	Oil content (A), oil loss (B) and moisture loss (C) (%)							
	Leaves stored under shade			Leaves stored under sun			Leaves stored in powdered form	
	A	B	C	A	B	C	A	B
0	1.3	-	-	-	-	-	2.70	-
1	1.2	7.7	47.3	1.12	13.84	51.30	-	-
2	1.1	15.4	60.1	1.1	15.38	63.76	-	-
3	1.1	15.4	65.4	1.1	15.38	65.54	-	-
4	1.1	15.4	65.6	1.1	15.38	65.58	-	-
5	1.1	15.4	65.7	1.1	15.38	65.66	-	-
6	1.1	15.4	65.7	1.1	15.38	65.72	-	-
7	1.1	15.4	65.8	1.1	15.38	65.78	-	-
15	1.1	15.4	65.8	1.1	15.38	65.80	-	-
30	1.1	15.4	65.8	1.1	15.38	66.00	1.90	29.63
90	1.1	15.4	65.8	-	-	-	1.85	31.48
150	1.1	15.4	65.8	-	-	-	1.50	44.44
210	1.1	15.4	65.8	-	-	-	1.33	50.74
270	1.1	15.4	65.8	-	-	-	1.10	59.26
360	1.05	19.2	65.8	-	-	-	-	-
CD=0.05	NS	-	-	NS	-	-	0.14	-

Note: CD = Critical difference; NS = Non-significant

### Essential Oil Composition

Of a total of 31 components identified (Table 2), the major components in the essential oil from fresh leaves were camphor (23.91%), 1,8-cineole (22.36%),  $\alpha$ -pinene (11.45%), camphene (5.82%), verbenone (5.81%),  $\alpha$ -terpineol + borneol (4.26%),  $\beta$ -pinene (4.05%), bornyl acetate (2.67%), myrcene (2.37%), limonene (2.16%) and linalool (1.11%). Most of the components were found to be affected by postharvest storage/drying. Amounts of  $\alpha$ -pinene, camphene and  $\beta$ -pinene were reduced substantially after 1 day of storage. However, concentrations of  $\alpha$ -pinene and camphene were observed to increase after 90 days while that of  $\beta$ -pinene, after 4 days of storage under shade. Under sun, the concentrations of  $\alpha$ -pinene and camphene were maximal after 30 days of storage while that of  $\beta$ -pinene, after 2 days of storage (Table 3). The concentrations of camphor and 1,8-cineole were observed to be generally higher in stored leaves than in fresh ones under both the conditions. The concentration of verbenone was highest after 1 day of storage in the shade and 3 days of storage in the sun (Tables 2-3).

The oil composition of the powdered leaves (Table 4) was quite different from the unpowdered ones. Overall, the former contained a higher percentage of oxygenated monoterpenoids (71.7-83.7%) than those in the latter (63.3-70.5% and 65.7-67.4% for shade-dried and sun-dried leaves respectively), probably due to a more favourable formation of oxidation products during postharvest storage. The amount of monoterpene hydrocarbons, however, was found to be highest in shade-dried leaves (19.7-31.1%) and lowest in powdered leaves (14.3-18.2%).

In general, most of the changes in essential oil composition of aromatic plants occur during the early hours of storage (initial 12-24 hours). These changes may be due to some physiological processes that continue even after the harvesting of the plant material and/or due to loss of some molecular constituents as the oil glands start to deteriorate on storage. Once the tissues become dried, the changes

**Table 2.** Changes in essential oil composition of rosemary (*Rosmarinus officinalis*) leaves stored under shade

Compound *	Number of days of storage														
	0	1	2	3	4	5	6	7	15	30	90	150	210	270	360
$\alpha$ -Pinene	11.4	6.72	11.1	11.4	11.6	12.1	10.6	11.7	11.3	10.6	15.6	13.7	13.5	15.5	11.1 9
Camphepane	5.82	3.20	4.91	5.12	5.29	5.13	4.53	4.95	4.70	4.45	6.3	5.9	5.6	6.1	6.05
$\beta$ -Pinene	4.05	3.10	4.12	3.97	4.32	4.06	3.77	4.15	3.26	2.85	2.2	1.1	0.4	0.2	3.33
Sabinene	t	-	-	-	-	-	-	-	-	-	t	t	t	-	-
Myrcene	2.37	2.28	2.39	2.35	2.84	2.58	2.75	3.20	2.45	2.71	2.4	1.5	1.4	1.7	1.53
$\alpha$ -Terpinene	0.31	0.29	0.22	0.29	0.61	0.22	0.55	t	0.32	0.71	0.4	0.2	0.4	0.6	0.24
Limonene	2.16	2.90	2.92	2.81	2.78	2.68	2.63	2.85	2.62	3.03	2.7	2.4	2.4	2.8	2.48
1,8-Cineole	22.3	21.4	25.3	24.5	24.6	24.5	24.5	26.3	24.0	24.9	26.6	27.8	28.4	27.0	24.4 4
$\beta$ -Phellandrene	t	-	t	-	0.27	t	0.23	t	t	0.37	-	t	t	-	-
(Z)- $\beta$ -Ocimene	0.67	0.78	0.72	0.77	0.98	0.85	0.83	0.77	0.91	0.98	0.8	0.4	0.4	0.4	0.57
$\gamma$ -Terpinene	0.18	0.13	0.11	0.10	0.09	0.11	t	0.11	0.11	t	t	t	t	t	0.13
p- Cymene	0.32	0.31	0.36	0.37	0.40	0.45	0.41	0.33	0.51	0.54	0.7	0.8	1.0	1.4	0.90
1-Octen-3-ol	0.33	0.11	0.24	0.24	0.23	0.28	0.20	0.49	0.24	0.21	t	t	0.1	0.1	0.31
(E)-Sabinene hydrate	0.46	0.55	0.68	0.83	0.69	0.72	0.66	0.77	0.54	0.39	t	t	0.1	0.1	0.40
Camphor	23.9	26.5	24.9	24.3	24.1	24.4	24.4	24.8	24.8	25.0	25.1	28.7	28.4	26.5	28.5 7
Chrysanthenone	0.26	0.32	0.27	0.26	0.25	0.25	0.27	0.24	0.25	0.24	0.1	-	-	-	0.28
Linalool	1.11	1.60	1.17	1.18	1.10	1.20	1.14	1.26	1.08	1.03	0.8	0.5	0.6	0.5	0.76
Linalyl acetate	0.39	0.50	0.47	0.46	0.40	0.42	0.45	0.41	0.41	0.37	0.1	-	t	-	0.30
Bornyl acetate	2.67	3.53	2.36	2.53	2.42	2.46	2.55	2.18	2.37	2.30	2.0	1.9	1.9	1.6	0.81
$\beta$ -Caryophyllene	0.75	1.41	0.86	1.24	1.00	1.18	1.21	1.00	1.38	1.09	1.2	0.3	0.8	0.9	0.30
Terpinen-4-ol	0.82	0.82	0.76	0.96	0.66	0.74	0.77	1.46	0.68	0.81	0.6	0.5	0.4	0.4	0.97
$\alpha$ -Humulene	0.45	0.82	0.68	0.58	0.71	0.82	0.85	0.71	0.80	0.62	0.8	0.1	0.4	0.5	0.63
$\alpha$ -Terpineol+borneo 1	4.26	5.50	4.35	4.09	4.28	4.39	4.44	3.78	4.40	4.05	3.8	6.4	5.9	6.0	6.83
Verbenone	5.81	7.26	4.80	5.19	3.96	5.25	5.44	3.23	5.71	4.58	6.3	4.2	4.5	4.1	4.79
Citronellol	t	0.32	0.19	0.16	0.14	0.18	0.14	0.12	0.16	t	t	t	t	t	0.11
Myrtenol	0.14	0.19	0.13	0.53	0.21	0.12	0.13	0.31	0.16	0.11	t	t	t	t	0.17
Geraniol	0.25	0.64	0.17	t	t	0.10	t	t	0.60	0.17	-	t	t	0.2	0.22
Caryophyllene oxide	t	0.45	0.31	t	0.17	0.26	t	t	0.20	0.90	-	0.1	0.1	0.1	0.10
Methyl eugenol	-	t	t	t	t	t	t	t	t	-	-	0.1	0.1	t	t
Eugenol	t	0.24	0.84	0.18	0.23	0.28	0.21	0.21	0.40	0.86	0.2	0.1	0.1	0.1	0.39
<b>Class composition</b>															
Monoterpene hydrocarbons	27.3	19.7	26.9	27.2	29.2	28.2	26.3	28.1	26.2	26.2	31.1	26.0	25.1	28.7	26.4 2
Oxygenated monoterpenes	62.7	69.5	66.4	65.4	63.3	65.3	65.4	66.2	65.9	65.1	65.5	70.2	70.5	66.6	69.3 5
Sesquiterpenes hydrocarbons	1.2	2.23	1.54	1.82	1.71	2	2.06	1.71	2.18	1.71	t	0.1	0.1	0.1	0.93
Oxygenated sesquiterpenes	t	0.45	0.31	t	0.17	0.26	t	t	0.20	0.90	2.0	0.4	1.2	1.4	0.10
<b>Total identified (%)</b>	91.3 0	91.9 7	95.1 7	94.5 1	94.4 1	95.8 9	93.9 0	96.0 9	94.5 1	93.9 9	98.6 0	96.7 0	96.9 0	96.8 0	96.8 0

\* Mode of identification: RI (retention index based on homologous series of n-alkanes: C<sub>8</sub>-C<sub>24</sub>), co-injection with standards compounds, and MS (GC-MS)

Note: t = trace (<0.10%)

**Table 3.** Changes in essential oil composition of rosemary (*Rosmarinus officinalis*) leaves stored in open (sun) condition

Compound (%)	Number of days of storage								
	1	2	3	4	5	6	7	15	30
$\alpha$ -Pinene	11.02	11.49	10.59	10.80	10.53	11.35	11.43	11.30	12.11
Camphepane	4.82	5.08	4.72	4.70	4.52	4.89	4.82	4.77	5.17
$\beta$ -Pinene	3.92	4.15	3.63	3.89	3.88	3.78	4.00	3.48	3.44
Myrcene	2.44	2.32	2.29	2.40	2.36	2.26	2.37	2.29	2.44
$\alpha$ -Terpinene	0.51	0.17	0.25	0.25	0.51	0.17	0.21	0.21	0.31
Limonene	2.89	2.93	2.89	2.81	2.67	2.71	2.93	2.67	3.01
1,8-Cineole	23.68	24.70	22.87	23.60	24.92	23.61	27.07	24.32	26.03
$\beta$ -Phellandrene	-	t	-	t	0.28	t	t	t	t
(Z)- $\beta$ -Ocimene	0.72	0.71	0.70	0.77	0.75	0.82	0.76	0.88	0.95
$\gamma$ -Terpinene	t	t	0.18	0.11	0.10	0.11	0.11	0.10	0.12
p-Cymene	0.33	0.41	0.36	0.41	0.41	0.37	0.41	0.46	0.61
1-Octen-3-ol	0.24	0.24	0.42	0.91	1.05	0.29	0.25	0.88	0.25
(E)-Sabinene hydrate	0.70	0.72	1.08	0.74	0.75	0.67	0.73	0.55	0.17
Camphor	25.16	25.67	23.09	25.00	24.68	24.49	26.08	25.87	25.14
Chrysanthrone	0.25	0.27	0.28	0.24	0.25	0.26	0.26	0.25	0.21
Linalool	1.22	1.19	1.11	1.20	1.18	1.04	1.21	1.10	1.00
Linalyl acetate	0.34	0.33	0.37	0.47	0.40	0.35	0.30	0.41	0.27
Bornyl acetate	2.60	2.54	2.43	2.50	2.38	2.40	2.01	2.24	2.05
$\beta$ -Caryophyllene	1.10	0.85	1.10	1.09	1.32	1.22	0.83	0.98	0.87
Terpinen-4-ol	0.78	0.80	0.77	0.76	0.78	0.65	0.68	0.79	0.78
$\alpha$ -Humulene	0.59	0.72	0.42	0.82	0.81	0.78	0.58	0.71	0.64
$\alpha$ -Terpineol+borneol	4.51	4.56	3.77	4.39	4.20	4.85	4.03	4.90	4.13
Verbenone	5.87	4.91	7.19	5.92	5.49	6.34	3.61	5.26	4.86
Citronellol	0.13	0.13	t	0.12	0.13	0.15	t	0.13	0.12
Myrtenol	0.20	0.22	0.32	0.31	0.41	0.27	t	0.48	0.31
Geraniol	0.26	t	0.11	t	t	t	t	t	t
Caryophyllene oxide	0.55	0.50	t	0.22	0.44	0.44	0.38	0.40	0.13
Methyl eugenol	t	t	-	t	t	t	t	t	t
Eugenol	0.20	0.78	1.96	0.18	0.25	0.70	0.62	0.29	0.54
<b>Class composition</b>									
Monoterpene hydrocarbons	26.65	27.26	25.61	26.14	26.01	26.46	27.04	26.16	28.16
Oxygenated monoterpenes	66.14	67.06	65.77	66.34	66.87	66.07	66.85	67.47	65.86
Sesquiterpenes hydrocarbons	1.69	1.57	1.52	1.91	2.13	2	1.41	1.69	1.51
Oxygenated sesquiterpenes	0.55	0.50	0	0.22	0.44	0.44	0.38	0.40	0.13
<b>Total identified (%)</b>	95.03	96.39	92.9	94.61	95.45	94.97	95.68	95.72	95.66

Note: t = trace (&lt;0.10%)

**Table 4.** Changes in the essential oil composition of rosemary (*Rosmarinus officinalis*) leaves stored in powdered form

Compound (% peak area)	RI	Number of days of storage				
		30	90	150	210	270
$\alpha$ -Pinene	1026	9.1	9.8	9.6	8.5	7.4
Campphene	1065	4.0	4.3	4.1	3.6	3.5
$\beta$ -Pinene	1105	1.4	1.3	0.3	0.1	0.3
Sabinene	1119	t	0.1	-	-	0.4
Myrcene	1158	0.9	1.1	0.2	0.3	0.9
$\alpha$ -Terpinene	1177	0.2	0.5	t	0.1	0.6
Limonene	1194	1.1	t	0.2	0.9	1.3
1,8-Cineole	1204	29.5	27.9	31.6	27.8	24.7
$\beta$ -Phellandrene	1206	-	t	-	t	0.1
(Z)- $\beta$ -Ocimene	1234	0.6	0.7	0.1	0.2	0.6
$\gamma$ -Terpinene	1240	-	-	t	-	0.2
p-Cymene	1271	0.3	0.4	0.4	0.6	1.1
1-Octen-3-ol	1411	t	t	t	t	0.6
(E)-Sabinene hydrate	1463	t	t	t	t	0.7
Camphor	1507	31.2	29.0	35.8	35.0	30.1
Chrysanthrone	1512	0.1	0.2	-	-	-
Linalool	1550	1.0	0.9	0.4	0.4	0.5
Linalyl acetate	1561	0.1	0.2	t	t	t
Bornyl acetate	1585	2.6	2.5	2.2	2.2	2.4
$\beta$ -Caryophyllene	1594	1.3	1.8	0.3	0.7	0.9
Terpinen-4-ol	1606	0.9	0.9	0.7	0.4	1.1
$\alpha$ -Humulene	1670	0.5	1.3	0.1	0.4	0.6
$\alpha$ -Terpineol+borneol	1682	5.4	5.8	7.3	9.1	6.8
Verbenone	1702	7.8	7.9	5.6	5.1	4.6
Citronellol	1778	t	0.1	-	0.2	0.1
Myrtenol	1792	t	0.1	-	0.1	t
Geraniol	1848	-	t	-	0.2	0.1
Caryophyllene oxide	1995	-	t	t	t	t
Methyl eugenol	2132	t	0.1	t	t	-
Eugenol	2192	0.2	0.3	0.1	0.2	t
<b>Class composition</b>						
Monoterpene hydrocarbons		17.6	18.2	14.9	14.3	16.4
Oxygenated monoterpenes		78.8	75.9	83.7	80.7	71.7
Sesquiterpenes hydrocarbons		1.8	3.1	0.4	1.1	1.5
Oxygenated sesquiterpenes		0	t	t	t	t
<b>Total identified (%)</b>		98.2	97.2	99	96.1	89.6

Note: t = trace (&lt;0.10%)

in the essential oil composition are mainly due to loss of molecules from stored biomass. So, if we look at the content of Table 2 again, the major changes in composition are noticed in leaves stored for 1 day (24 hours). Oxygenated monoterpenes (69.5%) dramatically increased when compared to those in the oil of fresh leaves (62.7%). Oxygenated monoterpenes which increased after 1 day were sabinene hydrate, camphor, bornyl acetate, linalool, linalyl acetate, verbenone,  $\alpha$ -terpineol + borneol, citronellol, geraniol, myrtenol and caryophyllene oxide. Thus due to increase (or decrease) in some components the relative percentages of other constituents automatically become less (or more). However, the changes notices on long storage are due to loss of oil constituents. Similar variations in essential oil

content and composition have also been noticed in other plant materials [17, 19, 20, 28]. Therefore, the results of the present study reinforce the fact that there are quantitative and qualitative differences in the essential oil of fresh and dried plant materials.

## CONCLUSIONS

The essential oil content of shade-dried and sun-dried rosemary leaves were not significantly different and oil loss was less than 20% after 1 year and 1 month respectively. In contrast, oil loss in powdered leaves was quite substantial (nearly 60% after 9 months). The oil composition of all stored leaves seemed to change continuously during storage. The monoterpene hydrocarbons content was lowest whereas the oxygenated monoterpenes content was highest in the powdered leaves compared with unpowdered leaves kept in the shade and sun.

During the process of shade drying the green colour of the leaves remained unchanged while the sun-dried leaves turned to brown. Rosemary leaves should therefore be dried and stored as such under shade condition. Storage in powdered form should also be avoided in order to prevent excessive oil loss.

## ACKNOWLEDGEMENTS

The authors are thankful to Integrated Ecodevelopment Research Programme (IERP) for financial support and to the Director of Central Institute of Medicinal and Aromatic Plants, Lucknow (UP) India for continuous encouragement.

## REFERENCES

1. A. C. Atti-Santos, M. Rossato, G. F. Pauletti, L. D. Rota, J. C. Rech, M. R. Pansera, F. Agostini, L. A. Serafini and P. Moyna, "Physio-chemical evaluation of *Rosmarinus officinalis* L. essential oils", *Braz. Arch. Biol. Technol.*, **2005**, 48, 1035-1039.
2. A. Porte, R. L. O. Godoy, D. Lopes, M. Koketsu, S. L. Goncalves and H. S. Torquillo, "Essential oil of *Rosmarinus officinalis* L. (Rosemary) from Rio de Janeiro, Brazil", *J. Essent. Oil Res.*, **2000**, 12, 577-580.
3. B. M. Lawrence, "Progress in essential oils", *Perf. Flav.*, **1986**, 11, 81-82.
4. F. M. E. A. Soliman, E. L. Kashoury, M. M. Fathy and M. H. Gonaid, "Analysis and biological activity of the essential oil of *Rosmarinus officinalis* L. from Egypt", *Flav. Fragr. J.*, **1994**, 9, 29-33.
5. I. Rasooli, M. H. Fakoor, D. Yadegarinia, L. Gachkar, A. Allmeh and M. B. Razaei, "Antimycotoxicogenic characteristics of *Rosmarinus officinalis* and *Trachyspermum copticum* L. essential oils", *Int. J. Food Microbiol.*, **2008**, 122, 135-139.
6. H. L. Madsen and G. Bertelsen, "Spices as antioxidants", *Trends Food Sci. Technol.*, **1995**, 6, 271-277.
7. A. R. Hras, M. Hadolin, Z. eljko Knez and D. Bauman, "Comparison of antioxidative and synergistic effects of rosemary extract with  $\alpha$ -tocopherol, ascorbyl palmitate and citric acid in sunflower oil", *Food Chem.*, **2000**, 71, 229-233.

8. P. Ramirez, F. J. Senorans, E. Ibanez and G. Reglero, "Separation of rosemary antioxidant compounds by supercritical fluid chromatography on coated packed capillary columns", *J. Chromatogr. A*, **2004**, *1057*, 241-245.
9. Y. Peng, J. Yuan, F. Liu and J. Ye, "Determination of active components in rosemary by capillary electrophoresis with electrochemical detection", *J. Pharm. Biomed. Anal.*, **2005**, *39*, 431-437.
10. G. Pintore, M. Usai, P. Bradesi, C. Juliano, G. Boatto, F. Tomi, M. Chessa, R. Cerri and J. Casanova, "Chemical composition and antimicrobial activity of *Rosmarinus officinalis* L. oils from Sardinia and Corsica", *Flav. Fragr. J.*, **2002**, *17*, 15-19.
11. M. H. Bolens, "The essential oil from *Rosmarinus officinalis* L.", *Perf. Flav.*, **1985**, *10*, 21-37.
12. J. C. Chalchat, R. P. Garry, A. Michet, B. Benjilali and J. L. Chabart, "Essential oils of rosemary (*Rosmarinus officinalis* L.): The chemical composition of oils of various origins (Morocco, Spain, France)", *J. Essent. Oil Res.*, **1993**, *5*, 613-618.
13. C. Boutekedjiret, F. Bentahar, R. Belabbes and J. M. Bessiere, "The essential oil from *Rosmarinus officinalis* L. in Algeria", *J. Essent. Oil Res.*, **1998**, *10*, 680-682.
14. L. Rahman, A. K. Kukreja, S. K. Singh, A. Singh, A. Yadva and S. P. S. Khanuja, "Qualitative analysis of essential oil of *Rosmarinus officinalis* L. cultivated in Uttarakhand hills, India", *J. Spices Arom. Crops*, **2007**, *16*, 55-57.
15. D. J. Daferera, B. N. Ziogas and M. G. Polissiou, "GC-MS analysis of essential oils from some Greek aromatic plants and their fungitoxicity on *Penicillium digitatum*", *J. Agric. Food Chem.*, **2000**, *48*, 2576-2581.
16. A. Elamrani, S. Zrira, B. Benjilali and M. Berrada, "A study of Moroccan rosemary oils", *J. Essent. Oil Res.*, **2000**, *12*, 487-495.
17. P. Ram, B. Kumar, A. A. Naqvi, R. S. Verma and N. K. Patra, "Post-harvest storage effect on quantity and quality of rose-scented geranium (*Pelargonium* sp. cv. 'Bourbon') oil in Uttarakhand", *Flav. Fragr. J.*, **2005**, *20*, 666-668.
18. N. Tigrine-Kordjani, F. Chemat, B. Y. Meklati, L. Tuduri, J. L. Giraudel and M. Montury, "Relative characterization of rosemary samples according to their geographical origins using microwave-accelerated distillation, solid-phase microextraction and Kohonen self-organizing maps", *Anal. Bioanal. Chem.*, **2007**, *389*, 631-641.
19. R. S. Verma, L. Rahman, C. S. Chanotiya, R. K. Verma, A. Chauhan, A. Yadav, A. K. Yadav and A. Singh, "Chemical composition of volatile fraction of fresh and dry *Artemisia capillaris* Thunb. from Kumaon Himalaya", *J. Essent. Oil Bearing Plants*, **2010**, *13*, 118-122.
20. R. S. Verma, R. K. Verma, A. Chauhan and A. K. Yadav, "Changes in the essential oil content and composition of *Eucalyptus citriodora* Hook during leaf ontogeny and leaf storage", *Indian Perfumer*, **2009**, *53*, 22-25.
21. G. R. Mallavarapu, M. Singh, R. S. C. Shekhar, S. Ramesh and S. Kumar, "Rosemary oil: Prospects of its production in India", *J. Med. Arom. Plant Sci.*, **2000**, *22*, 298-301.
22. A. S. Shawl, S. Nisar, T. Kumar and I. A. Nawchoo, "Essential oil composition of *Rosmarinus officinalis* L. cultivated in Kashmir valley, India", *Indian Perfumer*, **2008**, *52*, 47-49.

23. R. S. Verma, K. V. Sashidhara and A. Yadav, “Essential oil composition of blue flower ‘rosemary’ (*Rosmarinus officinalis* L.) from subtropical India”, *Acta Pharm. Sci.*, **2010**, 52, 426-429.
24. L. Rahman, S. P. S. Khanuja, R. K. Verma, R. S. Verma, S. Mishra, A. Singh, A. Chauhan, U. B. Singh, S. K. Sharma, A. K. Kukreja, M. P. Darokar, A. K. Shasany and B. V. Raju, “High essential oil yielding variety ‘CIM-Hariyali’ of *Rosmarinus officinalis* L.”, *J. Med. Arom. Plant Sci.*, **2008**, 30, 95-100.
25. N. W. Davies, “Gas chromatographic retention indices of monoterpenes and sesquiterpenes on methyl silicone and carbowax 20M phases”, *J. Chromatogr. A*, **1990**, 503, 1-24.
26. R. P. Adams, “Identification of essential oil components by gas chromatography/quadrupole mass spectrometry”, Allured Publishing Corporation, Carol Stream, Ill., **1995**.
27. W. G. Cochran and G. M. Cox, “Experimental Designs”, Asia Publishing House, New Delhi, **1959**.
28. P. A. Luning, T. Ebbenhorstseller, T. Derijk and J. P. Rozen, “Effect of hot-air drying on flavour compounds of bell peppers (*Capsicum annum*)”, *J. Sci. Food Agric.*, **1995**, 68, 355-365.

*Full Paper*

## **A comparative study of sequencing batch reactor and moving-bed sequencing batch reactor for piggery wastewater treatment**

**Kwannate Sombatsompop\*, Anusak Songpim, Sillapa Reabroi and Prapatpong Inkong-ngam**

Department of Civil and Environmental Engineering Technology, College of Industrial Technology, King Mongkut's University of Technology North Bangkok (KMUTNB), Bangkok, 10800, Thailand

\* Corresponding author, e-mail: kwn@kmutnb.ac.th

*Received: 16 August 2010 / Accepted: 3 June 2011 / Published: 6 June 2011*

**Abstract:** This research aims to comparatively study the efficiency of piggery wastewater treatment by the moving-bed sequencing batch reactor (moving-bed SBR) system with held medium, and the conventional sequencing batch reactor (SBR) system, by varying the organic load from 0.59 to 2.36 kgCOD/m<sup>3</sup>.d. The COD treatment efficiency of the SBR and moving-bed SBR was higher than 60% at an organic load of 0.59 kgCOD/m<sup>3</sup>.d and higher than 80% at the organic loads of 1.18-2.36 kgCOD/m<sup>3</sup>.d. The BOD removal efficiency was greater than 90% at high organic loads of 1.18-2.36 kgCOD/m<sup>3</sup>.d. The moving-bed SBR gave TKN removal efficiency of 86-93%, whereas the SBR system exhibited the removal efficiency of 75-87% at all organic loads. The amount of effluent suspended solids for SBR systems exceeded the piggery wastewater limit of 200 mg/L at the organic load of 2.36 kgCOD/m<sup>3</sup>.d while that for the moving-bed SBR system did not. When the organic load was increased, the moving-bed SBR system yielded better treatment efficiency than that of the SBR system. The wastewater treated by the moving-bed SBR system met the criteria of wastewater standard for pig farms at all organic loads, while that treated by the SBR system was not satisfactory at a high organic load of 2.36 kgCOD/m<sup>3</sup>.d.

**Keywords:** sequencing batch reactor (SBR), moving-bed SBR, moving-bed biofilm reactor, piggery wastewater treatment

## INTRODUCTION

Piggery wastewater is high in organic matter and consists of pig manure (urine and faeces), food waste and water from cleaning living quarters. Piggery wastewater is very difficult to treat because it contains a considerable amount of unstabilised organic matter and a high ammonia concentration. In Thailand, the average volume of piggery wastewater is in the range of 10-20 L/pig/day [1]. Generally, its average biochemical oxygen demand (BOD) value is in the range of 1,500-3,000 mg/L, and its average chemical oxygen demand (COD) value is in the range of 4,000-7,000 mg/L [1]. The Ministry of Natural Resources and Environment (Thailand) has recently introduced regulations for livestock wastewater control including effluent standards for pig farms, which states that the effluent from small- and medium-size pig farms must contain not more than 100 mg/L of BOD, 400 mg/L of COD, 200 mg/L of suspended solids and 200 mg/L of total Kjeldahl nitrogen (TKN) [2]. In order to comply with these regulations, an effective wastewater treatment system for both organic and nitrogen removal is required.

The biological process appears to be the method of choice for organic and nitrogen removal from animal waste because the chemicals for the process are relatively inexpensive and the treatment efficiency is relatively high [3-4]. The organic matter in piggery wastewater can be initially treated with anaerobic digestion. This process achieves an effective reduction of organic matter and pathogens and generates biogas, a valuable energy [5]. However, the effluent from anaerobic digestion of piggery wastewater contains a high amount of ammonia, which requires further removal by such methods as air stripping and coagulation-flocculation (physicochemical method) [6-7], treatment in a biofilm air-lift reactor or membrane bioreactor (physicobiological method) [4], and/or treatment in a sequencing batch reactor (biological method) in order to meet the quality standard for discharged effluent. The sequencing batch reactor (SBR) with the ability to remove nitrogen and organic matter in limited space has recently been used for piggery wastewater treatment [3, 8-10], either in aerobic/anoxic condition or in anaerobic digestion [8-10]. From the economical point of view, the biological treatment is preferred since its relative cost is lower than other physicochemical or physicobiological methods [11]. The SBR system can also be used to treat wastewater with high nitrogen content through nitrification-denitrification [12-13].

Over the last decade, there has been growing interest in the moving-bed biofilm reactor process for both municipal and industrial wastewater treatments, as compared to conventional biological processes and biofilter process, due to their greater compactness and need for less space, high tolerance to load impact, no sludge bulking problem as well as less dependence on final sludge separation and utilisation owing to the lack of sludge return [14-17]. At present, there are about 400 large-scale wastewater treatment plants from 22 different countries all over the world using the moving-bed process [18]. The development on the attached growth bioreactor by addition of a moving-bed medium in the case of high biomass concentration has created great interest [13, 15-16]. Due to its high removal efficiency and stable operation at high organic loads, some researchers [13,15-19] have employed the moving-bed bioreactor in treating slaughterhouse wastewater [13], phenolic wastewater [20], pesticide wastewater [21] and municipal wastewater [13-16,19].

As mentioned earlier, the piggery wastewater from the anaerobic digestion still contains high amounts of organic matter and ammonia and thus requires further treatment. Therefore, it is the

aim of this work to apply the SBR system with a moving-bed medium to the treatment and to compare the results with those obtained from the ordinary SBR system. Recent literature [13-21] has clearly indicated that such comparative study of moving-bed SBR and ordinary SBR systems, especially that utilising piggery wastewater, has been limited. This then becomes the main interest in our present work.

## MATERIALS AND METHODS

### Experimental Set-up

The SBR and moving-bed SBR systems each consisted of an acrylic reactor 40 cm high, 0.5 cm thick and 16 cm in diameter with a working volume of 6 L. One air pump system (Yamano AP-10, Japan) was used for supplying the air to the two reactors. The flow-in and flow-out rates of piggery wastewater were controlled by a level control (Omron, Japan) and solenoid valve (AirTac-2W025-08, China). The operational sequence of the SBR systems and the movements of all mechanical devices including the air pump system, solenoid valve and level control were controlled by a programmable logic controller (Omron ZEN-10C3AR-A-V2, Japan). The SBR and moving-bed SBR systems were installed and assembled as shown in Figure 1.

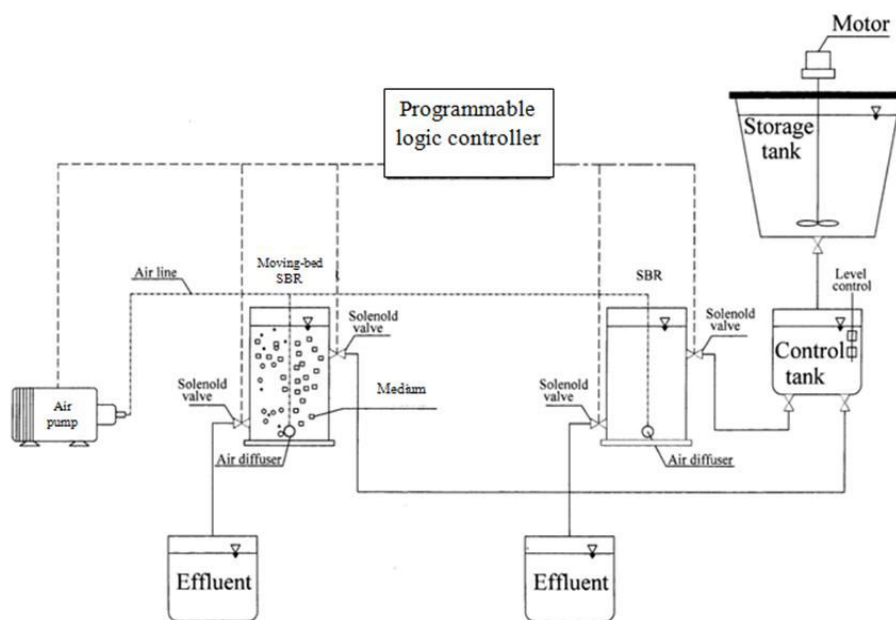


**Figure 1.** Schematic diagram of SBR and moving-bed SBR systems

Before starting each batch reactor, the piggery wastewater was fed into the reactor containing activated sludge. The activated sludge culture was obtained from Bangkok central wastewater treatment plant. The volatile suspended solids to suspended solids ratio of the activated sludge was 0.89. The activated sludge microorganisms was adapted to the piggery wastewater by cultivating in an aeration tank. The SBR and moving-bed SBR systems were operated batchwise for 10 days with aeration and mixing to obtain a dense culture of the activated sludge for use as inocula

for the two systems, which, after cultivating, had a mixed liquor suspended solids (MLSS) concentration of about 3,000 mg/L. Both systems worked 2 cycles per day. One cycle comprised the following stages: 1 h for filling, 8 h for reacting, 2 h for settling and 1 h for drawing and idling. During the drawing phase, the supernatant wastewater was decanted until the liquid volume in the reactor decreased to 2 L. Both systems were operated at a sludge retention time (SRT) of 10 days by wasting a certain amount of mixed liquor from the reactors everyday just before the settling period. The piggery wastewater was treated at 8 L/day for each system, and the hydraulic retention time (HRT) was 0.75 day. The dissolved oxygen (DO) concentration in each reactor was maintained by an air flow rate of 1.0 L/min. Throughout the study, the pH and ambient temperature were approximately  $7.5 \pm 0.5$  and  $27 \pm 2^\circ\text{C}$  respectively. Poly(vinyl chloride) sponge, which was cut in 1.5-cm cubes, was used as the floating medium in the moving-bed reactor. The sponge cubes were circulated in the reactor by air without any additional mixing equipment. The moving medium had a specific surface area of  $400 \text{ m}^2/\text{m}^3$  and a density of  $0.0145 \text{ g/cm}^3$  and was used at 20% fill fraction [% fill fraction =  $100 \times (\text{volume occupied by medium} / \text{reactor volume})$ ].

The piggery wastewater used in this experiment was taken from an anaerobic system of a pig farm in Nontaburi province. It was allowed to settle for 1 h and then filtered through a 1-mm mesh screen to remove any large particles. The wastewater in the influent tank was prepared daily by mixing the raw piggery wastewater with tap water to provide the feed wastewater with COD concentrations of 500, 1000, 1500 and 2000 mg/L, and organic loads of 0.59, 1.18, 1.77 and 2.36 kgCOD/m<sup>3</sup>.d respectively. The characteristics of a typical piggery wastewater sample from the anaerobic digestion are given in Table 1.

**Table 1.** Characteristics of raw piggery wastewater

Parameter	Unit	Concentration	Standard value for pig-farm effluent (Thailand) [2]
BOD	mg/L	1500-2300	100
COD	mg/L	4700-5900	400
Suspended Solids	mg/L	4000-8000	200
TKN	mg/L	300-500	200
NH <sub>3</sub> -N	mg/L	210-380	-
pH	-	7.5-8.5	5.5-9.0

### Analytical Methods

The samples collected from the influent and effluent wastewaters were analysed in terms of chemical oxygen demand (COD), biochemical oxygen demand (BOD), total Kjedahl nitrogen (TKN), ammonia-N and suspended solids according to "Standard Methods for the Examination of Water and Wastewater" [22]. The per cent removal efficiency of COD, BOD and TKN was defined as:  $[(\text{influent value} - \text{effluent value}) / \text{influent value}] \times 100$ .

Dissolved oxygen (DO) and pH measurements were monitored by a DO meter (Oxi 340i, WTW, Germany) and a pH meter (pH 340i, WTW, Germany) respectively. The sludge volume

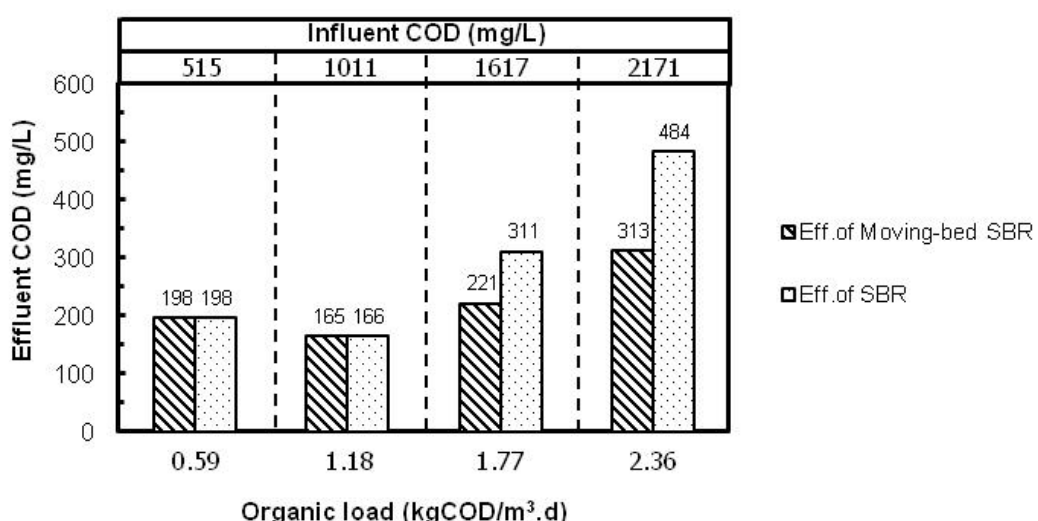
index (SVI), the volume in millilitre occupied by 1 g of a suspension after 30 min settling, was determined in 1-L graduated cylinders with the mixed liquor samples taken directly from the reactors at the end of the reaction period. SVI is typically used to monitor settling characteristics of activated sludge and other biological suspensions [22].

The attached biofilm on the medium was determined as biofilm mass after extraction from the medium. The experimental method for determining the attached biofilm followed the work of Andreottola et al [19]. The average errors for all experimental data were  $\pm 5\%$ .

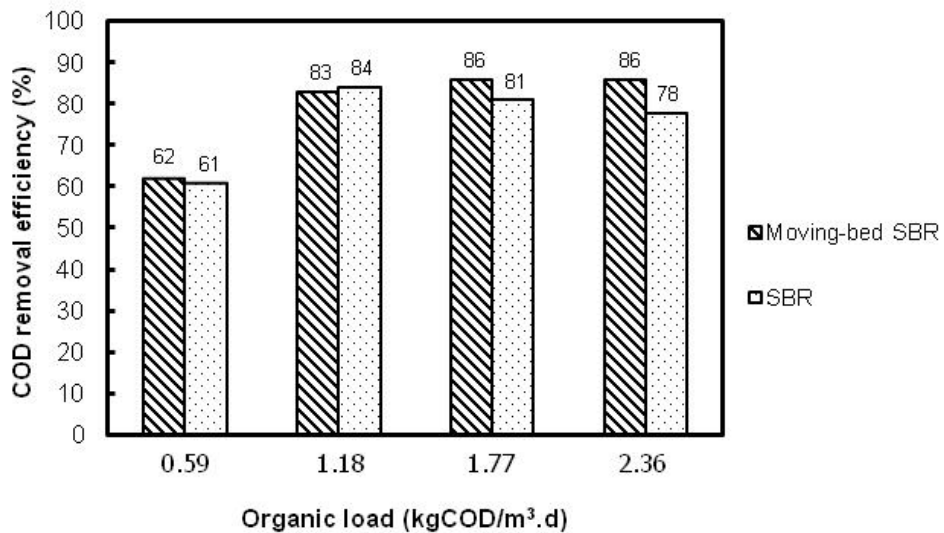
## RESULTS AND DISCUSSION

### COD and BOD Removal Efficiency

A set of experiments were performed at four different organic loads varying from 0.59 to 2.36 kgCOD/m<sup>3</sup>.d while the HRT was fixed at 0.75 day. Figure 2 shows the effluent COD in the two systems as a function of organic load. The results clearly show that as the organic load increased, so did the effluent COD, whose values were similar in both systems at the organic loads of 0.59 and 1.18 kgCOD/m<sup>3</sup>.d, whereas they were higher in the SBR system at the organic loads of 1.77 and 2.36 kgCOD/m<sup>3</sup>.d. At 2.36 kgCOD/m<sup>3</sup>.d the effluent COD in the SBR system did not pass the standard for piggery wastewater (COD of 400 mg/L) [2], while the piggery wastewater treated by the moving-bed SBR satisfied the standard criteria at all organic loads. The moving-bed SBR system was thus apparently more effective at a high organic load than the SBR system. This might be related to the fact that the circulating medium in the moving-bed SBR enhanced distribution of liquid flow and oxygen transfer. This then would enable the unsettled waste to be treated directly [15]. The relationship between COD removal efficiency and organic load for the two systems is shown in Figure 3. It can be seen that as the organic load increased the removal efficiency of the moving-bed SBR also increased or remained unchanged while that of the SBR gradually decreased at high organic loads.

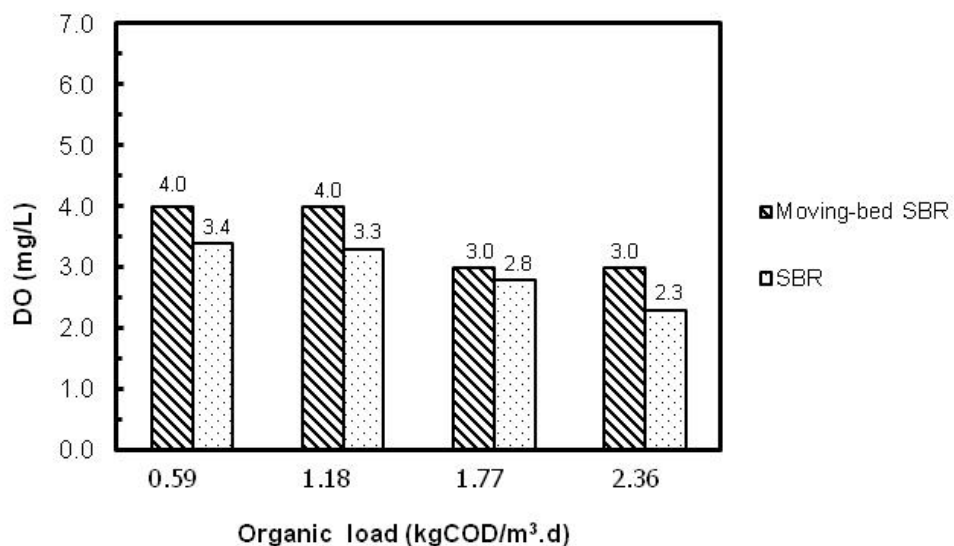


**Figure 2.** Relationship between effluent COD and organic load



**Figure 3.** Removal efficiency of COD as a function of organic load

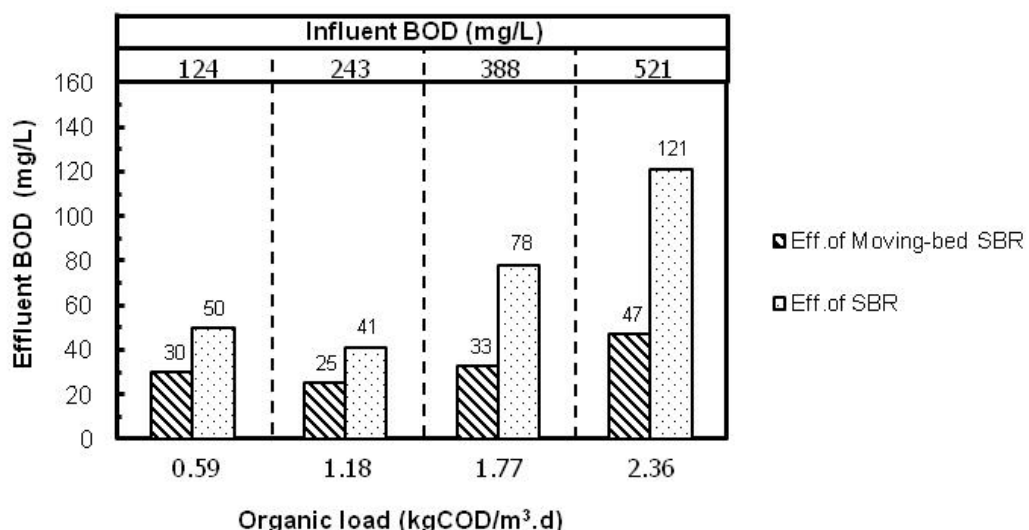
The values of DO in the effluents at different organic loads are given in Figure 4. The DO concentrations at all organic loads in the moving-bed SBR were greater than those in the SBR. These results substantiate the hypothesis that the moving-bed medium can assist in oxygen transfer and liquid distribution in the moving-bed SBR system.



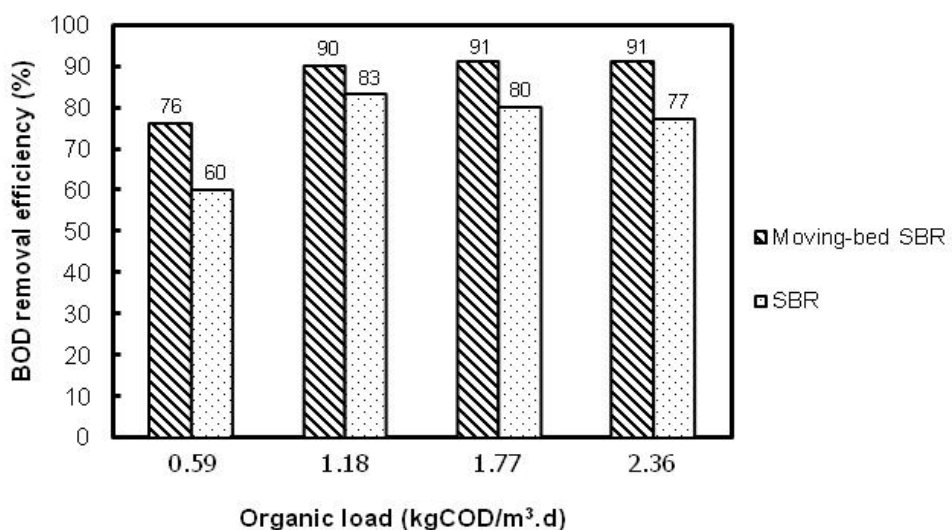
**Figure 4.** DO of effluents at different organic loads

The quality of the effluents from the two reactors in terms of BOD at different organic loads are shown in Figure 5. The BOD trends were similar with those of COD in Figures 3-4. The effluent BOD in the SBR system at the organic load of 2.36 kgCOD/m<sup>3</sup>.d did not pass the standard criterion (BOD of 100 mg/L), whereas the piggery wastewater treated with the moving-bed SBR satisfied the standard criterion at all organic loads. It can be seen from Figure 6 that the BOD removal efficiency

was greater than 90% at high organic loads (1.18-2.36 kgCOD/m<sup>3</sup>.d), which in this study were 2-4 times higher than those used by Sirianuntapiboon and Yommee [13], who reported that the moving-bed aerobic SBR gave higher than 95% COD and BOD removal efficiency when the system was operated to treat synthetic wastewater with an organic load of 0.528 kgBOD/m<sup>3</sup>.d. Thus, the moving-bed SBR seemed to effectively handle a high organic load and consistently provide a high BOD removal efficiency. The biofilm on the medium surface apparently facilitated more biodegradation in the system, thus accounting for the improved BOD removal.



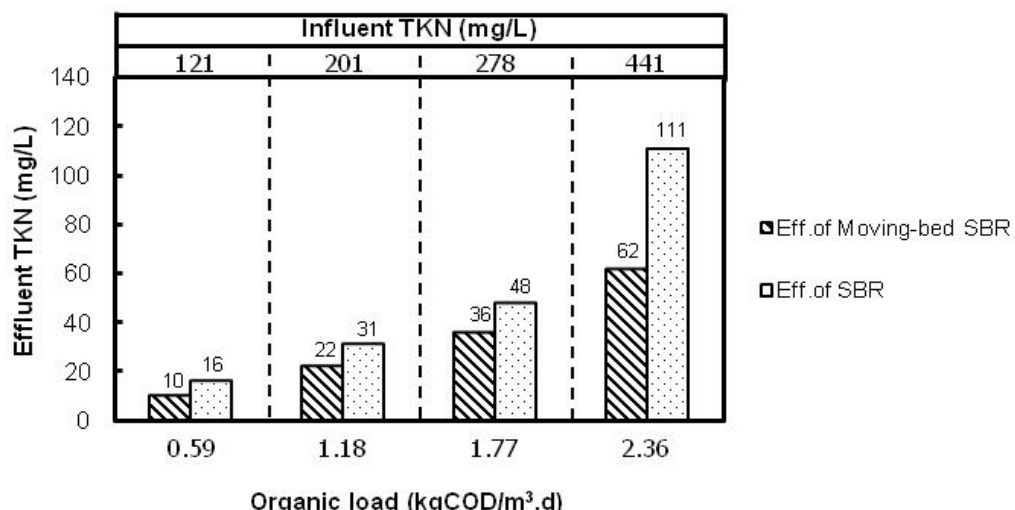
**Figure 5.** Effluent BOD at different organic loads



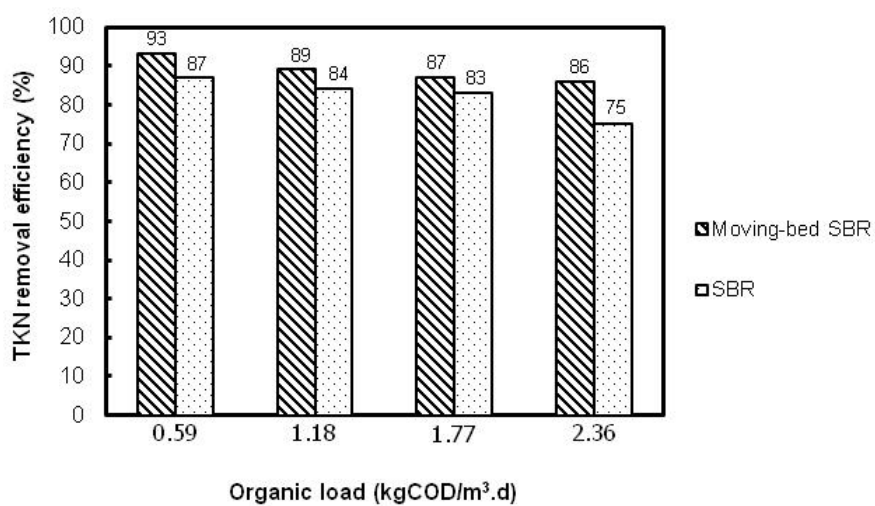
**Figure 6.** Relationship between BOD removal efficiency and organic load

### TKN and Ammonia Removal Efficiency

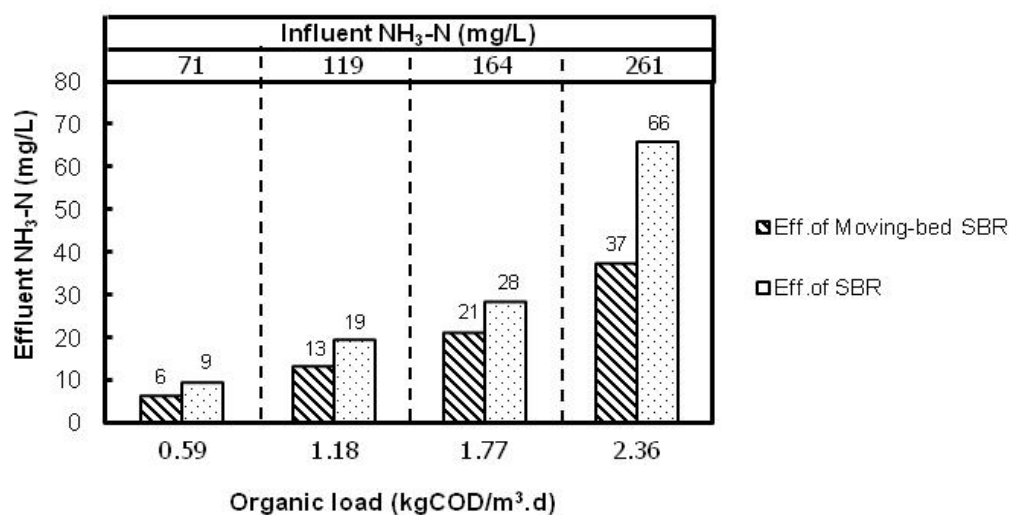
Figure 7 shows the relationship between TKN and organic load for the SBR and moving-bed SBR systems. It can be seen that influent and effluent TKN increased with increasing organic load for both systems, although the TKN effluents in both the SBR and moving-bed SBR satisfied the standard criterion at all organic loadings. Figure 8 presents relationship between TKN removal efficiency and organic load; the efficiency of the moving-bed SBR (86-93%) was better than that of the SBR (75-87%). The biofilm formation on the moving-bed medium, which led to a more efficient nitrification/denitrification process, could account for the increasing nitrogen removal [13,16]. As shown in Figure 9, the ammonia-N in the effluent of the moving-bed SBR was also lower than that of the SBR at all organic loads. This indicates that ammonium oxidation by oxygen occurred more efficiently in the moving-bed SBR, in agreement with the DO data presented in Figure 4.



**Figure 7.** Relationship between TKN and organic load

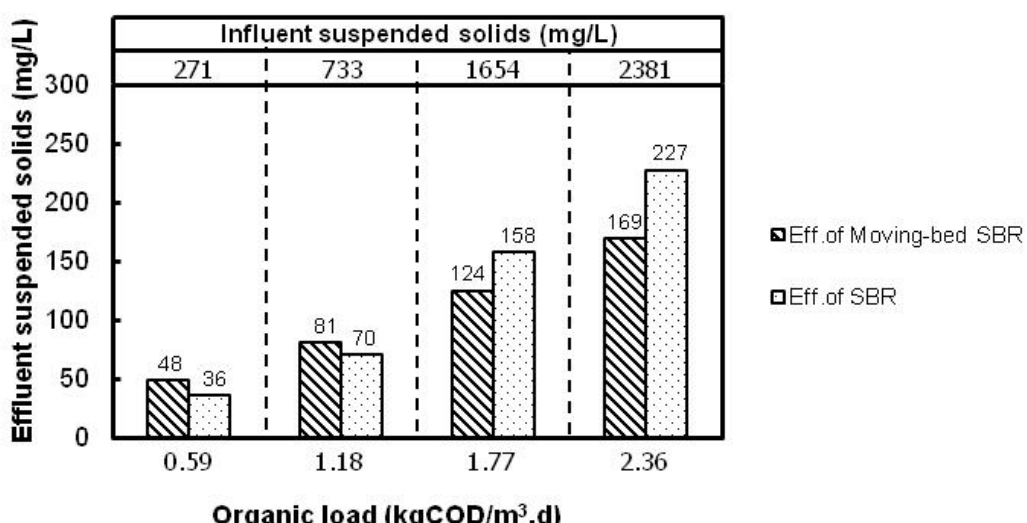


**Figure 8.** Relationship between TKN removal efficiency and organic load

**Figure 9.** Variation in effluent ammonia-N with organic load

#### Suspended Solids, Sludge Volume Index and Microscopic Examination

As expected, the effluent suspended solids from the two systems increased with increasing organic load as shown in Figure 10. It was found that for both systems the effluent suspended solids were similar at organic loads of 0.59 and 1.18 kgCOD/m<sup>3</sup>.d, while at organic loads of 1.77 and 2.36 kgCOD/m<sup>3</sup>.d they differed. At the organic load of 2.36 kgCOD/m<sup>3</sup>.d, the amount of effluent suspended solids from the SBR was 227 mg/L, which exceeded the limit of piggery wastewater standard of 200 mg/L, while the amount from the moving-bed SBR (169 mg/L) was still within the limit, thus again demonstrating a better performance of the moving-bed SBR over the conventional SBR system.

**Figure 10.** Variation in effluent suspended solids with organic load

SVI is an important parameter affecting the performance of a wastewater treatment system. Low SVI values (<100 mL/g) indicate good sedimentation characteristics of the sludge yielding high biomass concentrations in the aeration tank, whereas high SVI values (>>100 mL/g) reflect bulky sludge and low biomass concentrations in the aeration tank [12]. Figure 11 shows SVI as a function of organic load. It can be seen that the SVI for both reactors ranged from 40 to 60 mL/g, indicating that the sludge had good settling capability.

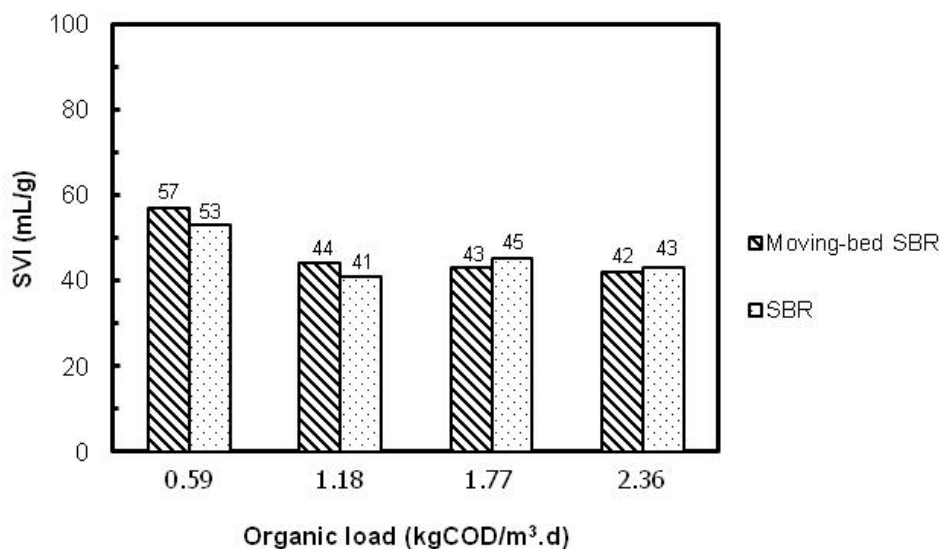
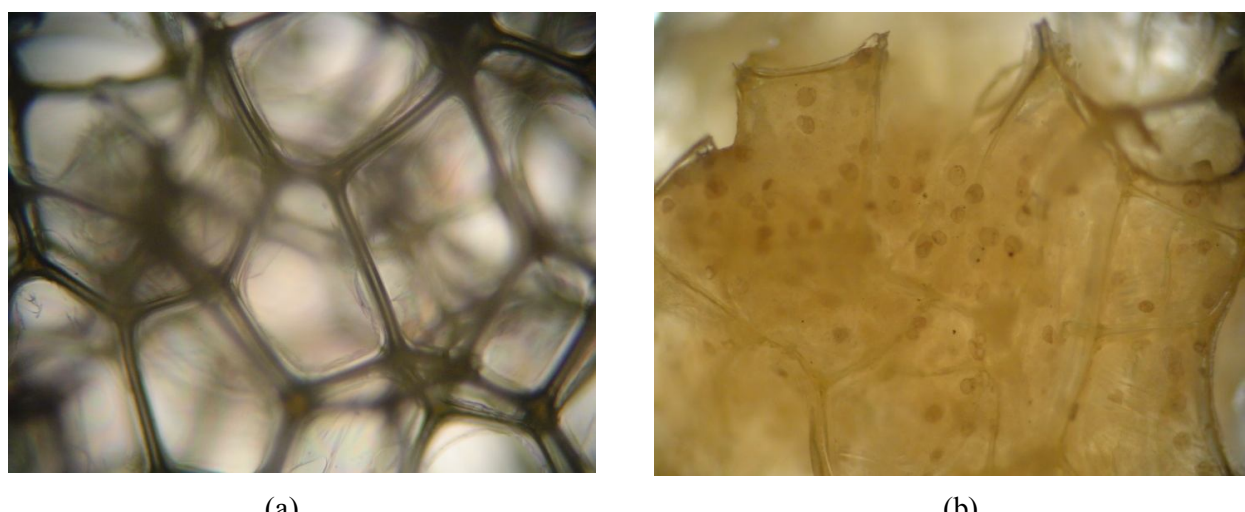


**Figure 11.** Variation in SVI with organic load

During the experiments, microscopic examination was carried out on samples of moving-bed medium taken from the moving-bed SBR. Typical results as in Figure 12 show that there was a large amount of biomass growing on the medium circulated in the reactor. This medium thus provided a large surface area for microbial growth during the operation. A large amount of the biofilm was found attached on the medium and could apparently handle a high organic load. The biofilm mass (mg MLSS/L) and biofilm mass of medium (mg/m<sup>2</sup>) presented the sludge quantities in the moving-bed SBR (Table 2). It can also be seen that the bio-sludge quantity increased with increasing organic load.

**Table 2.** Bio-sludge quantities of the moving-bed SBR

Organic load (kgCOD/m <sup>3</sup> .d)	Biofilm mass (mgMLSS/L)	Biofilm mass of medium (mg/m <sup>2</sup> )
0.59	328	3.0
1.18	367	3.4
1.77	396	3.6
2.36	424	3.9



(a)

(b)

**Figure 12.** Photographs of sponge medium surface ( $\times 10$  magnification): (a) without bio-sludge, (b) with bio-sludge

## CONCLUSIONS

The moving-bed SBR system could be operated effectively at a high organic load. The quality of the effluent from the moving-bed SBR in terms of COD, BOD, TKN and suspended solids met the criteria of wastewater standards for pig farms at all organic loads used, whereas the SBR system was not satisfactory at a high organic load of  $2.36 \text{ kgCOD/m}^3\text{.d}$ . The moving-bed SBR thus seems to be an efficient system for treatment of piggery wastewater with a high nitrogen and organic content.

## ACKNOWLEDGEMENTS

The authors would like to thank Mr. Chaiwat Kaewsri of Chiwat Farm, Nonthaburi province, for his kind support and supply of the raw piggery wastewater used in this research. The Thailand Research Fund (IRPUS Grant No: IPSS150067) is thanked for financial support. Thanks are also expressed to the vets at the Nonthaburi Department of Livestock Development for their help and suggestions.

## REFERENCES

1. "Piggery wastewater management and practice manual", Department of Livestock Development, Ministry of Agriculture and Cooperatives, Bangkok, **2004** (in Thai).
2. "Effluent standard for piggery wastewater", Water Pollution Act 122, part 125, Ministry of Natural Resources and Environment, Bangkok, **2005** (in Thai).

3. D. Obaja, S. Macé, J. Costa, C. Sans and J. Mata-Álvarez, "Nitrification, denitrification and biological phosphorus removal in piggery wastewater using a sequencing batch reactor", *Biores. Technol.*, **2003**, 87, 103-111.
4. H. S. Kim, Y. K. Choung, S. J. Ahn and H. S. Oh, "Enhancing nitrogen removal of piggery wastewater by membrane bioreactor combined with nitrification reactor", *Desalination*, **2008**, 223, 194-204.
5. R. Rajagopol, P. Rousseau, N. Bernet and F. Béline, "Combined anaerobic and activated sludge anoxic/oxic treatment for piggery wastewater", *Biores. Technol.*, **2011**, 102, 2185-2192.
6. B. Wichitsathai and N. Chuersuwan, "Piggery wastewater pretreatment by physic-chemical techniques", *Suranaree J. Sci. Technol.*, **2006**, 13, 29-37.
7. J. Dosta, J. Rovira, A. Galí, S. Macé and J. Mata-Álvarez, "Integration of a coagulation/flocculation step in a biological sequencing batch reactor for COD and nitrogen removal of supernatant of anaerobically digested piggery wastewater", *Biores. Technol.*, **2008**, 99, 5722-5730.
8. N. Bernet, N. Delgenes, J. C. Akunna, J. P. Delgenes and R. Moletta, "Combined anaerobic-aerobic SBR for the treatment of piggery wastewater", *Water Res.*, **2000**, 34, 611-619.
9. M. L. Duamer, F. Béline, F. Guiziou and M. Sperandio, "Effect of nitrification on phosphorus dissolving in a piggery effluent treated by a sequencing batch reactor", *Biosys. Eng.*, **2007**, 96, 551-557.
10. D. H. Kim, E. Choi, Z. Yun and S. W. Kim, "Nitrogen removal from piggery waste with anaerobic pre-treatment", *Wat. Sci. Technol.*, **2004**, 49, 165-171.
11. STOWA, "One reactor system for ammonia removal via nitrite", Report no.96-01, Utrecht, The Netherlands, **1996**.
12. F. Kargi and A. Uygur, "Nutrient removal performance of a sequencing batch reactor as a function of the sludge age", *Enzy. Microb. Technol.*, **2002**, 31, 842-847.
13. S. Sirianuntapiboon and S. Yommee, "Application of a new type of moving bio-film in aerobic sequencing batch reactor (aerobic-SBR)", *J. Envir. Manage.*, **2006**, 78, 149-156.
14. T. H. Lessel, "Upgrading and nitrification by submerged bio-film reactors—experiences from a large scale plant", *Water Sci. Technol.*, **1994**, 29, 167-174.
15. H. Ødegaard, "Advanced compact wastewater treatment based on coagulation and moving bed biofilm processes", *Water Sci. Technol.*, **2000**, 42, 33-48.
16. M. Kermani, B. Bina, H. Movahedian, M. M. Amin and M. Nikaeni, "Application of moving bed biofilm process for biological organics and nutrients removal from municipal wastewater", *American J. Envir. Sci.*, **2008**, 4, 675-682.
17. S. Chen, D. Sun and J. S. Chung, "Stimulaneous removal of COD and ammonium from landfill leachate using an anaerobic-aerobic moving-bed biofilm reactor system", *Waste Manage.*, **2008**, 28, 339-346.
18. B. Rusten, B. Eikebrokkk, Y. Ulgenes and E. Lygren, "Design and operations of the Kaldnes moving bed biofilm reactors", *Aquacult. Eng.*, **2006**, 34, 322-331.

19. G. Andreottola, P. Foladori and M. Ragazzi, “Upgrading of a small wastewater treatment plant in a cold climate region using a moving bed biofilm reactor (MBBR) system”, *Water Sci. Technol.*, **2000**, *41*, 177-185.
20. S. H. Hosseini and S. M. Borghei, “The treatment of phenolic wastewater using a moving bed bio-reactor”, *Process Biochem.*, **2005**, *40*, 1027-1031.
21. S. Chen, D. Sun and J. S. Chung, “Treatment of pesticide wastewater by moving-bed biofilm reactor combined with Fenton-coagulation pretreatment”, *J. Hazar. Mater.*, **2007**, *144*, 577-584.
22. L. S. Clesceri, A. D. Eaton, A. E. Greenberg, M. A. H. Franson and APHA, “Standard Methods for the Examination of Water and Wastewater”, 19<sup>th</sup> Edn., American Public Health Association, Washington, DC, **1996**.

© 2011 by Maejo University, San Sai, Chiang Mai, 50290 Thailand. Reproduction is permitted for noncommercial purposes.

***Maejo International  
Journal of Science and Technology***

ISSN 1905-7873

Available online at [www.mijst.mju.ac.th](http://www.mijst.mju.ac.th)

*Full Paper*

**LDPC concatenated space-time block coded system in multipath fading environment: Analysis and evaluation**

**Surbhi Sharma\*** and **Rajesh Khanna**

Department of Electronics and Communication Engineering, Thapar University, Patiala-147003,  
Punjab, India

\*Corresponding author, e-mail: surbhi.sharma@thapar.edu

*Received: 13 October 2010 / Accepted: 10 June 2011 / Published: 10 June 2011*

---

**Abstract:** Irregular low-density parity-check (LDPC) codes have been found to show exceptionally good performance for single antenna systems over a wide class of channels. In this paper, the performance of LDPC codes with multiple antenna systems is investigated in flat Rayleigh and Rician fading channels for different modulation schemes. The focus of attention is mainly on the concatenation of irregular LDPC codes with complex orthogonal space-time codes. Iterative decoding is carried out with a density evolution method that sets a threshold above which the code performs well. For the proposed concatenated system, the simulation results show that the QAM technique achieves a higher coding gain of 8.8 dB and 3.2 dB over the QPSK technique in Rician (LOS) and Rayleigh (NLOS) faded environments respectively.

**Keywords:** LDPC, STBC, modulation techniques, multipath fading environment

---

## INTRODUCTION

In recent years, error control codes have been revolutionised by the rediscovery of codes which are capable of approaching the theoretical limits of the Shannon's channel capacity. This has been impelled by discrete approaches to coding theory towards codes which are more closely tied to physical channel and soft decoding techniques. Coding theory is nearly ubiquitous in modern information society. From DVD to every phone call made with a digital cellular phone a coding technique is employed. Low-density parity-check (LDPC) codes are one of the codes which are fascinating researchers these days. From satellite communication to next-generation wireless communication systems including WiMaX, WLAN and UMTS, all are employing LDPC codes to achieve the upper limits of capacity and reduced bit error rates.

Multiple antenna systems have also attracted considerable interest for providing high data rate transmission in next-generation wireless communication systems. Reliable communication over fading channels is possible by exploiting the spatial diversity with the use of multiple transmitter or/and receiver antennas. This can be achieved by using spatial multiplexing or space-time codes. For space-time coding, Alamouti [1] introduced a simple transmitting scheme for two transmitter antennas, which achieves full diversity and has a fast ML decoding at the receiver. Motivated by Alamouti's scheme, Tarokh et al.[2] proposed a general coding scheme for any number of transmitter antennas, called orthogonal space-time block codes (OSTBC), which achieve full diversity with a fast ML decoding algorithm. In particular, the transmitted symbols can be decoded separately. Thus, the decoding complexity increases linearly rather than exponentially with the code size. There are two classes of space-time block codes from orthogonal designs. One class consists of codes from real orthogonal designs for real constellations such as pulse amplitude modulation (PAM). These codes are already well developed and have been utilised for the composition of quadratic forms. The other class consists of complex orthogonal designs for complex constellations such as quadrature amplitude modulation (QAM) and phase shift keying (PSK). Tarokh et al. [3] observed that it is not necessary for complex orthogonal designs to be square matrices since OSTBC allow non-square designs when the number of transmitter antennas ( $N_t$ ) is not equal to the number of receiver antennas ( $N_r$ ). Subsequently, they introduced the definition of generalised complex orthogonal designs and further introduced generalised complex orthogonal designs with linear processing. With these new definitions, there are space-time block codes from generalised complex orthogonal designs that can be used for any number of transmitter antennas. Research work of Su and Xia [4] presents a detailed discussion of space-time block codes from complex orthogonal designs for achieving high data rates using QAM signals in wireless communications. As space- time block codes provide substantial diversity gain and no coding gain, so there is a need for a concatenated channel coder along with a space-time coder. Among other channel codes, an LPDC code performs well near the Shannon capacity.

For single-antenna systems at the transmitter and receiver side, irregular LDPC codes [5-7] achieve better performance than other block codes for various fading channels. Kavcic et al. [8] derived a bound on Gallager codes using the density evolution method. Precisely in the additive white Gaussian noise (AWGN), reliable transmission was demonstrated [9] at low signal-to-noise ratios (SNR), and the transmission rate was extremely close to the Shannon channel limit. Extending the work to a single antenna at the transmitter and multiple receiver antennas is known as a single input multiple output (SIMO) system. Gounai and Ohtsuki [10] derived the SNR thresholds of regular/irregular LDPC codes for maximum-ratio combining (MRC), equal-gain combining (EGC) and selection combining (SC) schemes. All these combining techniques were evaluated without considering the presence of external interferers.

Sharma and Khanna [11] extended the work of SIMO systems in the presence of interferers using optimum combining. It was assumed that the desired signal and all interferers have equal power. The bit error rate has been evaluated for different values of signal to interference plus noise ratio (SINR). Currently efforts have been made to employ LDPC codes with a multiple transmitter and multiple receiver antenna system (known as a MIMO system). Lu et al. [12] used LDPC codes

as channel codes in a space-time orthogonal frequency division multiplexing (OFDM) system over correlated frequency- and time-selective fading channels. The performance of faded LDPC coded signal was simulated for different modulation techniques with MIMO systems. The work of Hou et al. [13] further proves the strength of properly designed LDPC codes across quasi-static and fast fading channels in MIMO systems. Gulati and Narayanan [14] demonstrated a significant improvement in performance by using LDPC codes of quasi-regular structure in space-time wireless transmission. With a relatively small number of transmitter antennas, LDPC codes of quasi-regular construction are able to achieve higher coding gain than previously proposed space-time trellis codes, turbo codes and convolution codes in quasi-static fading channels [15]. For the MIMO system concatenated with LDPC, no work comparing the performance of different modulation schemes in line-of-sight (LOS) and non-line-of-sight (NLOS) fading environments has been reported in the literature. Hence, in this paper the performance of concatenated LDPC codes and space-time block codes (STBC) (with complex orthogonal designs) on Rayleigh and Rician fading channels with M-ary phase shifting key (MPSK) and QAM techniques using Monte Carlo simulations is determined. The perfect channel state information (CSI) is assumed to be available on the receiver side. Evaluated results obtained through computer simulations when compared with the results of Lanxun and Weizhen [16] show that there is significant improvement in bit error rate (BER) even at a very low value of SNR.

The paper is organised as follows. Concatenation of LDPC-STBC, the focus of the paper, is discussed first. Next, the iterative decoding algorithm used to decode LDPC codes is considered. In the subsequent section, the results of the proposed system in various fading channels are presented and discussed. Then the results and discussion of various fadings are presented. Finally, the conclusions drawn are provided.

## CONCATENATED LDPC-STBC SYSTEM MODEL

The model considers a single-user system with  $N_t$  transmitter and  $N_r$  receiver antennas (where  $N_r \geq N_t$ ). The main focus is the performance evaluation of different modulation schemes using a base-band model of the system employing concatenated LDPC codes with density evolution methods and complex orthogonal space time block codes in various fading environments. The input to system is ‘ $K$ ’ uncoded bits that are mapped onto the LDPC coded bits of length ‘ $N$ ’ leading to ‘ $s$ ’ code words, and redundancy is given by  $M=N-K$ . The code rate is  $r = M/N$ . In the present work, irregular LDPC codes are considered. An irregular LDPC code consists of a parity check matrix  $H$  having a variable number of ‘1’s per row or per column. LDPC codes are designed by an appropriate construction of the corresponding parity check matrix  $H$  of size ( $M * N$ ) that is sparse in nature (the number of ‘1’s are very few in comparison to the number of ‘0’s for a given row), and is given by equation (1).

$$\mathbf{H} = [\mathbf{I}_{n-k} * \mathbf{P}^T] \quad (1)$$

where  $P$  is the parity sub-matrix,  $I_k$  is the identity sub-matrix of dimension ( $K \times K$ ) and  $(.)^T$  denotes the transpose. In the parity check matrix  $H$ , the number of variable nodes ‘ $N$ ’ corresponds to the

columns of  $H$ , and the number of check nodes ‘ $M$ ’ correspond to the rows of  $H$ . It is possible to associate  $H$  with a bipartite graph in one-to-one correspondence. Such a graph contains two kinds of nodes: variable node  $d_v$ , (associated with a column of  $H$ ) and check node  $d_c$  (associated with a row of  $H$ ). The encoded message is then sent to a space-time block coder where the encoded bit stream is converted into an OSTBC code matrix ‘ $X$ ’ of size  $(N_t \times N_r)$ . For example, an OSTBC code matrix  $U$  of size  $(3 \times 8)$  can be defined as follows [3]:

$$U = \begin{bmatrix} \mathbf{s}_1 & -\mathbf{s}_2 & -\mathbf{s}_3 & -\mathbf{s}_4 & \mathbf{s}_1^* & -\mathbf{s}_2^* & -\mathbf{s}_3^* & -\mathbf{s}_4^* \\ \mathbf{s}_2 & \mathbf{s}_1 & \mathbf{s}_4 & -\mathbf{s}_3 & \mathbf{s}_2^* & \mathbf{s}_1^* & -\mathbf{s}_4^* & -\mathbf{s}_3^* \\ \mathbf{s}_3 & -\mathbf{s}_4 & \mathbf{s}_1 & \mathbf{s}_2 & \mathbf{s}_3^* & -\mathbf{s}_4^* & \mathbf{s}_1^* & \mathbf{s}_2^* \end{bmatrix} \quad (2)$$

The ST encoder output is sent through a frequency flat channel with channel matrix  $H_c$  of size  $N_r \times N_t$ . The  $H_c$  is a complex Gaussian random matrix having independent and identically distributed entries. The output of the channel is faded and polluted by additive white Gaussian noise, which is assumed to be independent of all receiving antenna elements. On the receiver side, the received signal is first fed to a space-time block decoder. Thus the input-output state of the concatenated LDPC-STBC system is defined as:

$$\mathbf{y} = \mathbf{H}_{C \text{ } N_r N_t} \mathbf{s} + \mathbf{n} \quad (3)$$

where  $y$  is the received vector of size  $(N_r \times 1)$ ,  $s$  is the transmitted vector of size  $(N_t \times 1)$  and  $n$  is the additive white Gaussian noise vector of size  $(N_r \times 1)$ . The output of the STBC decoder is fed into the LDPC decoder, which decodes the signal using the following steps.

## LDPC DECODING

The decoding algorithm of LDPC codes is first specified in the probability domain and then the results are projected in the log-likelihood ratio (LLR) domain. Decoding of the low-density parity check codes traces the following steps:

1. Compute all the reliability values input to variable node.

First, the variable-node degree distribution,  $\lambda(x)$ , and the check-node degree distribution,  $\rho(x)$ , used to update the corresponding nodes of bipartite graph are found [17]. For a given graph with  $l$  branches, with the corresponding parity check matrix having  $l$  non-zero entries, the number of variable nodes ‘ $N$ ’ is given by:

$$N = l \sum_i \frac{\lambda_i}{i} = l \int_0^1 \lambda(x) dx \quad (4)$$

Similarly, the number of check nodes ‘ $M$ ’ is given by:

$$M = l \sum_j \frac{\rho_j}{j} = l \int_0^1 \rho(x) dx \quad (5)$$

2. Compute the LLR for each node by using a posteriori probability values.

To project the results in the LLR domain, let a binary random variable ‘x’ (having values in the set {0,1}) specified in the probability domain be given as

$$\lambda = (\lambda_1, \lambda_2, \dots, \lambda_{dv}) = \frac{P(x=0/\zeta_1, \dots, \zeta_{dv})}{P(x=1/\zeta_1, \dots, \zeta_{dv})}$$

where  $\zeta$  is the independent observation regarding the bit. The corresponding log-likelihood ratio ( $\Lambda$ ) is given as [18]:

$$\Lambda = \log(\lambda) \quad (6)$$

3. Compute the variable node output message and transfer the message to check node.

After calculating the LLR given in equation (6), the number of variable nodes can be calculated using equation (5). The output message at a given variable node ‘v’ of degree ‘j’ that is passed to the check node ‘c’ of degree ‘i’ is the summation of initial message  $m_0$  (the sample from channel or that corresponding to a priori information on the corresponding bit) and the input messages coming from ‘i’ check nodes connected to variable node v. (Initially the entire message coming from the check node is set to zero and after the first iteration, all messages coming at the variable node from the check node are considered independent.) Thus the  $j^{\text{th}}$  output message of a given variable node as shown in Figure 1 is given as

$$m_j^v = m_0 + \sum_{i=1}^{dv-1} m_i^v \quad (7)$$

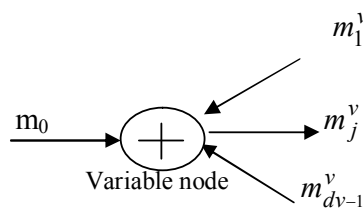


**Figure 1.** Variable node computation

The output message computed from Eq. (7) is transferred to the check node ‘c’. The  $j^{\text{th}}$  output message at the check node is given by Eq. (8) and the equivalent representation is shown in Figure 2 [19].

$$m_j^c = 2 \tanh^{-1} \prod_{i=1}^{dc-1} \tanh \frac{m_i^c}{2} \quad (8)$$

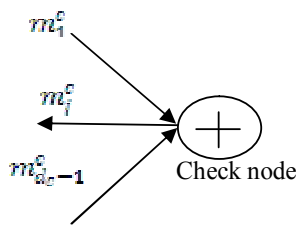


**Figure 2.** Check node computation

The computed check-node message form Eq. (8) is now transferred to the variable nodes.

#### 4. Compute the final reliability value.

At the end of the decoding process each variable node computes an output reliability value as follows:

$$m^v = m_0 + \sum_{i=1}^{dv-1} m_i^v \quad (9)$$

In other words, the output reliability value of a code word bit is the sum of all messages directed towards the corresponding variable node.

## RESULTS AND DISCUSSION

The results of the simulations have been obtained for the concatenated STBC-LDPC coding with two transmitter and three receiver antennas. In this paper we have considered transmission over Rayleigh flat fading and Rician fading channels. For Rician fading channel the Rician factors are considered as K=1 and 4. The channels are modelled as complex Gaussian distributions with a mean ‘m’ and covariance matrix R. In Rayleigh faded channels m=0, and for Rician faded channels the mean ‘m’ is the sum of the power in the line-of-sight and the local-mean scattered power. For both Rayleigh as well as Rician faded environments, R=I. The noise considered as additive is modelled as a circular symmetric complex Gaussian random variable with mean 0 and variance 1. In this paper a (180,360) irregular LDPC with a mean column weight of 3 has been employed. A frame consisting of 360 coded bits is sent from the LDPC encoder with all the bits with random values 0 and 1, which are then fed into the space-time block encoder. The results have been obtained from 1000 independent iterations of each frame, for each value of SNR varying from -10 to 20dB. Figure 3(a) shows the plot of the bit error rate (BER) for MPSK and QAM modulation schemes in Rayleigh and Rician faded environments. A more expanded view of Figure 3(a) is shown in Figure 3(b). From these figures it can be observed that for a BER of  $5 \times 10^{-1}$ , QPSK requires an SNR of 13.8 dB and QAM requires an SNR of 3.2 dB. QAM provides 8.8 dB coding gain over QPSK in a Rayleigh faded environment.

Similarly in a Rician faded environment for the same BER, QPSK and QAM require SNR of -2 dB and -5.2 dB respectively, providing a coding gain of 3.2 dB by using QAM over QPSK. The input SNR required for various constellations of PSK and QAM modulations at a BER of  $5 \times 10^{-1}$  is given in Table 1.

**Table 1.** SNR results for different modulation techniques at  $\text{BER} = 5 \times 10^{-1}$  in NLOS and LOS environments

Modulation scheme	SNR required in dB at BER of $5 \times 10^{-1}$	
	Rayleigh fading	Rician fading( $K=1$ )
QAM	-0.9	-5.2
BPSK	14	-3
QPSK	13.8	-2
8-PSK	>20	14.1
16-PSK	>21	20

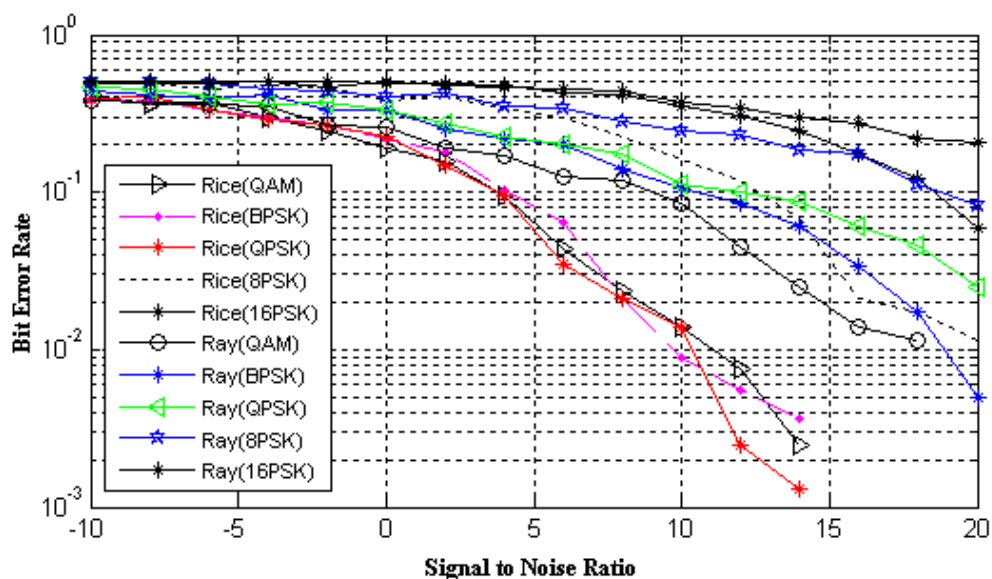


**Figure 3(a).** BER of concatenated STBC-LDPC scheme in Rayleigh and Rician fading with different modulation schemes

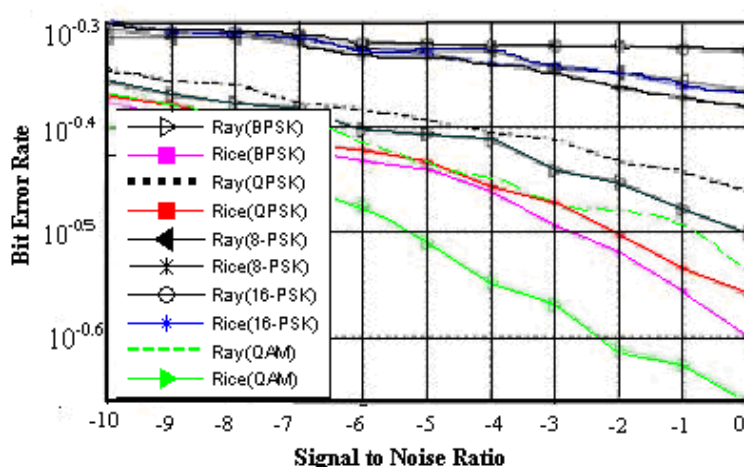


**Figure 3 (b).** An expanded view of Figure 3(a) in which a variation is shown for the lower value of SNR

Figure 4 provides a comparison of BER for various modulation schemes in a Rician fading environment for a varying Rice factor K ( $K = 1$  and  $4$ ). For a bit error rate of  $5 \times 10^{-1}$ , it is found that QAM outperforms the other modulation schemes in a Rician faded environment with  $K=1$ . A more comprehensible view of Figure 4(a) is shown in Figure 4(b), where it can be observed that QAM requires nearly half the power to achieve the same bit error rate when compared with the QPSK scheme despite having the same constellation size. Table 2 shows the SNR required by various modulation techniques to achieve a BER of  $5 \times 10^{-1}$  in a Rician faded environment. It illustrates that for the same BER, the QAM technique requires minimum power and a 16-psk signal requires maximum power. Figure 5 shows a normalised view of the BER of a concatenated LDPC-STBC scheme in Rayleigh and Rician faded environments.

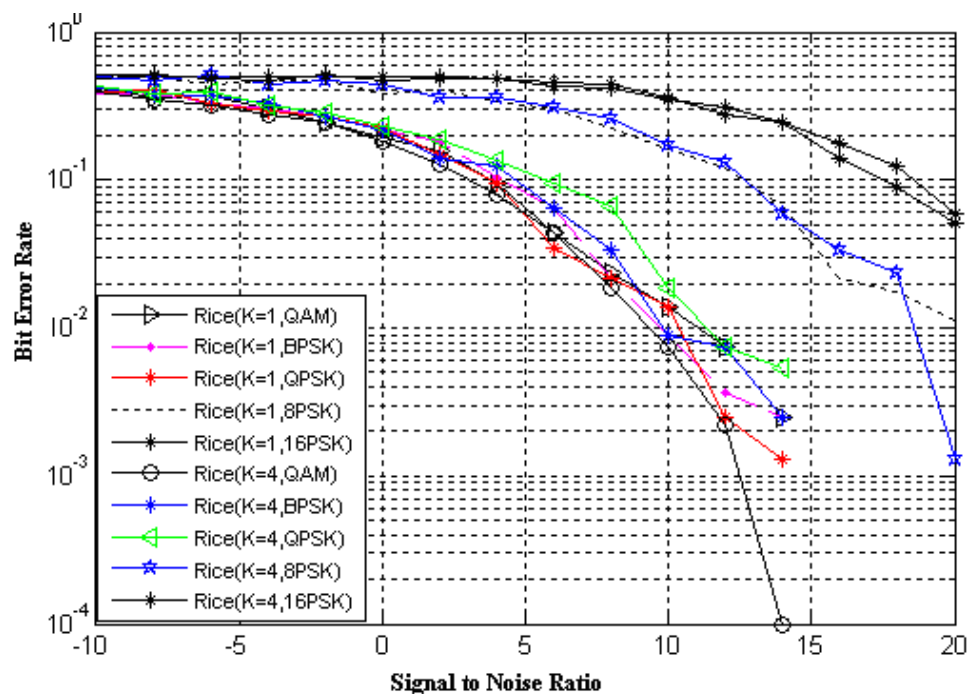


**Figure 4 (a).** BER of concatenated STBC-LDPC scheme in Rician fading with  $K=1, 2$

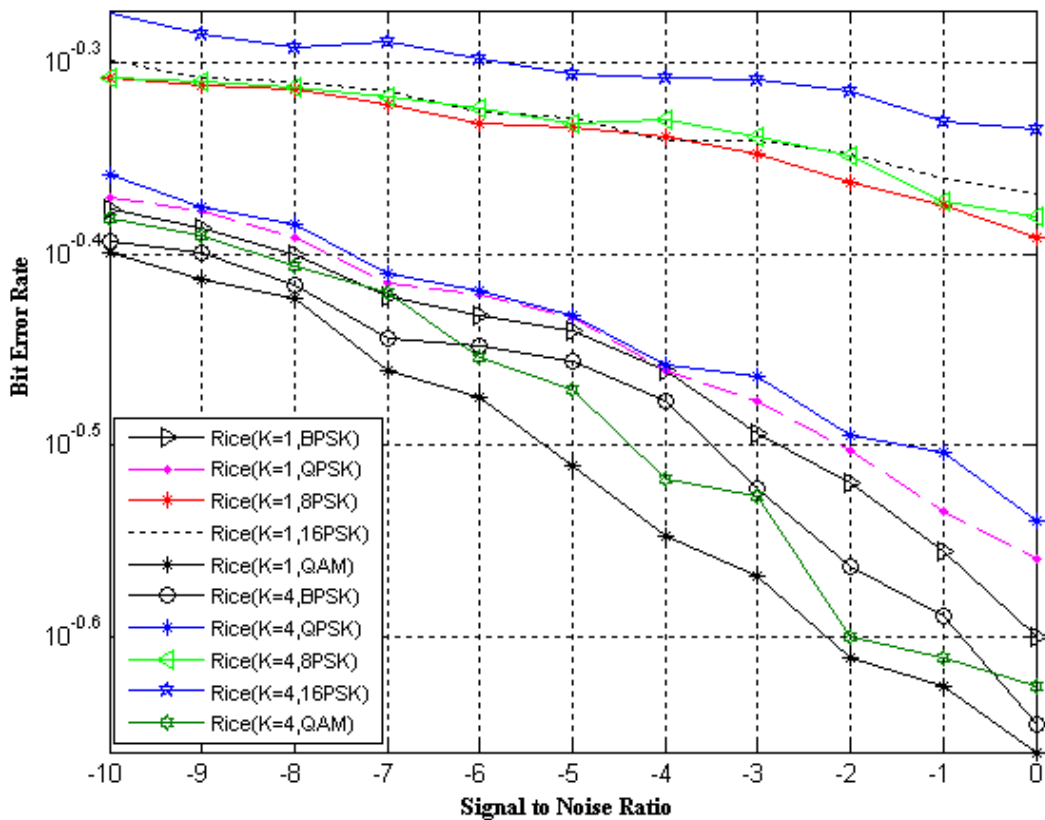


**Figure 4 (b).** A more comprehensive view of Figure 4(a) in which a variation is shown for lower values of SNR

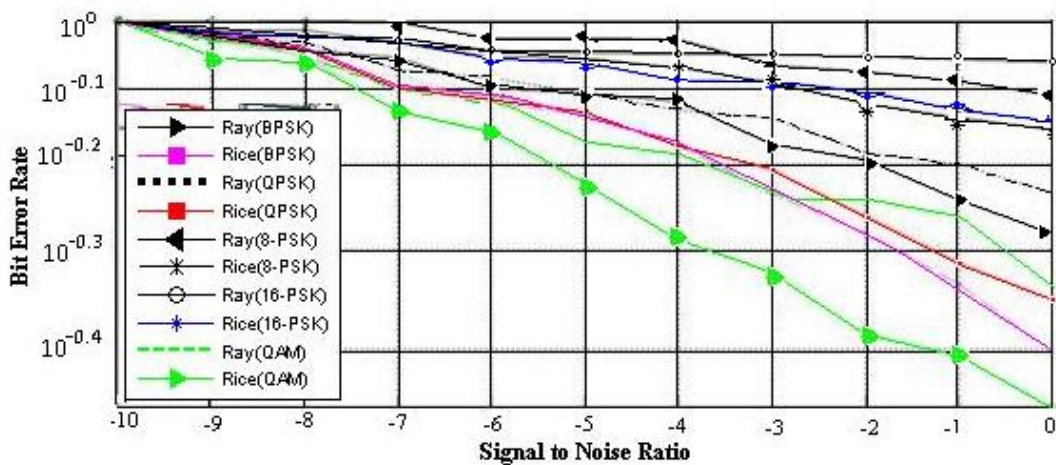


**Figure 5.** Normalised BER of concatenated STBC-LDPC scheme in Rayleigh-Rician fading

**Table 2.** SNR results for different modulation techniques at BER = $5 \times 10^{-1}$  in an LOS environment

Modulation scheme	SNR required in dB at BER of $5 \times 10^{-1}$	
	Rician fading (K=1)	Rician fading (K=4)
QAM	4.7	4.8
BPSK	6.1	6.2
QPSK	5.2	8.1
8-PSK	14	14.2
16-PSK	19.5	20

## CONCLUSIONS

The bit error rate performance of concatenated irregular LDPC codes has been evaluated in flat Rayleigh and Rician faded environments. Simulation results show that the quadrature amplitude modulation (QAM) technique with LDPC codes and complex orthogonal space-time block codes is able to achieve higher coding than QPSK modulation technique in all fading environments.

## ACKNOWLEDGEMENTS

The work is supported by UGC and AICTE India vide letter no. 31-1(PUN)(SR) 2008 TU and letter no. 8023/BOR/RID/RPS-105/2008-09.

## REFERENCES

1. S. M. Alamouti, "A simple transmit diversity technique for wireless communications", *IEEE J. Sel. Areas Commun.*, **1998**, 16, 1451-1458.
2. V. Tarokh, N. Seshadri and A. R. Calderbank, "Space-time codes for high data rate wireless communication: Performance criterion and code construction", *IEEE Trans. Inf. Theory*, **1998**, 44, 744-765.
3. V. Tarokh, H. Jafarkhani and A. R. Calderbank, "Space-time block codes from orthogonal designs", *IEEE Trans. Inf. Theory*, **1999**, 45, 1456-1467.
4. W. Su and X.-G. Xia, "On Space-time block codes from complex orthogonal designs", *Wireless Person. Commun.*, **2003**, 25, 1-26.
5. T. J. Richardson, M. A. Shokrollahi and R. L. Urbanke, "Design of capacity-approaching irregular low-density parity check codes", *IEEE Trans. Inf. Theory*, **2001**, 47, 619-637.
6. S.-Y. Chung, T. J. Richardson and R. L. Urbanke, "Analysis of sum-product decoding of low-density parity-check codes using a Gaussian approximation", *IEEE Trans. Inf. Theory*, **2001**, 47, 657-670.
7. O. Alamri, S. X. Ng, F. Guo, S. Zummo and L. Hanzo, "Nonbinary LDPC-coded sphere-packed transmit diversity", *IEEE Trans. Veh. Technol.*, **2008**, 57, 3200-3205.
8. A. Kavcic, X. Ma and M. Mitzenmacher, "Binary intersymbol interference channels: Gallager codes, density evolution, and code performance bounds". *IEEE Trans. Inf. Theory*, **2003**, 49, 1636-1652.

9. S.-Y. Chung, G. D. Forney Jr., T. J. Richardson and R. Urbanke, "On the design of low-density parity-check codes within 0.0045 dB of the Shannon limit", *IEEE Commun. Lett.*, **2001**, 5, 58-60.
10. S. Gounai and T. Ohtsuki, "Performance analysis of LDPC code with spatial diversity", Proceedings of IEEE 64<sup>th</sup> Vehicular Technology Conference, **2006**, Montreal, Quebec, pp.1-5.
11. S. Sharma and R. Khanna, "Analysis of LDPC with optimum combining", *Int. J. Electron.*, **2009**, 96, 803-811.
12. B. Lu, X. Wang and R. N. Krishna, "LDPC-based space-time coded OFDM systems over correlated fading channels performance: Analysis and receiver design", *IEEE Trans . Commun.*, **2002**, 50, 74-88.
13. J. Hou, P. H. Siegel, L. B. Milstein and H. D. Pfister, "Capacity-approaching bandwidth-efficient coded modulation schemes based on low-density parity-check codes", *IEEE Trans. Inf. Theory*, **2003**, 49, 2141-2155.
14. V. Gulati and K. R. Narayanan, "Concatenated space-time codes for quasi-static fading channels: Constrained capacity and code design", Proceedings of IEEE Global Telecommunication Conference, **2002**, Taipei, Taiwan, pp.1202-1206.
15. G. Li, I. J. Fair and W. A. Krzymien "Low-density parity-check codes for space-time wireless transmission", *IEEE Trans. Wireless Commun.*, **2006**, 5, 312-322.
16. W. Lanxun and L. Weizhen, "Quasi-orthogonal space time block codes (STBC) with full transmit rate concatenated LDPC codes", Proceedings of the 8<sup>th</sup> International Conference on Electronic Measurement and Instruments, **2007**, Xian, China, pp.3207-3210.
17. T. K. Moon, "Error Correction Coding: Mathematical Methods and Algorithms", Wiley-Interscience, London, **2005**, pp.641-648.
18. T. Richardson and R. Urbanke, "Modern Coding Theory", Cambridge University Press, Cambridge, **2008**, pp.459-464.
19. R. Gallager, "Low-density parity-check codes", *IRE Trans. Inf. Theory*, **1962**, 8, 21-28.

© 2011 by Maejo University, San Sai, Chiang Mai, 50290 Thailand. Reproduction is permitted for non-commercial purposes.

*Full Paper*

## **Agentless robust load sharing strategy for utilising heterogeneous resources over wide area network**

**Natthakrit Sanguandikul\* and Natawut Nupairoj**

Department of Computer Engineering, Chulalongkorn University, Bangkok 10110, Thailand

\* Corresponding author, e-mail: ramza\_th@hotmail.com

*Received: 2 November 2010 / Accepted: 20 June 2011 / Published: 22 June 2011*

---

**Abstract:** Resource monitoring and performance prediction services have always been regarded as important keys to improving the performance of load sharing strategy. However, the traditional methodologies usually require specific performance information, which can only be collected by installing proprietary agents on all participating resources. This requirement of implementing a single unified monitoring service may not be feasible because of the differences in the underlying systems and organisation policies. To address this problem, we define a new load sharing strategy which bases the load decision on a simple performance estimation that can be measured easily at the coordinator node. Our proposed strategy relies on a stage-based dynamic task allocation to handle the imprecision of our performance estimation and to correct load distribution on-the-fly. The simulation results showed that the performance of our strategy is comparable or better than traditional strategies, especially when the performance information from the monitoring service is not accurate.

**Keywords:** load sharing strategies, self-scheduling strategies, high performance computing, distributed systems, heterogeneous systems, load balancing, task assignment

---

### **INTRODUCTION**

For the past decades, there has been an emergence of the technologies for utilising a large number of computing resources over wide area network such as grid [1] and cloud computing [2]. A low-cost, high-performance system for computing-intensive applications [3] can be built by aggregating multiple computing clusters which may consist of either real physical resources or virtualised resources from external providers. Hence, the number of computing nodes and the complexity of the underlying system have been dramatically increased. In order to efficiently utilise

the available computing power, several resource monitoring frameworks and performance prediction methodologies have been proposed [4-7]. Although accurate performance prediction can greatly improve overall resource utilisation, these methodologies usually require a proprietary monitoring service to be implemented on all participating resources for collecting specific performance information. Hence, this requirement of implementing proprietary monitoring service might prevent the utilisation of cheaper or better computing resources due to the differences in their implemented systems or policies. In addition, predicting the execution time of a fine-grained task can be difficult on non-dedicated computing resources [8]. These limitations will hinder the possible applications in the upcoming computing technology such as those described in many-task computing (MTC) [9] where each job can consist of a large number of tasks which can be executed within a small computational time.

To address the problems in the traditional work, we propose a new load sharing strategy called agentless robust self-scheduling strategy (ARSS). As its name implies, our strategy can be used to assign the workload without the necessity of implementing any additional monitoring service in the computing resources while still being able to address the dynamic behaviour in the computing system. ARSS is based on self-scheduling strategies [10-11] and makes load decision according to performance metrics estimated at the coordinator node. The metrics used in our strategy are simple ones that represent how fast each computing resource can process the submitted workloads. Since these metrics can be obtained quickly and easily at the coordinator node which is responsible for assigning the workload, ARSS can use these estimations to make the load decision across different computing systems without any need to implement monitoring services in the participating resources. To compensate for the imprecision of these rough metrics, ARSS performs a dynamic task allocation to adjust the load distribution on-the-fly. The dynamic allocation is stage-based, consisting of both increasing and decreasing stages. The increasing stages are for improving the performance estimation accuracy while minimising the run-time by overlapping between computation and communication overheads over the wide area network (WAN). The decreasing stages are for smoothing the load imbalance near the end of the execution due to an inaccurate performance prediction. In addition, ARSS also includes an on-the-fly load distribution correction mechanism which performs the job-stealing on the leftover workload between stages in order to further minimise the effects of abrupt changes in computing power and of the performance estimation inaccuracy. Using this mechanism, ARSS does not require any agents installed on the participating resources while being very robust against the changes in the available computing power of the underlying system.

## **RELATED BACKGROUND AND ASSUMPTIONS**

In this section, we will describe the multi-organisational computing environment including the application model and other related work in the past.

## Multi-Organisational Computing Environment

Throughout this work, we assume that a computing system consists of several heterogeneous computing resources from different organisations. Let us assume that there are a total of  $N$  computing nodes aggregated from different  $M$  groups or clusters  $\{C_1, C_2 \dots C_M\}$ . These computing clusters communicate with each other over WAN with a propagation delay and bandwidth specified as  $\alpha_w$  and  $\beta_w$  respectively. The propagation delay and bandwidth within each cluster are defined to be  $\alpha_L$  and  $\beta_L$  respectively. The computing heterogeneity within our model will come from differences in the computing power between participating clusters while the computing nodes within the same cluster are homogeneous as illustrated by Chau and Fu [12]. Each cluster is assumed to have one local gateway which is responsible for distributing workloads submitted by users to the computing nodes within its own cluster based on local workload assignment strategy and which also handles the inter-cluster communications. In addition, one of the local gateways will also serve as the coordinator node which manages submitted jobs and assigns workloads to other clusters based on the global workload assignment strategy. Note that the local strategy can be varied depending on the owner of that particular cluster. Figure 1 illustrates an example of the multi-organisational computing system which involves multiple clusters from different organisations.

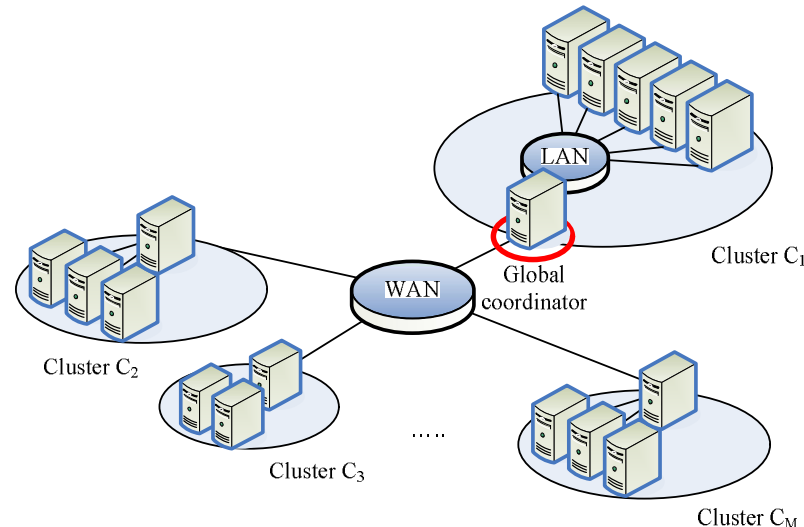


**Figure 1.** Multi-organisational computing environment

## Application Model

We define our application model to represent computing intensive applications including those from many-task computing. This class of application contains a large number of small tasks which can be from thousands to billions. This common pattern can be found in many scientific applications from a wide range of domains such as astronomy, physics, astrophysics, pharmaceuticals, bioinformatics, biometrics, neuroscience, medical imaging, chemistry, climate modelling, economics and data analytics [13]. This amount of tasks will cause the performance

degradation to time-consuming decision-making strategies due to high queuing and dispatching overheads. Since the expected run-time of small tasks is difficult to predict, the problem of inaccurate prediction will also affect the overall performance. Although we can group small tasks together to address this problem, this methodology will make it even harder to make the load decision given heterogeneous computing resources.

Our work focuses on fine-grained computationally intensive applications where the data sets are not large or have been prepared beforehand. Each task within a submitted application can be either independent or dependent on other tasks. If there are dependency between tasks, we assume each task can retrieve necessary information from the result files created by previously executed tasks similar to loosely-coupled applications defined by Zhang et al [14]. Hence, we define an application model consisting of  $U$  unit tasks whose computation and communication sizes vary. The distribution of computation sizes of unit tasks can be grouped into four distinct classes, viz. uniform, increasing, decreasing, and random distributions. These classes can represent popular applications, e.g. Matrix Multiplication, Successive Over-Relaxation, Reverse Adjoint Convolution, LU Decomposition and Gauss Jordan Elimination [15].

## Related Work

The self-scheduling strategy (SS) has been famous for its simplicity for making load decision during the execution. This strategy dynamically assigns only one unit task for each request for an idle computing resource. With this behaviour, it can achieve an almost perfect load balancing because every computing resource will finish within one task of each other. However, this strategy suffers from high communication overheads. To address this problem while maintaining simplicity, many variations of SS have been proposed [16-19]. One of them, called ‘factoring self-scheduling’ (FSS), is famous for its robustness [20]. This strategy assigns a workload into multiple stages. In the first stage, FSS distributes the largest chunk and proportionally decreases the chunk size in the subsequent stages. During each stage, every processor will receive an equal chunk size of workload. The FSS can reduce communication overheads by sending large chunks at the beginning while achieving sub-optimal run-time by sending small chunks near the end of computation.

To further address heterogeneity within the computing system, ‘weighted factoring self-scheduling’ (WFSS) [21] was proposed as an extension of FSS. In this strategy, the amount of total unit tasks allocated during each stage is the same as in FSS. However, unlike FSS, WFSS utilises pre-execution information of the computing resources as weighted values to assign workloads allocated within each stage. One of the major weaknesses of this strategy is that the load decision is made based on static information. Thus, WFSS performs quite poorly in the dynamic multi-organisational computing environment.

One of the descendants of FSS, called ‘adaptive weighted factoring’ (AWF) [22], addresses this problem by extending WFSS with an adaptive weighted value called ‘weighted average performance’ (WAP). This weighted value is re-calculated at every stage using the newly obtained computing rates of each resource. Therefore, the pre-execution information will be used as a weighted value during the first stage only. With this average value, AWF can address the dynamic behaviour of the heterogeneous computing system. However, since AWF assigns half of the available

workloads during the first stage, the problem of inaccurate pre-execution information can still affect the performance of this strategy.

In addition to SS, our proposed strategy is also based on the concept of increasing and decreasing stages. Utilising increasing and decreasing stages has been introduced in one of the traditional strategies [23]. However, that strategy requires specific information about the underlying system for determining the appropriate chunk sizes during the increasing and decreasing stages. Hence, it needs the monitoring service to be installed on the participating resources and its performance can also be highly affected by information inaccuracy. Although the load sharing strategy that focuses on practical usage [24] addresses inaccurate performance information by assigning the  $N$  smallest tasks to each node in order to compare their real performance, this behaviour requires the knowledge about the computation size of each task for creating the performance ranking of the computing resources.

### Description of ARSS

Our proposed strategy aims for two important goals. First, the strategy must be non-intrusive such that it can assign the workload to participating resources using performance estimation at the coordinator node without relying on any monitoring services at the computing nodes. Second, the strategy must be robust enough against information inaccuracy due to the performance estimation and dynamic behaviour of the underlying system. In order to achieve these goals, our proposed strategy divides the entire unit tasks and assigns them in multiple stages. At each stage, the allocated unit tasks for that particular stage will be further divided into chunks and assigned to participating clusters with respect to their performance. ARSS will begin with the increasing stages and end with the decreasing stages. The increasing stages will allow ARSS to overlap communication overheads over WAN with computation overheads and to also collect more accurate performance metrics of the participating clusters, while the decreasing stages will ensure the robustness against both the information inaccuracy and the dynamic behaviour of the underlying system. Equation 1 illustrates how our strategy calculates the amount of unit tasks allocated for stage  $j$  ( $S_j$ ) where  $U$  is the total number of unit tasks and  $j$  starts from 1 until it reaches the last stage, which is  $2(\log_2 U - 1)$ . An example of how ARSS assigns 8,192 unit tasks for each stage is shown in Figure 2.

$$S_j = \begin{cases} \left\lceil \frac{U}{2^{(\log_2 U - j + 1)}} \right\rceil & j \leq \log_2 U - 1 \\ \left\lceil \frac{U}{2^{(j+2-\log_2 U)}} \right\rceil & \text{otherwise} \end{cases} \quad (1)$$

During each stage, the coordinator node will assign tasks to participating clusters and estimate their performance based on the number of assigned tasks and the interval time between requests. Since this information is derived based on the interval time between requests, the coordinator node does not have these metrics at the beginning of the execution. Thus, the coordinator node will assign an equal number of unit tasks to all clusters at the first stage. In the

subsequent stages, ARSS will dynamically adjust the assigned tasks based on the pre-defined number of tasks in each stage and the relative performance of the computing resources.

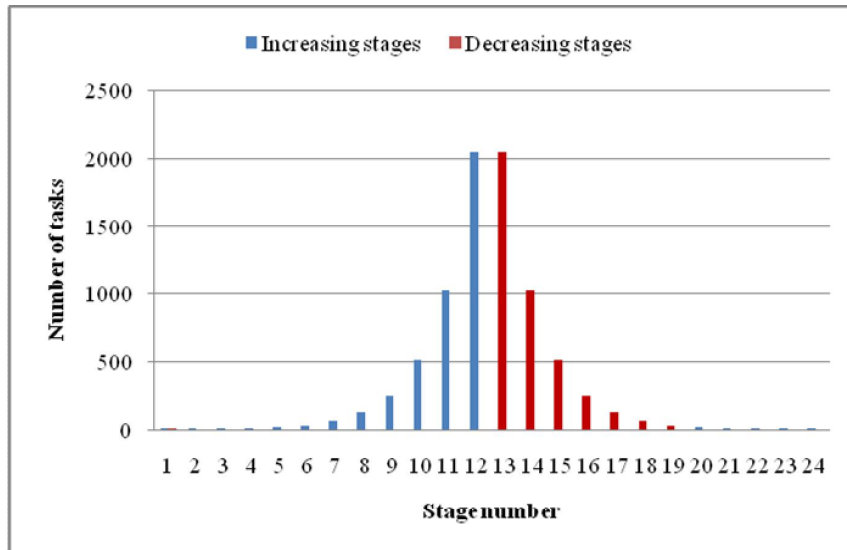


**Figure 2.** Number of unit tasks allocated within each stage

Let  $R_{i,j}$  represent the number of tasks executed per second by cluster  $i$  during stage  $j$ . In an ideal case, all resources will finish their execution of all assigned tasks of stage  $j$  at the same time before entering the next stage,  $j+1$ . However, because  $R_{i,j}$  is an estimation at the coordinator node, it can be inaccurate. Thus, while some clusters may complete the execution of stage  $j$  and be ready to move further to stage  $j+1$ , other clusters may still be in the middle of the execution of stage  $j$ . This behaviour will create a load imbalance and can degrade the overall execution time. To address this problem, our strategy performs a job-stealing mechanism called “stage-warping”. By including the leftover tasks of the previous stage when allocating tasks for the next stage, this technique will make sure that every cluster will progress through each stage at the same pace until the end of the execution. Given  $L_{j-1}$  as the number of leftover tasks from the previous stages  $j-1$ , the number of tasks assigned to cluster  $i$  during the current stage  $j$  ( $A_{i,j}$ ) can be specified as

$$A_{i,j} = \frac{R_{i,j-1}}{\sum_{k=1}^M R_{k,j-1}} (L_{j-1} + S_j) \quad (2)$$

From equation 2, we can see that the leftover workload in the previous stage  $j-1$  will be reassigned together with other tasks allocated for the current stage  $j$ . In other words, this behaviour will allow other computing resources to steal the workload from computing resources which have been slower than expected due to the estimation error of our performance metrics.

## RESULTS AND DISCUSSION

### Simulation Environment for Performance Evaluation

The performance of our strategy was evaluated by creating a large-scale computing system using ns-2 simulator [25]. To ensure the validity of our simulation experiments, we compared the results with those from the actual computing environments, i.e. TERA and PLUTO clusters in Thaigrid [26]. TERA cluster belongs to Kasetsart University while PLUTO cluster belongs to Chulalongkorn University. Table 1 presents the parameters for our simulations collected from the actual environment. Note that the unit time represents the computation time for one computing node in each cluster to execute one row multiplication of the submitted matrix multiplication program. Using parameters from real environments, we simulated the SS strategy in our simulator and compared the results of using the strategy on the TERA and PLUTO clusters as presented in Figure 3. The obtained results clearly show that our model can accurately predict the parallel performance of computationally intensive application over the computing clusters.

**Table 1.** Simulation parameters for evaluating the accuracy of the test environment

Variable	Value
Unit time (TERA)	0.083s
Unit time (PLUTO)	0.117s
Number of unit tasks	2000
LAN propagation delay	30µs
LAN bandwidth	1000Mbps

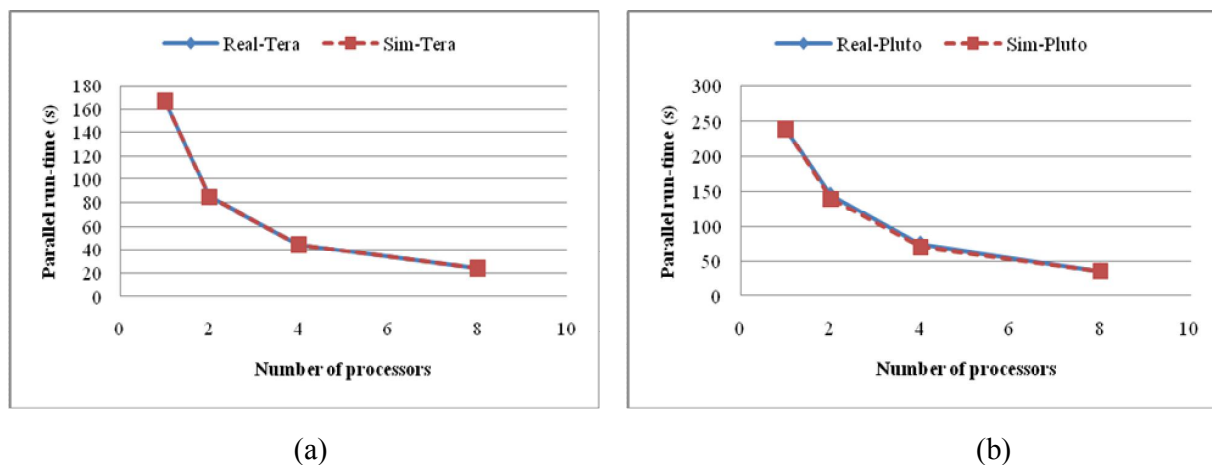


**Figure 3.** Comparison between real and simulated environments: a) TERA; b) PLUTO

Since this work focuses on the global strategy, the local strategy in all clusters is defined as SS. We define a uniformly distributed random variable to represent the actual computing power within each node to simulate the randomness of the available computing power as proposed by Casanova [27]. The specified computing power was varied within  $\pm 30\%$  from the expected value.

The computing heterogeneity was simulated by changing the expected value of the computing power. Let  $H$  represent the computing heterogeneity, which is the computing ratio between the fastest and slowest clusters in the system ( $p_{fastest} / p_{slowest}$ ) [28]. Unless specified otherwise, the environment in our simulation is assumed to be highly heterogeneous where  $H$  is specified as 10 [29]. We assume that it takes 1 second to execute a task whose computation size is 1 task unit on the computing resource with computing power specified as 1 power unit. As for the prediction error from the monitoring service, a uniform distribution random variable is used to represent the prediction error. The range of the prediction error is defined to be  $\pm 30\%$ . The other related parameters for simulating a large-scale multi-organisational computing environment are summarised in Table 2.

**Table 2.** Related parameters for simulating multiple-cluster environments

Variable	Value
Number of clusters ( $M$ )	4
Total computing nodes ( $N$ )	128
Total computing power ( $P$ )	128
Inter-cluster propagation delay ( $\alpha_w$ )	30ms
Inter-cluster bandwidth ( $\beta_w$ )	2Mb/s
Intra-cluster propagation delay ( $\alpha_L$ )	1ms
Intra-cluster bandwidth ( $\beta_L$ )	100Mb/s
Number of tasks ( $U$ )	16,384
Total computation size ( $W$ )	16,384
Total communication size ( $V$ )	16,384 kB

### Overall Performance Comparison

To evaluate the performance of load sharing strategies, the ARSS and four other load sharing strategies, namely chunk self-scheduling (CSS), one-time, WFSS and AWF, were simulated on two different computing environments, i.e. homogeneous and highly heterogeneous environments. In our simulation, CSS always assigned a fixed-size chunk of eight unit tasks to the requesting cluster. For one-time strategy, the entire workload was proportionally assigned all at once to participating resources with respect to the performance information obtained from the monitoring service. Finally, the performance of the predecessor of AWF, which is WFSS, was also evaluated. Unlike AWF, WFSS uses only the estimators obtained from the monitoring service for distributing the workload at every stage.

As illustrated in Figure 4, all strategies performed better in a homogeneous environment. The parallel run-times of CSS suffered from large communication overheads and load imbalance, especially when the underlying system was highly heterogeneous. Although we could reduce the communication overheads by assigning the workload within only one round, the performance of the

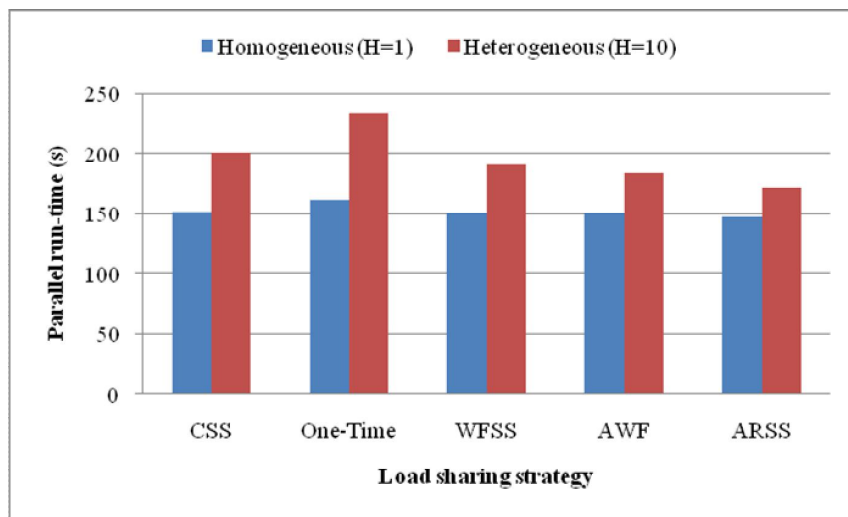


**Figure 4.** Parallel run-times over two different environments

one-time strategy was the worst on both systems because of an excessive load imbalance due to inaccurate information. WFSS and AWF performed equally well in a homogeneous system. However, AWF outperformed WFSS in a highly heterogeneous system because of its ability to adjust weight values for making load decision during the execution. Finally, ARSS performed as well as WFSS and AWF over a homogeneous system although it had to spend additional time during the increasing stages for obtaining accurate performance metrics. With exponentially increasing and decreasing task allocation during the increasing and decreasing stages, ARSS did not suffer from large communication overheads like CSS. The prediction error from the monitoring service did not affect the performance of ARSS because it used its own simple performance metrics calculated during the execution. Therefore, ARSS achieved the best parallel run-time over a highly heterogeneous system, given inaccurate performance information from the monitoring service.

#### Effect of Information Inaccuracy from Monitoring Services

The behaviour of the traditional strategies which rely on performance information from the monitoring service was evaluated. As mentioned earlier, we modelled the prediction errors as upper- and lower-bound percentages of the uniformly distributed random variable.

In Figure 5, it is quite obvious that AWF performs best when the estimated value is accurate (zero prediction error). As the prediction error increases, AWF will perform worse. The reason behind this behaviour is the characteristic of AWF. Since AWF assigns half of the available workload during the first stage, the problem of inaccurate information given a large prediction error can affect the performance of this strategy despite its effort to adjust the accuracy of the weighted values during the execution in the subsequent stages. On the contrary, the prediction error from the monitoring service does not affect the performance of our strategy. This is due to the fact that ARSS relies only on its simple performance metrics obtained by the coordinator node during the execution instead of using the values measured by the monitoring services.

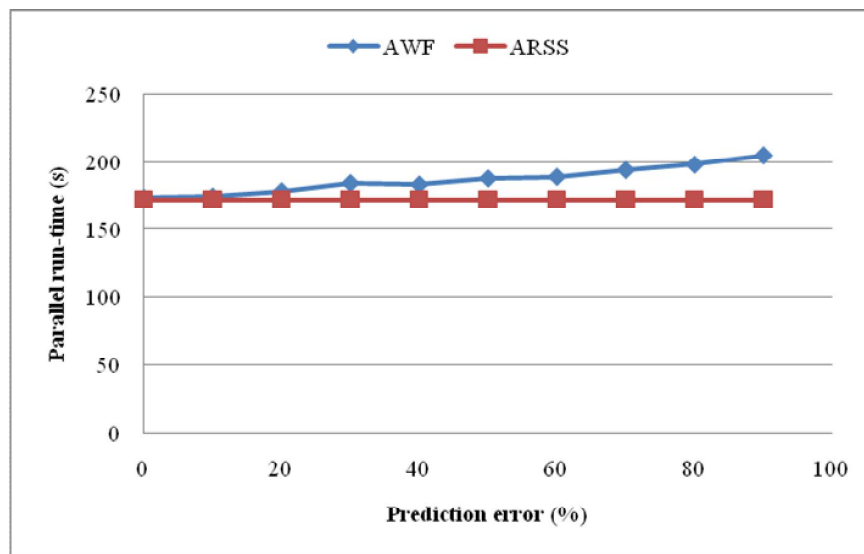


**Figure 5.** Parallel run-times with different prediction errors from monitoring service

### Effect of Computing Heterogeneity

The differences in the computing power between participating clusters can increase the risk of load imbalance. Unintentionally sending one additional task to a computing cluster ten times slower than other clusters can result in a very bad parallel run-time because other clusters have to wait until that cluster finishes. Figure 6 illustrates the performance of load sharing strategies with different values of computing heterogeneity ( $H$ ).

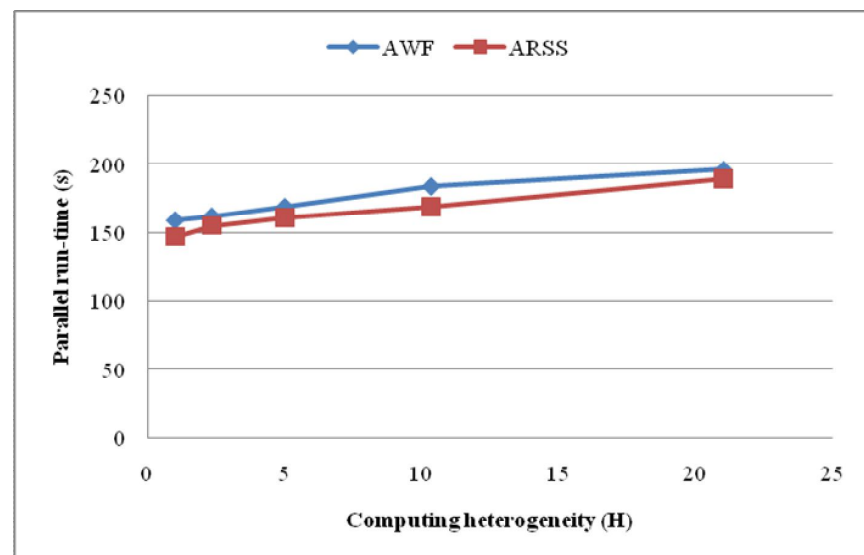


**Figure 6.** Parallel run-times at different values of computing heterogeneity

As shown in Figure 6, the parallel run-times of both strategies increases when the underlying system becomes more heterogeneous. However, since ARSS utilises job-stealing technique to ensure that every cluster enters the same stage throughout the entire execution, it can perform better than AWF over different values of computing heterogeneity.

### **Effect of Communication Overheads**

Large communication overheads can degrade the performance of load sharing strategies. The effect of communication overheads was evaluated by focusing on two parameters: the propagation delay in WAN and the communication size of the submitted application. The effect of propagation delay in WAN on different load sharing strategies is shown in Figure 7.

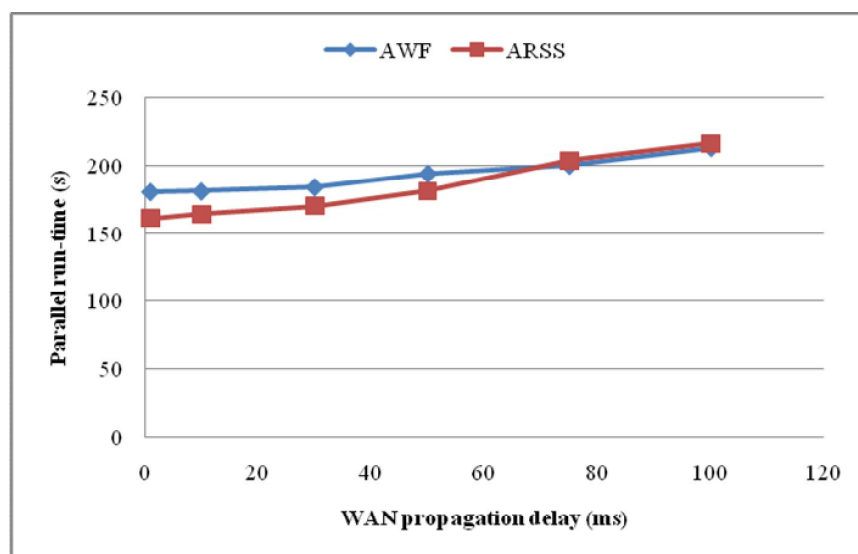


**Figure 7.** Parallel run-times at different WAN propagation delays

The obtained results illustrate that the performance of ARSS is better than that of AWF when the propagation delay in WAN is low. Since the accuracy of simple performance metrics used by ARSS decreases with propagation delay, the parallel run-times of both strategies become comparable when the WAN propagation delay is large.

From Figure 8, it can be seen that the performance of ARSS is much better than that of AWF when the communication size is large. The explanation for this behaviour is that AWF assigns workload in a decreasing fashion. Therefore, it suffers from a large amount of communication overheads during the first stage. Since ARSS starts the execution with the increasing stages, it can overlap the communication overheads with the computation time for each cluster. Note that, in our experiments, we do not consider the data-intensive applications with large communication sizes. In real life, large data sets which may be up to terabytes in total are usually pre-fetched to the computing resources before the execution begins in order to hide the communication overheads. Therefore, it is uncommon to assume that these large data sets will be transferred during run-time.

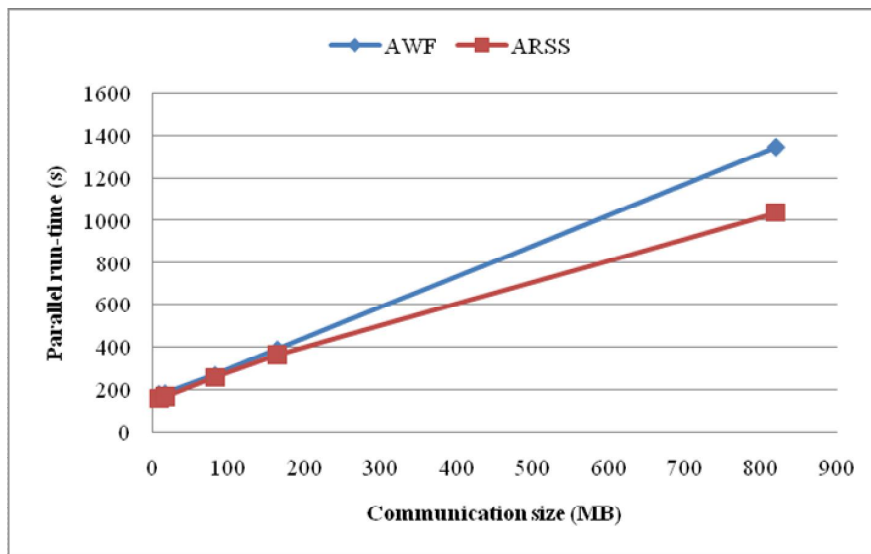


**Figure 8.** Parallel run-times at different communication sizes

### Effect of Application Pattern

Since ARSS will use the first half of total unit tasks to collect performance metrics, the characteristic of the submitted application can affect its performance. However, as shown in Figure 9, it can be seen that the performance of ARSS is barely changed given four different classes of applications. If an application has constant-size tasks, ARSS can perform better than AWF because the performance metrics obtained during the increasing stages are accurate. In the case of an application with increasing-size tasks, the performance of AWF is not good since the size of the unit tasks near the end of the execution, which will be used to balance the workload assigned during the previous stage, is large. In contrast to AWF, ARSS gradually increases the chunk size at the beginning and also gradually decreases it near the end of the execution. Although this behaviour will add a small amount of communication overheads, it provides stability to ARSS even when the computation size of each task is not the same.

### Effect of Total Number of Unit Tasks

The number of unit tasks in a submitted application is also one of the important factors because it can affect the accuracy of the obtained performance metrics used by ARSS. Since we keep the same total computation size for every test, the computation size of each task will be larger when the total number of unit tasks is decreased. From Figure 10, it can be seen that the performance of ARSS is still comparable or even better than AWF given a limited number of unit tasks. This behaviour shows that ARSS is robust enough to obtain good results even with a small number of unit tasks.

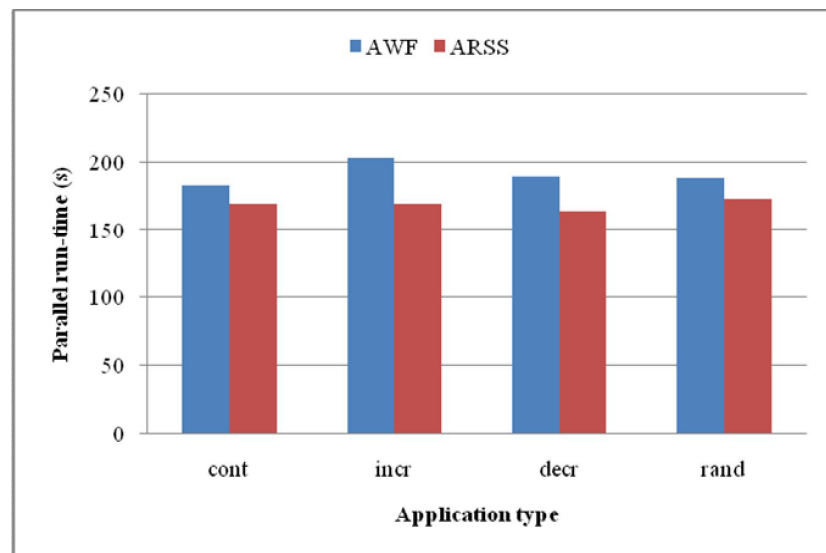


**Figure 9.** Parallel run-times for four different applications: those with constant-size (cont), increasing-size (incr), decreasing-size (decr), and randomized-size (rand) tasks

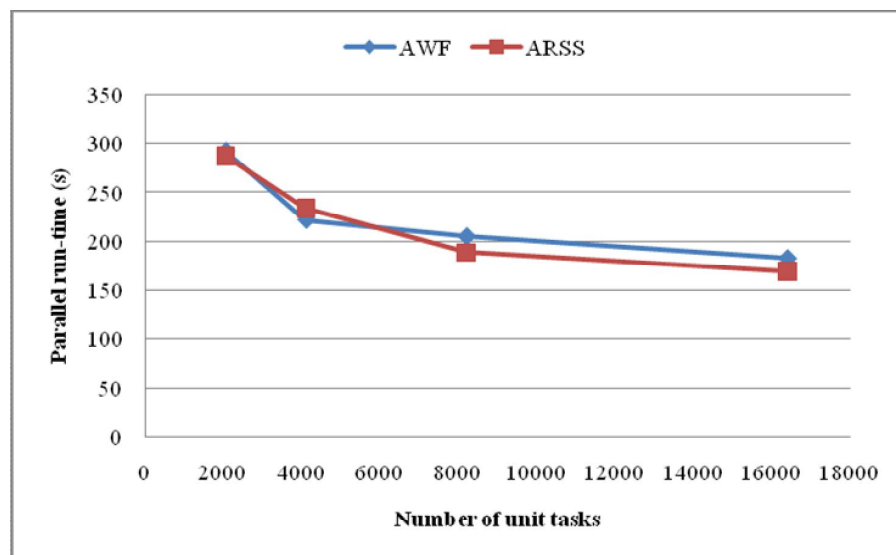


**Figure 10.** Parallel run-times for different number of unit tasks

## CONCLUSIONS

We have proposed a new global strategy called agentless robust self-scheduling strategy (ARSS) for large-scale multi-organisational computing systems. Unlike other traditional strategies, our proposed strategy can make load decision without any proprietary monitoring services installed at the participating resources. In order to address communication overheads in WAN and dynamic behaviour over a heterogeneous computing system, our strategy divides an entire computation into multiple stages. The increasing stages during the beginning of the execution are for obtaining an

accurate estimation of the computing power of each resource and also for overlapping the communication overheads. After that, the decreasing stages will eliminate the load imbalance until the end of the execution. During each stage, our strategy addresses the dynamic behaviour of the underlying system by assigning workload according to the performance metrics obtained in the previous stages. We also introduce a stage-warping technique to further handle the performance estimation errors. This technique will allow clusters to steal workload from those slower-than-expected clusters. The experimental results have shown that the proposed strategy can achieve a comparable or better performance compared to that of other traditional strategies. Our strategy is therefore non-intrusive and efficient at utilising heterogeneous resources over WAN, which definitely will be served as the computing platform for the next generation.

## REFERENCES

1. I. Foster, C. Kesselman and S. Tuecke, "The anatomy of the grid: Enabling scalable virtual organizations", *Int. J. High Perform. Comput. Appl.*, **2001**, 15, 200-222.
2. R. Buyya, C. S. Yeo, S. Venugopal, J. Broberg and I. Brandic, "Cloud computing and emerging IT platforms: Vision, hype, and reality for delivering computing as the 5th utility", *Future Generat. Comput. Syst.*, **2009**, 25, 599-616.
3. R. Moreno-Vozmediano, R. S. Montero and I. M. Llorente, "Elastic management of cluster-based services in the cloud", Proceedings of the 1st Workshop on Automated Control for Datacenters and Clouds, **2009**, Barcelona, Spain, pp.19-24.
4. J. S. Vetter and D. A. Reed, "Real-time performance monitoring, adaptive control, and interactive steering of computational grids", *Int. J. High Perform. Comput. Appl.*, **2000**, 14, 357-366.
5. B. Tierney, B. Crowley, D. Gunter, J. Lee and M. Thompson, "A monitoring sensor management system for grid environments", *Cluster Comput.*, **2001**, 4, 19-28.
6. R. Biswas, M. Frumkin, W. Smith and R. Van der Wijngaart, "Tools and techniques for measuring and improving grid performance", *Lect. Notes Comput. Sci.*, **2002**, 2571, 45-54.
7. R. Wolski, "Experiences with predicting resource performance on-line in computational grid settings", *Perform. Eval. Rev.*, **2003**, 30, 41-49.
8. X. H. Sun and M. Wu, "Grid harvest service: A system for long-term, application-level task scheduling", Proceedings of the 17th IEEE International Parallel and Distributed Processing Symposium, **2003**, Nice, France, pp.25-33.
9. I. Raicu, I. T. Foster and Y. Zhao, "Many-task computing for grids and supercomputers", Proceedings of ACM Workshop on Many-Task Computing on Grids and Supercomputers, **2008**, Austin, USA, pp.1-11.
10. C. P. Kruskal and A. Weiss, "Allocating independent subtasks on parallel processors", *IEEE Trans. Software Eng.*, **1985**, 11, 1001-1016.
11. P. Tang and P. C. Yew, "Processor self-scheduling for multiple-nested parallel loops", Proceedings of the International Conference on Parallel Processing, **1986**, Harrisburg, USA, pp. 528-535.

12. S. C. Chau and A. W. C. Fu, “Load balancing between heterogeneous computing clusters”, *Lect. Notes Comput. Sci.*, **2004**, 3032, 75-82.
13. R. Buyya, M. Murshed, D. Abramson and S. Venugopal, “Scheduling parameter sweep applications on global Grids: a deadline and budget constrained cost-time optimization algorithm”, *Softw. Pract. Exper.*, **2005**, 35, 491-512.
14. Z. Zhang, A. Espinosa, K. Iskra, I. Raicu, I. Foster and M. Wilde, “Design and evaluation of a collective IO model for loosely coupled petascale programming”, Proceedings of ACM Workshop on Many-Task Computing on Grids and Supercomputers, **2008**, Austin, USA, pp.1-10.
15. Y. W. Fann, C. T. Yang, S. S. Tseng and C. J. Tsai, “An intelligent parallel loop scheduling for multiprocessor systems”, *J. Inform. Sci. Eng.*, **2000**, 16, 169-200.
16. C. D. Polychronopoulos and D. J. Kuck, “Guided self-scheduling: A practical scheduling scheme for parallel supercomputers”, *IEEE Trans. Comput.*, **1987**, 36, 1425-1439.
17. T. H. Tzen and L. M. Ni, “Trapezoid self-scheduling: A practical scheduling scheme for parallel compilers”, *IEEE Trans. Parallel Distr. Syst.*, **1993**, 4, 87-98.
18. A. T. Chronopoulos, R. Andonie, M. Benche and D. Grosu, “A class of loop self-scheduling for heterogeneous clusters”, Proceedings of the IEEE Annual International Conference on Cluster Computing, **2001**, Newport Beach, USA, pp.282-291.
19. K. W. Cheng, C. T. Yang, C. L. Lai and S. C. Chang, “A parallel loop self-scheduling on grid computing environments”, Proceedings of the International Symposium on Parallel Architectures, Algorithms and Networks, **2004**, Kaohsiung, Taiwan, pp.409-414.
20. S. F. Hummel, E. Schonberg and L. E. Flynn, “Factoring: A method for scheduling parallel loops”, *Comm. ACM*, **1992**, 35, 90-101.
21. S. F. Hummel, J. Schmidt, R. N. Uma and J. Wein, “Load-sharing in heterogeneous systems via weighted factoring”, Proceedings of the ACM Symposium on Parallelism in Algorithms and Architectures, **1996**, Padua, Italy, pp.318-328.
22. I. Banicescu and V. Velusamy, “Performance of scheduling scientific applications with adaptive weighted factoring”, Proceedings of the 15th IEEE International Parallel and Distributed Processing Symposium, **2001**, San Francisco, USA, pp.791-801.
23. Y. Yang and H. Casanova, “RUMR: Robust scheduling for divisible workloads”, Proceedings of the 12th High Performance Parallel and Distributed Computing, **2003**, Seattle, USA, pp. 114-123.
24. Y. C. Lee and A. Y. Zomaya, “Practical scheduling of bag-of-tasks applications on grids with dynamic resilience”, *IEEE Trans. Comput.*, **2007**, 56, 815-825.
25. S. McCanne and S. Floyd, “ns-2 network simulator”, <http://www.isi.edu/nsnam/ns/>. (Accession date: 20 Feb. **2006**)
26. V. Varavithya and P. Uthayopas, “ThaiGrid: Architecture and overview”, *NECTEC Tech. J.*, **2000**, 2, 219-224.
27. H. Casanova, “Simgrid: A toolkit for the simulation of application scheduling”, Proceedings of the 1st IEEE/ACM International Symposium on Cluster Computing and the Grid, **2001**, Brisbane, Australia, pp.430-437.

28. C. T. Yang, K. W. Cheng and W. C. Shih, “On development of an efficient parallel loop self-scheduling for grid computing environments”, *Parallel Comput.*, **2007**, 33, 467-487.
29. K. Lu, R. Subrata and A. Y. Zomaya, “On the performance-driven load distribution for heterogeneous computational grids”, *J. Comput. Syst. Sci.*, **2007**, 73, 1191-1206.

© 2011 by Maejo University, San Sai, Chiang Mai, 50290 Thailand. Reproduction is permitted for noncommercial purposes.

Full Paper

## **Utilisation of vegetable oils in the production of lovastatin by *Aspergillus terreus* ATCC 20542 in submerged cultivation**

**Pattana Sripalakit<sup>1,2,\*</sup>, Janya Riunkesorn<sup>2</sup> and Aurasorn Saraphanchotiwitthaya<sup>2,3</sup>**

<sup>1</sup> Department of Pharmaceutical Chemistry and Pharmacognosy, Faculty of Pharmaceutical Sciences, Naresuan University, Phitsanulok 65000, Thailand

<sup>2</sup> Pharmaceutical Biotechnology Research Unit, Faculty of Pharmaceutical Sciences, Naresuan University, Phitsanulok 65000, Thailand

<sup>3</sup> Department of Pharmaceutical Technology, Faculty of Pharmaceutical Sciences, Naresuan University, Phitsanulok 65000, Thailand

\* Corresponding author, e-mail: [pattanas@nu.ac.th](mailto:pattanas@nu.ac.th)

Received: 27 August 2010 / Accepted: 21 July 2011 / Published: 21 July 2011

**Abstract:** The effect of vegetable oils as a supplementary carbon source during the production of lovastatin by *Aspergillus terreus* ATCC 20542 in submerged culture was investigated. The six vegetable oils tested were sesame oil, sunflower oil, soya bean oil, corn oil, palm oil and olive oil. Lovastatin concentration and biomass were measured. Lovastatin production was higher in several oil-containing media compared to control medium. In particular, palm oil and soya bean oil significantly improved lovastatin production. Yields with palm oil and soya bean oil were 4.5- and 1.4-fold higher respectively, compared with control. Sesame oil and corn oil, however, had a negative effect on lovastatin production. Biomass was proportional to vegetable oil concentration, but an excessive vegetable oil concentration resulted in a lower yield of lovastatin. Thus, some vegetable oils appear to be excellent adjuvants for improving efficiency of lovastatin production.

**Keywords:** lovastatin, *Aspergillus terreus*, vegetable oils, submerged culture

### **INTRODUCTION**

Lovastatin (Figure 1) was the first potent cholesterol-lowering drug to be approved [1]. It acts by competitively inhibiting 3-hydroxy-3-methylglutaryl coenzyme A (HMG-CoA) reductase which catalyses the rate-limiting step of cholesterol biosynthesis [2]. Lovastatin is produced as a

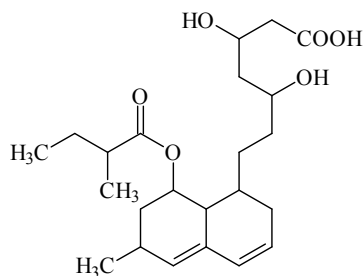


**Figure 1.** Lovastatin ( $\beta$ -hydroxy acid form)

secondary metabolite of the polyketide pathway by various fungi including *Penicillium* spp. [3], *Monascus* spp. [4], *Trichoderma* spp. [5] and *Aspergillus terreus* [2]. *A. terreus* is known to be the best lovastatin-producing species [6]. Several studies have extensively investigated methods for increasing lovastatin production in *A. terreus*. Many literature reports have focused on culture medium optimisation [7-15]. Further studies have addressed the development of mutant strains [16], the culturing environment [17] and the solid-state fermentation [18-20].

Carbon and nitrogen sources have dominant roles in the fermentation process because these are the major culture nutrients involved in the formation of biomass and metabolites [11]. Vegetable oils are essential components of industrial fermentation media and they are routinely supplemented into media during the production of antibiotics [21]. Vegetable oils are used as sole carbon sources, supplemental carbon sources, anti-foaming agents and precursors during antibiotic synthesis. There are many examples of the successful utilisation of vegetable oils in the production of antibiotics including erythromycin [21], tetracycline [22], cephamycin C [23], cephalosporin C [24], clavulanic acid [25] and gentamicin [26].

However, there seem to be no published reports of the application of vegetable oils in lovastatin production. Thus, we have undertaken to investigate the applicability of a range of vegetable oils to enhancing lovastatin productivity of *A. terreus*. This study also reports an optimised culture medium and culture environment for lovastatin production.

## MATERIALS AND METHODS

### Chemicals

Standard lovastatin ( $\beta$ -hydroxy acid form) ( $\geq 98\%$  purity) was obtained from Sigma Chemical Co. (St. Louis, MO). Yeast extract (Fluka Chemie GmbH, Buchs, Switzerland), corn steep liquor (Sigma Chemical, Co.), lactose (Ajax Finechem, NSW, Australia), D-(+)-glucose monohydrate (Riedel-de Haen Laborchemikalien GmbH, Seelze, Germany) and potato dextrose agar (Merck KGaA, Darmstadt, Germany) were used in the culture medium. Cooking vegetable oils tested were as follows: corn oil (refined, Mass Marketing Co. Ltd, Samutprakarn, Thailand), olive oil (extra virgin, Rafael Salgado SA, Madrid, Spain), palm oil (refined, P.S. Pacific Co. Ltd, Petchburi, Thailand), sesame oil (Chaiseri Co. Ltd, Chiang Mai, Thailand), soya bean oil (refined, Morakot Industries Public Co. Ltd, Samutprakarn, Thailand) and sunflower oil (refined, Thanakorn Vegetable

Oil Products Co. Ltd, Samutprakarn, Thailand). All other chemicals, trace elements and solvents were of reagent grade and obtained from standard sources.

### **Microorganisms and Culture Medium**

A standard fungal strain of *A. terreus* ATCC 20542 was obtained from the American Type Culture Collection (Manassas, VA). The fungal cells were kept in the form of a revivable freeze-dried culture and reactivated by culturing on potato dextrose agar slants in an incubator (Memmert GmbH & Co. KG, Schwabach, Germany) at 30°C for 3 days. In each experiment, the refreshed fungal strain was maintained on agar and subcultured into the primary seed culture medium. A basal culture medium, previously reported by Casas Lopez et al. [9], was optimised for this study and contained the following in 1 L of distilled water: 10 g lactose, 8 g yeast extract, 1.51 g KH<sub>2</sub>PO<sub>4</sub>, 0.52 g MgSO<sub>4</sub>.7H<sub>2</sub>O, 0.40 g NaCl, 1 mg ZnSO<sub>4</sub>.H<sub>2</sub>O, 2 mg Fe(NO<sub>3</sub>)<sub>3</sub>.9H<sub>2</sub>O, 0.04 mg biotin and 1 mL trace element solution. One litre of the trace element solution contained 100 mg NaB<sub>4</sub>O<sub>7</sub>.10H<sub>2</sub>O, 50 mg MnCl<sub>2</sub>.4H<sub>2</sub>O, 50 mg Na<sub>2</sub>MoO<sub>4</sub>.2H<sub>2</sub>O and 250 mg CuSO<sub>4</sub>.5H<sub>2</sub>O. The pH of the medium was adjusted to 6.5 using 0.1 N NaOH before sterilisation. The seed culture was prepared in a 250-mL Erlenmeyer flask containing 100 mL of medium, which was kept on an orbital shaker (Revco Scientific Inc., Asheville, NC) at 220 rpm for 5 days at room temperature. All aseptic techniques were conducted in a laminar air flow cabinet (Forma Scientific Inc., Marietta, OH).

### **Optimisation of Culture Conditions**

A 1.0-mL volume of dispersed spores from the seed medium was added to each flask containing 100 mL of the basal culture medium. The effects of incubation temperature, incubation period and shaking rate on lovastatin production were then examined. Experiments were performed at 25°C and 30°C, orbital shaker speeds of 150 and 220 rpm, and five fermentation periods of 5, 7, 9, 12 and 14 days, while all other conditions remained fixed.

### **Screening of Carbon and Nitrogen Sources**

A 1.0-mL volume of dispersed spores from the seed medium was added to 100 mL of the basal culture medium contained in each flask with different carbon and nitrogen sources. Various medium compositions were tested by varying the carbon and nitrogen sources as follows—lactose and yeast extract; lactose and corn steep liquor; glucose and yeast extract; glucose and corn steep liquor—all with a ratio of 10:8 g L<sup>-1</sup>. Further, the mass ratios, i.e. 8:10, 10:8, 12:6 and 14:4 g L<sup>-1</sup>, of the carbon:nitrogen sources were tested, based on the results of preliminary experiments. The total mass of carbon and nitrogen sources was fixed at 18 g L<sup>-1</sup>.

### **Effects of Different Vegetable Oils on Lovastatin Production**

A 1.0-mL volume of dispersed spores from the seed medium was added to 100 mL of the basal culture medium contained in each flask with different vegetable oils. Experiments were performed by testing six different vegetable oils at a concentration of 1% v/v. A subsequent study tested the effects of using different concentrations (0.5%, 1%, 2% and 3% v/v) of two vegetable oils on lovastatin production.

## HPLC Analysis

Each culture medium was separated from the fungal mass at the end of the incubation period and adjusted to pH 3. The clear broth (50 mL) was extracted with ethyl acetate (50 mL) by vigorously mixing for 10 min in a separating funnel. After separation, the organic layer was evaporated and dried. The residue volume was then adjusted to 2.0 mL with a mobile phase (composition described later in this section), filtered through a 0.45- $\mu\text{m}$  nylon syringe filter and transferred to a sample vial. One hundred microlitres was analysed by an HPLC system that consisted of a solvent delivery system (Varian 9012, Varian, Palo Alto, CA) and a variable wavelength UV-Vis detector (Varian 9050, Varian) equipped with a Rheodyne 7725 sample injector (Rohnert Park, CA) which was fitted with a 100- $\mu\text{l}$  sample loop. Chromatographic separation was conducted using an ODS Hypersil® C-18 column (250  $\times$  4.6 mm i.d.; 5- $\mu\text{m}$  particle diameter; 250Å average pore size) (Thermo Electron Corporation, Waltham, MA) and a mobile phase containing 55% acetonitrile, 12% methanol and 33% phosphate buffer saline (pH 4.0) at a flow rate of 1.0 mL min<sup>-1</sup>. Detected at 238 nm, lovastatin peak was located at a retention time of 14 min. Produced lovastatin content was obtained from its concentration in the culture medium determined by a calibration curve of the authentic sample between 1–20  $\mu\text{g mL}^{-1}$ .

## Measurement of Dry Cell Weight

The culture broth was filtered with a Whatman filter membrane No. 1. The total mycelia obtained were washed with distilled water, dried in an oven for 24 h at 70°C and equilibrated at room temperature before measurement of the dry cell weight.

## RESULTS AND DISCUSSION

### Optimisation of Culture Conditions

The different culture temperature of 25°C and 30°C had no significant effects on lovastatin production. However, an agitation speed of 150 rpm gave higher lovastatin production compared with 220 rpm. The lovastatin yield increased rapidly between day 3 and day 5, presumably because lovastatin is a secondary metabolite and its accumulation in mycelia appears to be growth-related. The maximum lovastatin yield was achieved on day 7, after which the yield slowly decreased (Figure 2). The decrease in lovastatin concentration after day 7 might be attributable to an insufficient amount of lactose relative to yeast extract and because the nitrogen source could also inhibit lovastatin formation [27]. This production time-course corresponded to others reported by Saminee et al. [6] and Lopez et al. [9]. Lovastatin is an intracellular product, so the product accumulation approximately correlates with cell growth [19]. These results indicate that the cultivation process may be concluded on day 7. Based on these finding, these operating conditions were used in the next experiments.

### Screening of Carbon and Nitrogen Sources

The optimum carbon and nitrogen sources for submerged cultures of *A. terreus* have been widely investigated [7–10]. In the present study, different types of carbon and nitrogen sources were

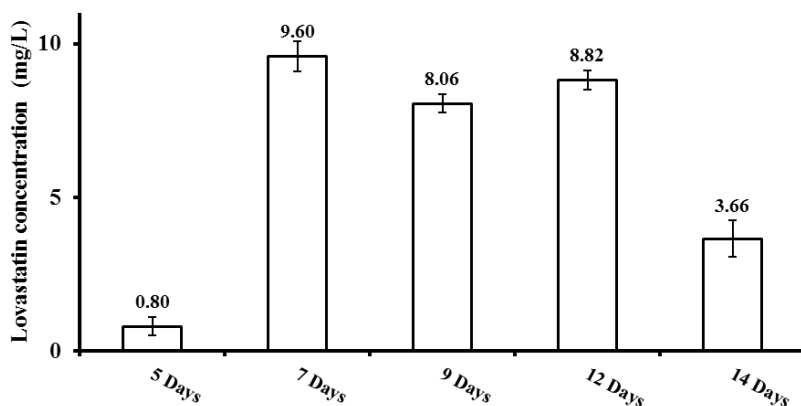


**Figure 2.** Time-course of lovastatin production by *A. terreus* ATCC 20542 (n = 3)

found to affect lovastatin production. Optimal lovastatin production was found when using 10 g L<sup>-1</sup> glucose and 8 g L<sup>-1</sup> corn steep liquor as carbon and nitrogen sources respectively. This medium yielded a lovastatin titre of 33.00 mg L<sup>-1</sup> within 7 days of culture, a 2.8-fold increase in lovastatin production when compared with that from a basal medium containing 10 g L<sup>-1</sup> lactose and 8 g L<sup>-1</sup> yeast extract (Figure 3). These results did not agree with those obtained by Lopez et al. [9] and Lai et al. [10], who preferred lactose and yeast extract as carbon and nitrogen sources rather than glucose and corn steep liquor. The inconsistency might stem from differences in the culture environments as well as the composition and concentration of other culture medium components.

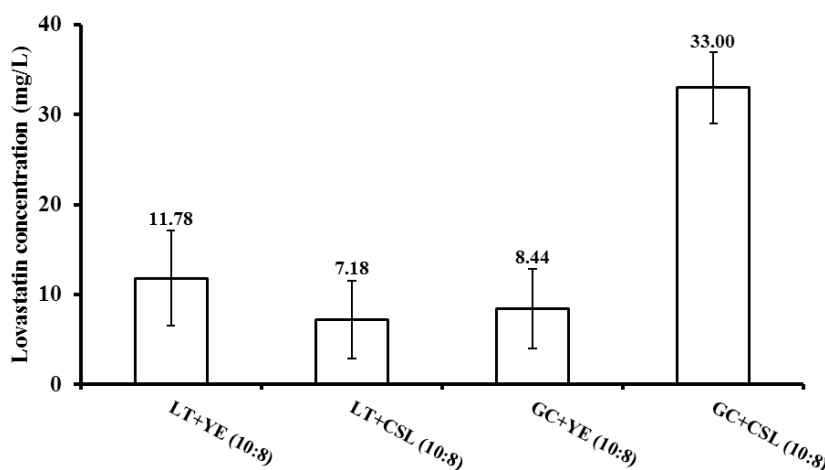


**Figure 3.** Lovastatin production in cultures containing different carbon and nitrogen sources (g L<sup>-1</sup>) for *A. terreus* ATCC 20542 (LT = lactose; GC = glucose; YE = yeast extract; CSL = corn steep liquor) (n = 3)

A second set of experiments involved testing the effects of using different glucose:corn steep liquor mass ratios on lovastatin yield. A mass ratio of 12:6 resulted in the highest production (Figure 4). These results agreed with the reports by Hajjaj et al. [8] and Lopez et al. [9]. Lovastatin yield can thus be increased when the carbon source is nonlimiting and growth is only arrested by nitrogen

source limitation. Based on these findings, glucose and corn steep liquor with a mass ratio of 12:6 was used in the next experiments.

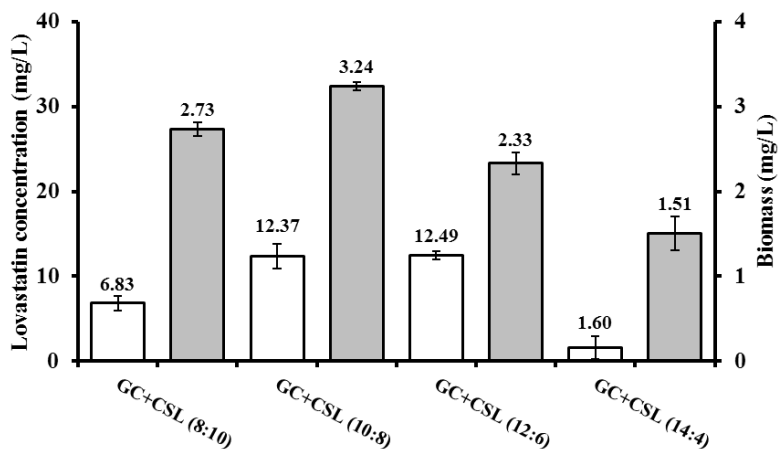


**Figure 4.** Lovastatin production (light bars) and biomass (dark bars) derived from cultures of *A. terreus* ATCC 20542 with different carbon:nitrogen mass ratios ( $\text{g L}^{-1}$ ) ( $n = 3$ )

#### Effects of Various Vegetable Oils on Lovastatin Production

Separate submerged cultures were grown for 7 days in Erlenmeyer flasks, each containing 100 mL of the production medium and 1% (v/v) of each of the six vegetable oils. Figure 5 shows the effects of various vegetable oils on lovastatin production in two different media containing lactose:yeast extract (10:8) and glucose:corn steep liquor (12:6). Most vegetable oils increased the product yield compared with control, with the exceptions of sesame oil and corn oil. The highest production levels were found with palm oil in the basal medium and soya bean oil in the optimised medium. The maximum production levels were  $15.94 \text{ mg L}^{-1}$  (palm oil in basal medium) and  $41.85 \text{ mg L}^{-1}$  (soya bean oil in optimised medium), which were approximately 4.5- and 1.4-fold greater than those obtained from the oil-free controls in basal and optimised media respectively. Soya bean oil was also known to have positive effects on tetracycline [22], cephalexin C [23] and gentamicin [26] production.

In order to find the optimal oil concentration, the experiments were repeated using soya bean oil and palm oil at concentrations of 0.5, 1, 2, and 3% (v/v). The resulting lovastatin and biomass production are shown in Figure 6, which indicates that palm oil and soya bean oil had a similar performance. An oil concentration of 0.5% resulted in the highest lovastatin production for both palm oil and soya bean oil; higher concentrations tended to give lower yields. It is interesting to note that the biomass increased with increasing oil concentration, which suggests that cell growth is related to vegetable oil concentration. These results agreed with a previous report [9], which showed that metabolic pathways governing the synthesis of lovastatin from a carbon source were slower than pathways converting carbon to biomass.

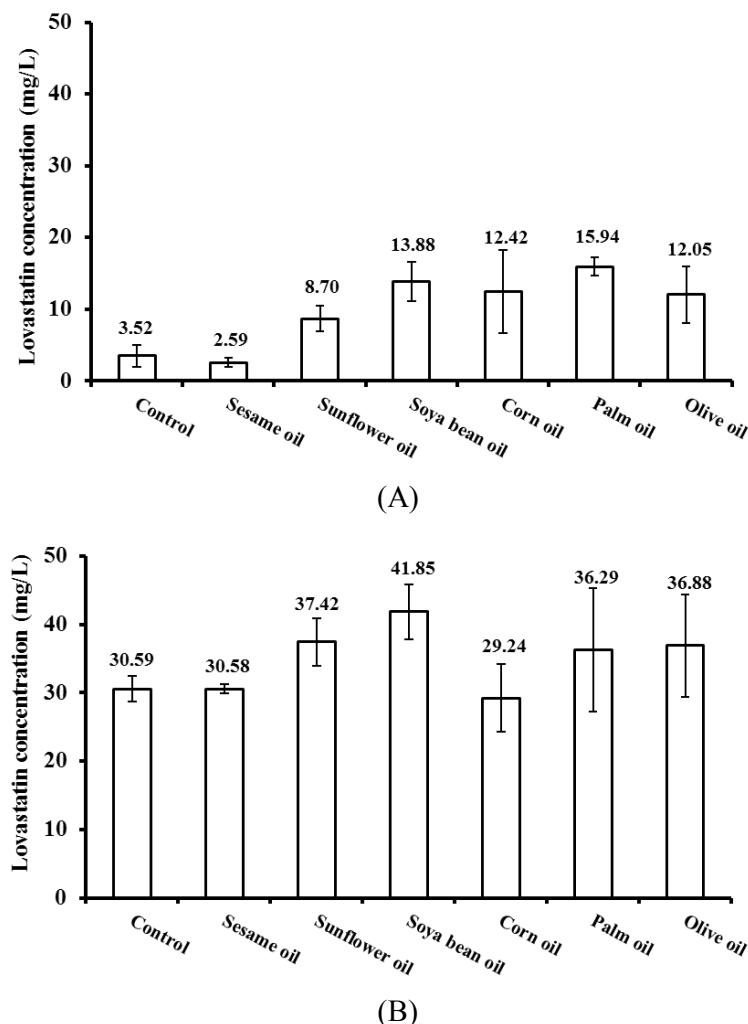


**Figure 5.** Effects of 1% (v/v) concentration of vegetable oils on lovastatin production by *A. terreus* ATCC 20542 in medium containing (g L<sup>-1</sup>): (A) lactose:yeast extract (10:8), and (B) glucose:corn steep liquor (12:6) (n = 3)

Although vegetable oils may have a key role as a supplementary carbon source, the data available are still not sufficient to identify any specific components of the vegetable oils used that may be the key factors affecting lovastatin production. Further investigations are required to test different combinations of fatty acids and other components of vegetable oils to identify any major factors affecting lovastatin production.

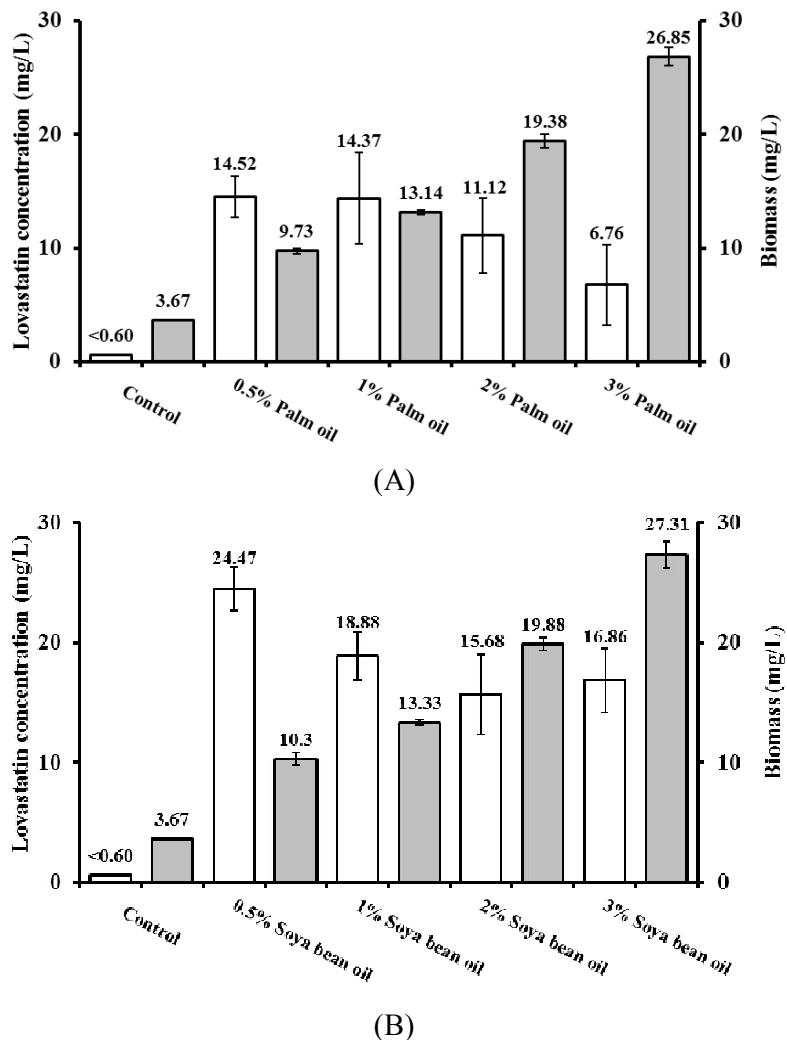


**Figure 6.** Effects of concentration of palm oil (A) and soya bean oil (B) on lovastatin (light bar) and biomass (dark bar) production by *A. terreus* ATCC 20542 in a medium containing (g L<sup>-1</sup>) lactose:yeast extract (10:8) (n = 3)

## CONCLUSIONS

Vegetable oils are a promising substrate as additional carbon and energy source for lovastatin production by *A. terreus* in a submerged culture. Of the six vegetable oils tested, palm oil and soya bean oil significantly improved lovastatin production when present at low levels in the culture medium. The degree of cell growth was also closely associated with the vegetable oil concentration. The type of carbon and nitrogen sources used and their mass ratio also affected lovastatin production.

## ACKNOWLEDGEMENTS

This work was supported by a research grant from the Faculty of Pharmaceutical Sciences and the Division of Research Administration, Naresuan University.

## REFERENCES

1. M. Manzoni and M. Rollini, "Biosynthesis and biotechnological production of statins by filamentous fungi and application of these cholesterol-lowering drugs", *Appl. Microbiol. Biotechnol.*, **2002**, *58*, 555-564.
2. A. W. Alberts, J. Chen, G. Kuron, V. Hunt, J. Huff, C. Hoffman, J. Rothrock, M. Lopez, H. Joshua, E. Harris, A. Patchett, R. Monaghan, S. Currie, E. Stapley, G. Albers-Schonberg, O. Hensens, J. Hirshfield, K. Hoogsteen, J. Liesch and J. Springer, "Mevinolin: A highly potent competitive inhibitor of hydroxymethylglutaryl-coenzyme A reductase and cholesterol-lowering agent", *Proc. Natl. Acad. Sci. USA*, **1980**, *77*, 3957-3961.
3. A. Endo, M. Kuroda and Y. Tasujita, "ML-236A, ML-236B and ML-236C, new inhibitors of cholestrogenesis produced by *Penicillium citrinum*", *J. Antibiot. (Tokyo)*, **1976**, *29*, 1346-1348.
4. S. Negishi, Z. Cai-Huang, K. Hasumi, S. Murakawa and A. Endo, "Productivity of monacolin K (mevinolin) in the genus *Monascus*", *J. Ferment. Eng.*, **1986**, *64*, 509-512.
5. A. Endo, K. Hausami, A. Yamada, R. Shimoda and H. Takeshima, "The synthesis of compactin (ML-236B) and monacolin K in fungi", *J. Antibiot. (Tokyo)*, **1986**, *39*, 1609-1610.
6. S. M. Samiee, N. Moazami, S. Haghghi, F. A. Mohseni, S. Mirdamadi and M. R. Bakhtiari, "Screening of lovastatin production by filamentous fungi", *Iran. Biomed. J.*, **2003**, *7*, 29-33.
7. M. S. Kumar, S. K. Jana, V. Senthil, V. Shashanka, S. V. Kumar and A. K. Sadhukhan, "Repeated fed-batch process for improving lovastatin production", *Process Biochem.*, **2000**, *36*, 363-368.
8. H. Hajjaj, P. Niederberger and P. Dubac, "Lovastatin biosynthesis by *Aspergillus terreus* in a chemically defined medium" *Appl. Environ. Microbiol.*, **2001**, *67*, 2596-2602.
9. J. L. C. Lopez, J. A. S. Perez, J. M. F. Sevilla, F. G. A. Fernandez, E. M. Grima and Y. Chisti, "Production of lovastatin by *Aspergillus terreus*: effects of the C:N ratio and the principal nutrients on growth and metabolite production", *Enzyme Microb. Technol.*, **2003**, *33*, 270-277.
10. L. S. T. Lai, C. C. Pan and B. K. Tzeng, "The influence of medium design on lovastatin production and pellet formation with a high-producing mutant of *Aspergillus terreus* in submerged cultures", *Process Biochem.*, **2003**, *38*, 1317-1326.
11. J. L. C. Lopez, J. A. S. Perez, J. M. F. Sevilla, F. G. A. Fernandez, E. M. Grima and Y. Chisti, "Fermentation optimization for the production of lovastatin by *Aspergillus terreus*: Use of response surface methodology", *J. Chem. Technol. Biotechnol.*, **2004**, *79*, 1119-1126.
12. M. Bizukojc, B. Pawlowska and S. Ledakowicz, "Supplementation of the cultivation media with B-group vitamins enhances lovastatin biosynthesis by *Aspergillus terreus*", *J. Biotechnol.*, **2007**, *127*, 258-268.
13. L. S. T. Lai, C. S. Hung and C. C. Lo, "Effects of lactose and glucose on production of itraconic acid and lovastatin by *Aspergillus terreus* ATCC 20542", *J. Biosci. Bioeng.*, **2007**, *104*, 9-13.
14. E. M. R. Porcel, J. L. C. Lopez, J. A. S. Perez and Y. Chisti, "Lovastatin production by *Aspergillus terreus* in a two-staged feeding operation", *J. Chem. Technol. Biotechnol.*, **2008**, *83*, 1236-1243.

15. Z. Jia, X. Zhang and X. Cao, "Effects of carbon sources on fungal morphology and lovastatin biosynthesis by submerged cultivation of *Aspergillus terreus*", *Asia-Pac. J. Chem. Eng.*, **2009**, *4*, 672-677.
16. M. A. V. Ferron, J. L. C. Lopez, J. A. S. Perez, J. M. F. Sevilla and Y. Chisti, "Rapid screening of *Aspergillus terreus* mutants for overproduction of lovastatin", *World J. Microbiol. Biotechnol.*, **2005**, *21*, 123-125.
17. L. S. T. Lai, T. H. Tsai, T. C. Wang and T. Y. Cheng, "The influence of culturing environments on lovastatin production by *Aspergillus terreus* in submerged cultures", *Enzyme Microb. Technol.*, **2005**, *36*, 737-748.
18. H. R. Valera, J. Gomes, S. Lakshmi, R. Gururaja, S. Suryanarayan and D. Kumar, "Lovastatin production by solid state fermentation using *Aspergillus flavipes*", *Enzyme Microb. Technol.*, **2005**, *37*, 521-526.
19. P. L. Wei, Z. N. Xu and P. L. Cen, "Lovastatin production by *Aspergillus terreus* in solid-state fermentation", *J. Zhejiang Univ. Sci. A*, **2007**, *8*, 1521-1526.
20. J. G. Banos, A. Tomasini, G. Szakacs and J. Barrios-Gonzalez, "High lovastatin production by *Aspergillus terreus* in solid-state fermentation on polyurethane foam: An artificial inert support", *J. Biosci. Bioeng.*, **2009**, *108*, 105-110.
21. J. Hamed, F. Malekzadeh and A. E. Saghafinia, "Enhancing of erythromycin production by *Saccharopolyspora erythraea* with common and uncommon oils", *J. Ind. Microbiol. Biotechnol.*, **2004**, *31*, 447-456.
22. A. M. Jones and M. A. Porter, "Vegetable oils in fermentation: Beneficial effects of low-level supplementation", *J. Ind. Microbiol. Biotechnol.*, **1998**, *21*, 203-207.
23. Y. S. Park, I. Momose, K. Tsunoda and M. Okabe, "Enhancement of cephamycin C production using soybean oil as the sole carbon source", *Appl. Microbiol. Biotechnol.*, **1994**, *40*, 773-779.
24. J. H. Kim, J. S. Lim and S. W. Kim, "The improvement of cephalosporin C production by fed-batch culture of *Cephalosporium acremonium* M25 using rice oil", *Biotechnol. Bioprocess Eng.*, **2004**, *9*, 459-464.
25. G. L. Maranesi, A. Baptista-Neto, C. O. Hokka and A. C. Badino, "Utilization of vegetable oil in the production of clavulanic acid by *Streptomyces clavuligerus* ATCC 27064", *World J. Microbiol. Biotechnol.*, **2005**, *21*, 509-514.
26. D. B. Choi, S. S. Park, B. K. Ahn, D. H. Lim, Y. W. Lee, J. H. Moon and D. Y. Shin, "Studies on production of gentamicin from *Micromonosporas purpurea* using crude vegetable oils", *Process Biochem.*, **2008**, *43*, 835-841.
27. M. Bizukojc and S. Ledakowicz, "A macrokinetic modelling of the biosynthesis of lovastatin by *Aspergillus terreus*", *J. Biotechnol.*, **2007**, *130*, 422-435.

*Full Paper*

## **Effects of forest road clearings on understory diversity beneath *Alnus subcordata* L. stands in Iran**

**Seyed A. Hosseini<sup>\*</sup>, Hamid Jalilvand, Mohammad R. Pourmajidian and Aidin Parsakhooh**

Department of Forestry, Faculty of Natural Resources, Sari Agricultural Sciences and Natural Resources University, P.O. Box 737, Mazandaran, Iran

\* Corresponding author, e-mail: Ata\_hosseiny2002@yahoo.com

*Received: 1 March 2011 / Accepted: 21 July 2011 / Published: 22 July 2011*

---

**Abstract:** This study was conducted in Darab Kola forest which is located east of Sari city. After confirming the identity of Alder trees (*Alnus subcordata* L., Betulaceae) at the edge of forest roads, the cross section geometry was classified into without earth works and with earth works. Road clearing limits were divided into less than 10 metres and 10-15 metres. The understory density and canopy cover underneath Alder stands were measured in 20 micro plots. The diversity of woody and herbaceous plant species was calculated by the Simpson index. The results indicated that the canopy cover at the edge of cross sections without earth works was greater than that of sections with earth works at a probability level of 5%. In both classes, the percentage of *Rubus hyrcanus* L. canopy cover on filled slopes was more than that on cut slopes, whereas the percentage of canopy cover of this species and of bare soil was similar, as well as the biodiversity indices for both sides of cross sections without earth works.

**Keywords:** understory diversity, forest road clearing, *Alnus subcordata* L.

---

### **INTRODUCTION**

The water balance of roads depends on the geometry and on the course of the road through the land [1]. It has been demonstrated that the locations of the trees on the down-slope and up-slope of roads affect the foliage discolouration level. Mean foliage discolouration level of trees was highest in the down-slope plots, followed by up-slope and forest interior plots [1]. Roadside soil receives at least twice as much rainfall water as other areas and the interception of subsurface flows by roads further increases the water availability in road side areas [2].

The environmental effects of forest roads were categorised into abiotic and biotic categories. For abiotic conditions, the effects of roads on hydrology, geomorphology, natural disturbances and edaphic properties were studied [3-4]. In a pine forest, Delgado et al. [5] detected a highly significant gradient of soil temperature along asphalt roads and a significant light gradient for both asphalt and unpaved roads. The biotic consequences are divided into genetic factors and plant and wildlife population situations [6].

Forest roads create edge effects on plant communities through fragmenting habitats and introducing disturbances [7-8]. These effects may vary with the width of roads as well as the geometry of road cross sections [9-10]. Solar radiation, soil moisture content, and soil temperature in gaps created by forest roads are significantly greater than adjacent closed canopy plots [11-12]. Gaps have significantly less exchangeable base cations (K, Ca and Mg) compared to forest plots with mineral soil (0–25 cm). Gaps also have significantly more dissolved organic N and extractable nitrates at 25–50 cm, indicating increased nutrient leaching in gaps. In situ N mineralisation is significantly greater in gaps and roadside plots compared to forest plots [13-15]. Zhou et al. [16] showed that wide and narrow roads have different edge effects. For wide roads, plant diversity and soil moisture tend to increase, whereas herbaceous biomass tends to decrease from the road edge to the forest interior.

The objective of this study is to assess the edge effects of wide (10-15 m) and narrow (less than 10 m) roadside clearings of forest roads on plant species diversity under the alder trees in the Darab Kola forest, Mazandaran, Iran. The effects of the geometry of forest road cross sections including those with earth works and without earth works on plant species diversity was investigated.

## **STUDY AREA AND METHODS**

Darab Kola forest with an area of 2,612 hectares is located in south-east Sari city in Mazandaran province, Iran. The latitude, longitude and elevation ranges of this forest are 36° 33' 20" to 36° 33' 30" N, 52° 14' 40" to 52° 31' 55" E and 180-800 metres above sea level respectively. The average slope of the forest is about 40%. The forest has four types of soil consisting of (I) non-developed randzin to washed randzin soil, (II) brown soil with an alkaline pH, (III) washed brown calcic soil and (IV) washed brown pseudoclay (Figure 1). The climate is very moist with average temperature ranging from 26.1 °C in August to 7.5 °C in February. The mean annual air temperature is 16.7 °C. The region receives 983.8 mm of precipitation annually. Minimum and maximum rainfall is 36.1 to 119.8 mm, which occur in July and November respectively.

The cross section shapes were classified into that without earth works and that with earth works (Figure 2). In addition, roadside clearings were divided into that less than 10 metres and that between 10-15 metres wide. According to the cross section shapes of forest roads and clearing classes, the understory density and canopy cover in were measured in 20 1×1-m plots. All data were collected in July 2009. The diversity of woody and herbaceous plant species was calculated by Simpson's index ( $\lambda$ ) :

$$\lambda = 1 - \sum \left[ \frac{n_i(n_i - 1)}{N(N-1)} \right]$$

where  $n_i$  is number of individuals of species  $i$  in the sample and  $N$  is total number of individuals in the sample.

The data were analysed by the ANOVA procedure using SAS software. Statistical significance was judged at  $p < 0.05$ . When the analysis was statistically significant, the Student Newman Keuls (SNK) test for separation of means was performed.

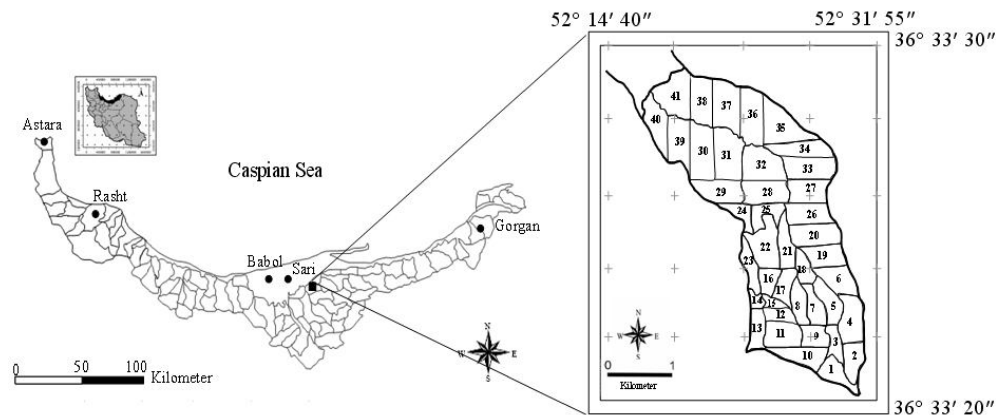


**Figure 1.** Location of the study area

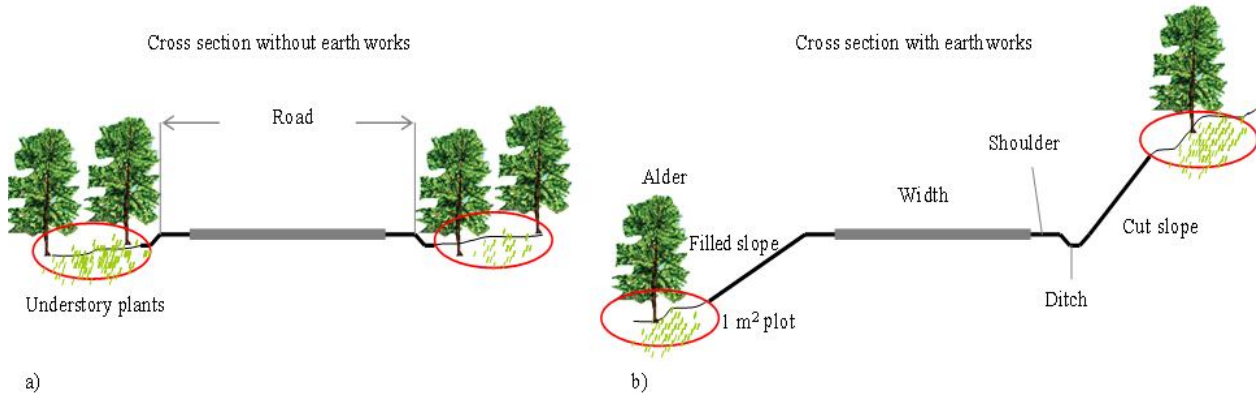


**Figure 2.** (a) Cross section without earth works; (b) cross section with earth works

## RESULTS AND DISCUSSION

Our results indicate that the percentage of canopy cover of *Diospyrus lotus* L. was affected by the clearing size of the forest road at a probability level of 5% (Table 1). In road cross sections both with and without earth works, the percentage of *Rubus hyrcanus* L. canopy cover on filled

slopes was more than that on cut slopes. The percentage of canopy cover of this species and that of bare soil were similar, as well as the biodiversity indices for both sides of cross sections without earth works. The percentage of bare soil on cut slopes was more than that on filled slopes (Table 2).

**Table 1.** ANOVA for independent effect of the clearing size (0-10m and 10-15 m) on canopy coverage of woody and non-woody plant species along Darab Kola forest road

Species	Habit	SS	MS	F
<i>Oplismenus undulatifolius</i> (Ard) P. Beauv	Herb	726.01	726.01	3.52 ns
<i>Rubus hyrcanus</i> Juz.	Shrub	649.80	649.80	0.58 ns
<i>Lamium album</i> L.	Herb	211.25	211.25	1.98 ns
<i>Phyllitis scolopendrium</i> (L.) Newm	Herb	0.11	0.11	0.15 ns
<i>Urtica dioica</i> L.	Herb	2.81	2.81	1.00 ns
<i>Equisetum</i> sp.	Herb	31.25	31.25	3.51 ns
<i>Chelidonium majus</i> L.	Herb	1.25	1.25	0.07 ns
<i>Mentha</i> sp.	Herb	5.00	5.00	1.19 ns
<i>Petris cretica</i> L.	Herb	2.81	2.81	0.84 ns
<i>Hedera helix</i> L.	Vine	0.00	0.00	0.00 ns
<i>Hypericum androsaemum</i> L.	Herb	0.01	0.01	0.01 ns
<i>Euphorbia amygdaloides</i> L.	Herb	3.20	3.20	1.39 ns
<i>Acer insigne</i> L.	Tree	0.61	0.61	0.29 ns
<i>Brachypodium sylvaticum</i> (Huds.) Beauv.	Herb	9.11	9.11	1.56 ns
<i>Convolvulus arvensis</i> L.	Vine	165.31	165.31	1.83 ns
<i>Carex silvatica</i> (L.) Auct.	Herb	7.81	7.81	1.84 ns
<i>Diospyrus lotus</i> L.	Tree	68.45	68.45	1.55*
<i>Rumex acetossa</i> L.	Herb	16.20	16.20	4.32 ns
<i>Viola odorata</i> L.	Herb	28.80	28.80	0.50 ns
<i>Potentilla reptens</i> L.	Herb	0.31	0.31	1.00 ns
<i>Oxalis corniculatum</i> L.	Herb	1.25	1.25	1.00 ns
Bare soil		0.31	0.31	1.00 ns
Total plant coverage		1.25	1.25	1.00 ns

Note: SS = Sum of squares of error; MS = Mean square; F = Value calculated by dividing MS source with MS error in SAS software; \* = Significant in probability level of 5 %; ns = Not significant

The Simpson index revealed that in clearings 10-15 m wide, the diversity of understory species on cut slopes was significantly greater than that on filled slopes at cross sections with earth works (Table 3). Understory species diversity was higher on roads with clearings of 10-15 m. We found increased numbers of both native and exotic species associated with increased width clearings (Table 4). In Shawnigan Lake on southern Vancouver Island of British Columbia, it has been proved that after 27 years of thinning and fertilisation, there was little effect on understory

**Table 2.** ANOVA for independent effect of the cross section type (with earth works and without earth works) on canopy coverage of woody and non-woody species along Darab Kola forest road

Species	Habit	SS	MS	F
<i>Oplismenus undulatifolius</i> (Ard) P. Beauv	Herb	632.81	632.81	2.92 ns
<i>Rubus hyrcanus</i> L.	Shrub	42.05	42.05	0.05 ns
<i>Lamium album</i> L.	Herb	162.45	162.45	1.57 ns
<i>Phyllitis scolopendrium</i> (L.) Newm	Herb	0.11	0.11	0.16 ns
<i>Urtica dioica</i> L.	Herb	2.81	2.81	1.00 ns
<i>Equisetum</i> sp.	Herb	5.00	5.00	0.56 ns
<i>Chelidonium majus</i> L.	Herb	5.00	5.00	0.30 ns
<i>Mentha</i> sp.	Herb	5.00	5.00	1.18 ns
<i>Petris cretica</i> L.	Herb	2.81	2.81	0.90 ns
<i>Hedera helix</i> L.	Vine	5.00	5.00	2.76 ns
<i>Hypericum androsaemum</i> L.	Herb	1.51	1.51	0.76 ns
<i>Euphorbia amygdaloides</i> L.	Herb	8.45	8.45	3.60 ns
<i>Acer insigne</i> L.	Tree	0.11	0.11	0.06 ns
<i>Berachypodium silvaticum</i> L.	Herb	7.81	7.81	0.09 ns
<i>Convolvulus arvensis</i> L.	Vine	1.51	1.51	0.35 ns
<i>Carex sylvatica</i> (L.) Auct.	Herb	405.00	405.00	9.34**
<i>Diospyrus lotus</i> L.	Tree	0.20	0.20	0.05 ns
<i>Polygonum</i> sp.	Herb	186.05	186.05	3.38 ns
<i>Rumex acetossa</i> L.	Herb	0.31	0.31	1.00 ns
<i>Viola odorata</i> L.	Herb	1.25	1.25	1.00 ns
<i>Potentilla reptens</i> L.	Herb	0.31	0.31	1.00 ns
<i>Oxalis corniculatum</i> L.	Herb	1.25	1.25	1.00 ns
Bare soil		20.00	20.00	3.04 ns
Total plant coverage		3850.31	3850.31	13.76***

Note: SS = Sum of squares of error; MS = Mean Square; F = Value calculated by dividing MS source with MS error in SAS software; \*\*, \*\*\* = Significant in probability level of 1 and 0.1 % respectively; ns = Not significant

vegetation in terms of species richness or vegetation cover [9]. An effective way to conserve species diversity is to protect specific substrate types, e.g. tree trunks, stumps and coarse woody debris [9].

The plant diversity on cut slopes was significantly higher than that on filled slopes in clearings of 10-15 metres (Figure 3). No significant difference between cut and filled slopes was for plant diversity in clearings of less than 10 metres. In cross sections without earth works, none of the measured variables showed a statistically significant difference between the right and left sides of the road clearings (Figure 4).

Bartemucci et al. [3] found that light transmission through the canopy influenced the structure and function of understory plants more than their diversity and composition. This is likely due to the strong effect of the upper understory layers, which tend to homogenise light levels at the forest

**Table 3.** Canopy cover percentage of woody and non-woody plant species in the two clearing classes with earth works

Species	≤10 m clearing width		10-15 m clearing width	
	Cut slope	Filled slope	Cut slope	Filled slope
<i>Oplismenus undulatifolius</i> (Ard) P. Beauv	7.8	7.0	5.5	2.5
<i>Rubus hyrcanus</i> L.	24.7	57.5	19.2	69.0
<i>Lamium album</i> L.	2.0	12.7	1.5	4.0
<i>Phyllitis scolopendrium</i> (L.) Newm	0.0	0.0	0.5	0.0
<i>Urtica dioica</i> L.	0.0	0.0	0.0	1.5
<i>Equisetum</i> sp	0.0	0.0	0.0	1.5
<i>Chelidonium majus</i> L.	0.0	2.0	0.0	0.0
<i>Mentha</i> sp.	0.0	0.0	0.0	1.0
<i>Petris cretica</i> L.	0.0	1.0	0.0	1.5
<i>Hedera helix</i> L.	0.5	0.5	1.0	0.0
<i>Hypericum androsaemum</i> L.	0.9	0.0	0.3	0.0
<i>Euphorbia amygdaloides</i> L.	1.3	0.8	0.5	0.0
<i>Acer insigne</i> L.	0.5	0.0	1.3	0.0
<i>Berachypodium silvaticum</i> L.	5.5	1.0	2.5	0.0
<i>Convolvulus arvensis</i> L.	0.8	1.0	0.8	0.0
<i>Carex sylvatica</i> (L.) Auct.	0.0	0.0	0.7	0.0
<i>Diospyrus lotus</i> L.	1.5	0.5	0.0	0.0
Bare soil	54.5	16.0	64.0	18.5

floor regardless of forest type. The understory community acts as a filter, thereby reducing light levels at the forest floor to uniformly low levels [15].

Zhou et al. [16] demonstrated that forest roads tend to increase plant biomass mainly because of increased light availability, but reduce plant diversity probably due to increased competition at the edges of forests. These findings have important implications for forest conservation and landscape planning so as to maximise biodiversity and minimise habitat fragmentation and edge effects.

The abruptness of microclimate and canopy gradient is slightly higher in a laurel forest than in a pine forest due to a higher edge contrast in the former [8]. The depth of the road edge effect found in laurel and pine forests is small, but it can have cumulative effects on forest microclimate and forest associated biota at the island scale. It has been proven that the mean canopy cover on roadsides is less than the forest interior [10].

Along roadsides, coarse woody debris cover and litter depth and cover were lowest, and the abundance and diversity of native species were also lower [11]. Figure 5 shows some plants in the study area. It was apparent that the right and left sides of the road with different cleared widths had no significant effect on canopy coverage of herbaceous plants and regeneration of woody species, especially for *Rubus hyrcanus* (Table 4). Roads supported a greater diversity of plants as a result of

**Table 4.** Canopy cover percentage of woody and non-woody plant species in the two clearing classes without earth works

Species	≤10 m clearing width		10-15 m clearing width	
	Left	Right	Left	Right
<i>Oplismenus undulatifolius</i> (Ard) P. Beauv	12.3	19	9	5
<i>Rubus hyrcanus</i> L.	37	42.7	40.5	56
<i>Lamium album</i> L.	1	5.3	0.5	2
<i>Phyllitis scolopendrium</i> (L.) Newm	0.5	0	0.3	0
<i>Equisetum</i> sp.	0	0	3.5	0
<i>Chelidonium majus</i> L.	0.5	0	0.5	3
<i>Mentha</i> sp.	1	0	0.5	1.5
<i>Petris cretica</i> L.	0	0	0	1
<i>Hypericum androsaemum</i> L.	0	0.8	1	0.5
<i>Acer insigne</i> L.	0.7	0.4	0.5	0.5
<i>Sepholantara</i> sp.	1	0	0.5	0.5
<i>Berachypodium silvaticum</i> L.	2.5	7	2	0
<i>Convolvulus arvensis</i> L.	1	0.5	0	0
<i>Carex sylvatica</i> L.	3.7	2.3	9.7	3
<i>Tussila</i> sp.	1	0	2	1
<i>Polygonum</i> sp.	3.7	0	7.5	1
<i>Rumex acetossa</i> L.	0	0	0	0.5
<i>Viola odorata</i> L.	0	0	1	0
<i>Potentilla reptens</i> L.	0	0	0.5	0
<i>Oxalis corniculatum</i> L.	0	0	0	1
<i>Diospyrus lotus</i> L.	0.6	1	0	0
Bare soil	33.5	21	20.5	23.5

variation in topographic features. The management of roadside vegetation should take this into account and avoid disturbance of marginal vegetation as far as possible. Drain cleaning should be done only when necessary and mechanical clearance of roadside scrub for safety purpose would be preferable to using herbicides [12]. The main reasons for the presence of non-native species along roads are disturbance of soil and vegetation during construction, altered light conditions, as well as intentionally introduced plants (ornamentals) [14].

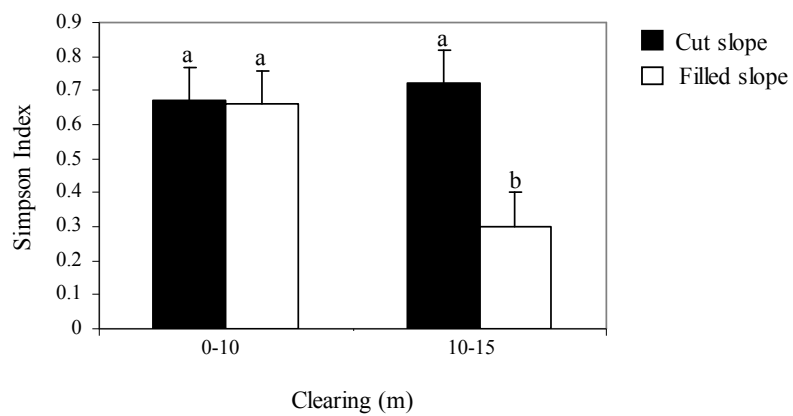


**Figure 3.** Comparison of plant diversity for different clearing widths with earth works  
(Letters a and b indicate different groups according to SNK test ( $p < 0.05$ ).)

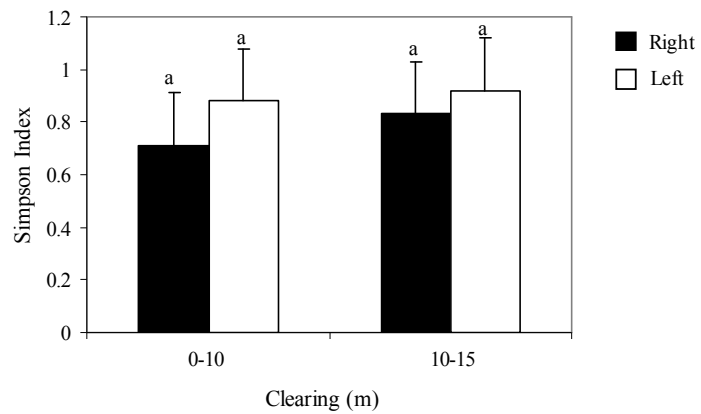


**Figure 4.** Comparison of plant diversity for different clearing widths without earth works  
(Letter a indicates same group according to SNK test ( $p < 0.05$ )).



**Figure 5.** Some plants along the Darab Kola forest road

## CONCLUSIONS

Canopy coverage was observed to show a significant effect on plant species diversity. The understory below Alder stands had significantly more species and higher species richness than the understory of other areas. This result suggests that Alder canopies create conditions to support more understory species. The percentage of bare soil on cut slopes was more than that on filled slopes. Simpson's index revealed that in clearing widths of 10-15 m, the diversity of the understory plants on cut slopes was significantly greater than that on filled slopes with earth works. Despite the importance of road gaps in the dynamics and management of many forest types, very little is known about the medium to long-term understory plant dynamics associated with this disturbance. It is proposed that the effects of roads on the chemical and physical properties of forest soils and consequently the effect on vegetation cover be investigated using PC-ORD or CANOCO softwares in future studies.

## REFERENCES

1. E. Akuzu, H. Eroglu, T. Sonmez, H. A. Yolasigmaz and T. Sariyildiz, "Effects of forest roads on foliage discoloration of oriental spruce by *Ips typographus* (L.)", *Afric. J. Agri. Res.*, **2009**, 4, 468-473.
2. J. R. Arevalo, J. D. Delgado, R. Otto, A. Naranjo, M. Salas and J. Andes-Palacios, "Exotic species in the roadside plant communities through an altitudinal gradient in Tenerife and Gran Canaria (Canary Islands)", *Plant Ecol. Evol. Syst.*, **2005**, 7, 185-202.
3. P. Bartemucci, C. Messier and C. D. Canham, "Overstory influences on light attenuation patterns and understory plant community diversity and composition in southern boreal forests of Quebec", *Can. J. For. Res.*, **2006**, 36, 2065-2079.
4. A. Cerdà, "Soil water erosion on road embankments in eastern Spain", *Sci. Total Environ.*, **2007**, 378, 151-155.
5. D. Delgado, N. L. Arroyo, J. R. Arevalo and J. Fernandez-placios, "Edge effects of roads on temperature, light, canopy cover and canopy height in laurel and pine forests (Tenerife, Canary Islands)", *Landsc. Urban Plan.*, **2007**, 81, 328-340.
6. S. Flory and C. Keith, "Invasive shrub distribution varies with distance to roads and stand age in eastern deciduous forests in Indiana, USA", *Plant Ecol.*, **2006**, 184, 131-141.
7. J. L. Gelbard and J. Belnap, "Roads as conduits for exotic plant invasions in a semiarid landscape", *Conserv. Biol.*, **2003**, 17, 420-432.
8. M. J. Hansen and A. P. Clevenger, "The influence of disturbance and habitat on the presence of non-native plant species along transport corridors", *Biol. Conserv.*, **2005**, 125, 249-259.
9. F. He and H. J. Barclay, "Long-term response of understory plant species to thinning and fertilization in a Douglas-fir plantation on southern Vancouver Island, British Columbia", *Can. J. For. Res.*, **2000**, 30, 566-572.
10. M. N. Karim and A. U. Mallik, "Roadside revegetation by native plants I. Roadside microhabitats, floristic zonation and species traits", *Ecol. Eng.*, **2008**, 32, 222-237.
11. J. N. Negishi, R. C. Sidle, S. Noguchi, A. R. Nik and R. Stanforth, "Ecological roles of roadside fern (*Dicranopteris curranii*) on logging road recovery in Peninsular Malaysia: Preliminary results", *For. Ecol. Manage.*, **2006**, 224, 176-186.
12. E. Osma, İ. İ. Özyigit, V. Altay and M. Serin, "Urban vascular flora and ecological characteristics of Kadıköy district, Istanbul, Turkey", *Maejo Int. J. Sci. Technol.*, **2010**, 4, 64-87.
13. B. C. Scharenbroch and J. G. Bockheim, "Impacts of forest gaps on soil properties and processes in old growth northern hardwood-hemlock forests", *Plant Soil.*, **2007**, 294, 219-233.
14. D. Suresh and S. Paulsamy, "Phenological observation and population dynamics of six uncommon medicinal plants in the grasslands of Nilgiris, Western Ghats, India", *Maejo Int. J. Sci. Technol.*, **2010**, 4, 185-192.
15. C. Vaidhayakarn and J. F. Maxwell, "Ecological status of the lowland deciduous forest in Chang Kian Valley, Chiang Mai, northern Thailand", *Maejo Int. J. Sci. Technol.*, **2010**, 4, 268-317.

16. T. Zhou, S. Peng, J. Wu, J. Liu and K. Wu, "Edge effects of roads on forest plant diversity and ecosystem properties: A case study from southern China", The Preliminary Program for 95th Ecological Society of America (ESA) Annual Meeting, 1-6 August **2010**, Pennsylvania, USA.

© 2011 by Maejo University, San Sai, Chiang Mai, 50290 Thailand. Reproduction is permitted for noncommercial purposes.

***Maejo International  
Journal of Science and Technology***

ISSN 1905-7873

Available online at [www.mijst.mju.ac.th](http://www.mijst.mju.ac.th)

*Full Paper*

**Dynamic changes in enzyme activities and phenolic content  
during in vitro rooting of tree peony (*Paeonia suffruticosa*  
Andr.) plantlets**

Zhenzhu Fu<sup>1</sup>, Panpan Xu<sup>1</sup>, Songlin He<sup>1,\*</sup>, Jaime A. Teixeira da Silva<sup>2</sup> and Michio Tanaka<sup>2</sup>

<sup>1</sup>Faculty of Forestry, Henan Agricultural University, No.95 Wenhua Road, Zhengzhou 450002, China

<sup>2</sup>Department of Horticultural Science, Faculty of Agriculture and Graduate School of Agriculture, Kagawa University, Miki-cho, Ikenobe 2393, Kagawa-ken 761-0795, Japan

\* Corresponding author, e-mail: hsl213@163.com

Received: 15 April 2011 / Accepted: 4 July 2011 / Published: 28 July 2011

**Abstract:** The dynamic changes of phenolic content and peroxidase (POD), polyphenol oxidase (PPO), indole-3-acetic acid oxidase (IAAO) and phenylalanine ammonia lyase (PAL) activities were assessed during the in vitro rooting process of three cultivars of tree peony (*Paeonia suffruticosa* Andr.). These changes in enzyme-related activity and phenolic content—observed at the level of the whole plant—differed during the first 20 days of the rooting process in easy-to-root ‘Feng Dan Bai’ cultivar and difficult-to-root ‘Wu Long Peng Sheng’ and ‘Tai Ping Hong’ cultivars, and in most cases they were actually opposite. The ease with which ‘Feng Dan Bai’ was able to root was closely related to the activity of all four enzymes (POD, PPO, IAAO, PAL) as well as to the phenolic content.

**Keywords:** tree peony, *Paeonia suffruticosa*, rooting, enzyme activities, phenolic content, dynamic changes

---

## INTRODUCTION

Tree peony (*Paeonia suffruticosa* Andr, Paeoniaceae) is a perennial woody flowering ornamental plant and a famous traditional flower in China [1-2]. Tree peony tissue culture is in vogue since traditional breeding methods have limitations [3]. However, it has not yet been able to meet the requirements for mass production due to difficulty in rooting and the low root quality of plantlets in vitro [4]. Therefore, solving the problem of rooting in vitro may be a key for a breakthrough in tree peony tissue culture.

There is a close relationship between the occurrence of adventitious roots in plants and their peroxidase (POD, EC 1.11.1.7), polyphenoloxidase (PPO, EC 1.10.3.1), indole-3-acetic acid oxidase (IAAO, no EC number) and phenylalanine ammonia lyase (PAL, EC 4.3.1.5) activities as well as their phenolic content. These enzymes have different functions during rooting [5-6]. Increasing POD activity is a rooting signal in the induction and formation of root primordia [7-8]. POD is involved in auxin metabolism and in the lignification of cell walls in the presence of phenolic compounds [9]. PPO is the main enzyme causing the oxidation of phenolic compounds; it can also catalyse phenolic compounds and IAA to form IAA-phenolic complexes, which promote the occurrence and development of adventitious roots [10]. IAAO affects the occurrence of adventitious roots in plants by oxidising IAA and changing its levels [11-12]. PAL is a key enzyme involved in the synthesis of phenolic compounds [13-14]. PAL activity and total phenolic content of lettuce plants and *Phalaenopsis* orchids were significantly correlated with browning [5-6,15]. There is a yet-to-be-disproved train of thought that an important difference between easy-to-root and difficult-to-root cultivars lies in the difference in the content of phenolic compounds: the former is thought to contain less polyphenols than the latter [16].

In order to provide a theoretical and mechanistic basis for the establishment of efficient rooting during the tissue culture of tree peony, this experiment aims to determine the dynamic changes in POD, PPO, IAAO and PAL activities and total phenol content during the in vitro rooting culture of tree peony cultivars in order to establish whether a relationship between the activities of these enzymes and the phenolic metabolism exists. If a correlation between rooting ability and enzyme activity could be established, this would open up a gateway for molecular manipulation of the plants to increase the level of those enzymes that would permit greater and more successful in vitro rooting, and hence for a successful micropropagation of this ornamental plant. Since rooting and root formation are both poorly understood and equally poorly achieved for this ornamental, an understanding of the enzymatic and biochemical dynamics is expected to provide vital clues to how better to try and improve its in vitro rooting.

## MATERIALS AND METHODS

### Chemicals and Reagents

All chemicals and reagents used in this study were of tissue culture or HPLC grade. Murashige and Skoog (MS) medium [17] and woody plant medium (WPM) [18] were made fresh from MS stocks and WPM stocks respectively. Other more important chemicals and reagents were purchased from the following companies: Phytagel, Folin-Ciocalteu's reagent and agar powder from Solarbio Science and Technology Co. Ltd., Beijing, China; 1-naphthaleneacetic acid (NAA) from Huixing Chemical Reagents Ltd., Shanghai, China; 6-benzylaminopurine (6-BA), indole-3-acetic acid (IAA) and indole-3-butyric acid (IBA) from Boao Biotech Co. Ltd., Shanghai, China; guaiacol and L-phenylalanine from Guangfu Chemical Institute, Tianjin, China; catechol, gallic acid and polyvinylpyrrolidone-30 (PVP-30) from Ke Miou Chemical Reagents Development Centre, Tianjin, China; trichloroacetic acid, ferric chloride and sucrose from Guanghua Chemical Reagents Ltd., Guangzhou, China; manganese chloride from Xilong Chemical Factory, Shantou, China; 2,4-

dichlorophenol from China National Pharmaceutical Industry Corp. Ltd., Shanghai, China;  $\beta$ -mercaptoethanol from Tianrui Chemical Co. Ltd., Shanghai, China. Phosphate and borate buffers were made fresh.

### **Plant Material and Culture Media**

The axillary buds of tree peony from uniform, clonally propagated in vitro stock mother plants, originally derived from 5-year-old ex vitro plants, were used. Three tree peony cultivars ('Feng Dan Bai', 'Wu Long Peng Sheng' and 'Tai Ping Hong') were gathered from Luoyang City in February, 2010.

Axillary buds were placed on MS medium supplemented with 0.3 mg/l of NAA, 0.3 mg/l of 6-BA and 3% of sucrose and solidified by 7.5 g/l of agar powder in 100-ml flasks (three axillary buds per flask) after sterilisation of the culture at  $24\pm1^{\circ}\text{C}$ . The flasks were placed under a 12-h photoperiod at  $36 \mu\text{mol m}^{-2}\text{s}^{-1}$ . After 35 days, standardised shoots formed (4-5 leaves, ~5 cm in height, and no roots), and these were used as explants for all subsequent experiments.

### **Assay Methods**

Adventitious shoots (one per flask) were transferred to WPM supplemented with 4 mg/l of IBA and 3% of sucrose, and solidified by 2.0 g/l of Phytagel for culture under the same conditions as for shoot induction. No antioxidant compounds were added to the medium. The enzyme activities and total phenolic content of whole plantlets were determined after culturing for 0, 1, 2, 3, 4, 5, 7, 9, 12, 15 and 20 days. Ten plantlets were cut into small pieces and mixed, and 0.5-g aliquots were used in enzyme assays. Each treatment contained 10 replicates and was repeated three times.

All media used were adjusted to pH 5.8 (measured with a pH-3B meter, Hongyi Instrument Co., Shanghai, China) with 1 M NaOH before autoclaving at  $121^{\circ}\text{C}$  for 15 min at 121 psi.

#### *POD activity*

The plantlets (0.5 g) from different rooting culture periods were ground immediately on ice by adding 5 ml of phosphate buffer (pH 7.0). The crude enzyme extract was obtained after centrifugation at  $12085\times g$  for 15 min at  $4^{\circ}\text{C}$ . POD activity was measured following the Guaiacol method [19]. Briefly, 0.3 ml of crude enzyme, 2.0 ml of phosphate buffer (pH 7.0), 0.5 ml of 0.2% aqueous guaiacol and 0.5 ml of 0.15%  $\text{H}_2\text{O}_2$  were mixed. POD absorbance values were recorded immediately at 470 nm using a UV-3200 spectrophotometer (Mei Puda Instrument Co., Shanghai, China). One unit of POD activity is equivalent to an increase in 0.01 times the amount of enzyme for 1 g of fresh weight/min.

#### *PPO activity*

The plantlets (0.5 g) from different rooting culture periods were ground immediately on ice by adding 5 ml of phosphate buffer (pH 6.0). The crude enzyme extract was obtained after centrifugation at  $12085\times g$  for 15 min at  $4^{\circ}\text{C}$ . PPO activity was measured according to Zhu et al. [20]. Briefly, 0.1 ml crude enzyme, 3.9 ml phosphate buffer (pH 6.0) and 1 ml 0.1 M aqueous catechol

were mixed in a 30°C water bath for 10 min. Then 2 ml of 20% trichloroacetic acid was added quickly to stop the reaction. PPO absorbance values were recorded immediately at 525 nm. One unit of PPO activity is equivalent to an increase in 0.01 times the amount of enzyme for 1 g of fresh weight/min.

#### *IAAO activity*

The activity of IAAO, extracted by the same method as that for PPO, was measured according to Zhang [21]. Briefly, 1 ml crude enzyme, 2 ml 1 mM aqueous MnCl<sub>2</sub>, 1 ml 1 mM aqueous 2,4-dichlorophenol, 2 ml 1 mM aqueous IAA and 5 ml phosphate buffer (pH 6) were mixed in a 30°C water bath for 30 min. Then 2 ml of this mixture and 4 ml of reaction solution (1.0 ml 0.5M FeCl<sub>3</sub> + 50 ml 35% perchloric acid) were mixed in the dark in a 30°C water bath for 30 min. IAAO absorbance values were recorded at 530 nm. One unit of IAAO activity was expressed in terms of µg of IAA degraded/g fresh weight/h.

#### *PAL activity*

The plantlets (0.5 g) from different rooting culture periods were ground immediately on ice with addition of 5 ml pre-cooled 0.1 M borate buffer (pH 8.8, containing 5 mM β-mercaptoethanol and 0.25 g PVP-30). The supernatant was used for the determination after centrifugation at 12085×g for 15 min at 4°C. PAL activity was measured by the method of Li [22] with minor modifications. Briefly, 1 ml crude enzyme, 1 ml 0.02 M L-phenylalanine in borate buffer (pH 8.8) and 2 ml distilled water were mixed in a 30°C water bath for 30 min. PAL absorbance values were measured at 290 nm using water as control. One unit of PAL activity is equivalent to an increase in 0.01 times the amount of enzyme for 1 g of fresh weight/h.

#### *Total phenolic content*

Polyphenols were extracted by a methanol and water extraction method [23]. Plantlets (0.5 g) from different rooting culture periods were placed in a 55°C water bath for 30 min after grinding in 5 ml of 40% methanol. A crude extract of polyphenols was obtained after centrifugation at 3000×g for 10 min. Polyphenols content was determined by the Folin-Ciocalteu method [24]. Briefly, 1.0 ml of crude polyphenol extract, 1.0 ml of distilled water, 0.5 ml of Folin-Ciocalteu's reagent and 0.5 ml of 7.5% Na<sub>2</sub>CO<sub>3</sub> were mixed for the reaction to take place at room temperature for 1 h. Absorbance values were then recorded at 765 nm using water as control. Gallic acid was used as standard. The total phenolic content was expressed as µg/g fresh weight.

#### *Morphological parameters*

Rooting percentage, average number of roots/plant, and root length (i.e. total length of all roots/total root number) of the three cultivars were determined after 60 days of rooting since root tips would emerge, on average, within 30-40 days while all roots appeared within 40-50 days of culture. The rooting index (RI) [25] was calculated as: RI = average number of roots/plant × root length × % rooting (where % rooting = (number of plants that formed roots / total number of plants)

$\times 100$ ). RI is a composite indicator for the measurement of root conditions that can fully explain the degree of difficulty of in vitro rooting.

#### *Experimental design and statistical analyses*

In all experiments, each treatment had 10 samples per treatment (tissue culture and biochemical experiments) and was repeated in triplicate. Means were separated by one-way analysis of variance and significant differences were assessed using Duncan's multiple range test at  $P = 0.05$  using DPS software version 3.01.

## RESULTS AND DISCUSSION

### **Rooting**

The rooting percentage and RI were significantly different ( $P < 0.05$ ) among the three tree peony cultivars. The rooting percentage of 'Feng Dan Bai' was highest (51.72%) with RI of 5.2, while rooting percentages of 'Wu Long Peng Sheng' and 'Tai Ping Hong' were lowest, i.e. 13.8 and 14.29% respectively (RI = 1.94 and 1.61 respectively; Table 1). From the results it can be concluded that 'Feng Dan Bai' is an easy-to-root cultivar while 'Wu Long Peng Sheng' and 'Tai Ping Hong' are difficult-to-root cultivars.

**Table 1.** Rooting in three tree peony cultivars (n = 30)

Cultivar	Root number	Root length (cm)	Rooting percentage	Rooting index (RI)
Feng Dan Bai	$2.8 \pm 0.2$ a	$3.59 \pm 0.6$ b	$51.72 \pm 3.23$ a	$5.2 \pm 0.71$ a
Wu Long Peng Sheng	$2.0 \pm 1$ a	$7.03 \pm 2.16$ a	$13.8 \pm 5.48$ b	$1.94 \pm 1.14$ b
Tai Ping Hong	$2.25 \pm 0.58$ a	$5.02 \pm 1.5$ ab	$14.29 \pm 5.2$ b	$1.61 \pm 0.7$ b

Note: Each value is the mean  $\pm$  SD of triplicate. Different letters within a column indicate significant difference at  $P < 0.05$  according to DMRT.

### **POD Activity**

POD activity changed during the in vitro rooting of the three tree peony cultivars (Figure 1). The change in POD activity of 'Feng Dan Bai' showed a jagged trend, peaking twice on the 3<sup>rd</sup> and 9<sup>th</sup> days. The activity was significantly different ( $P < 0.05$ ) from that of 'Tai Ping Hong' and 'Wu Long Peng Sheng' in the early days of rooting culture. The activity of 'Tai Ping Hong' and 'Wu Long Peng Sheng' was not significantly different, although a similar jagged trend was observed, albeit with a lower amplitude.

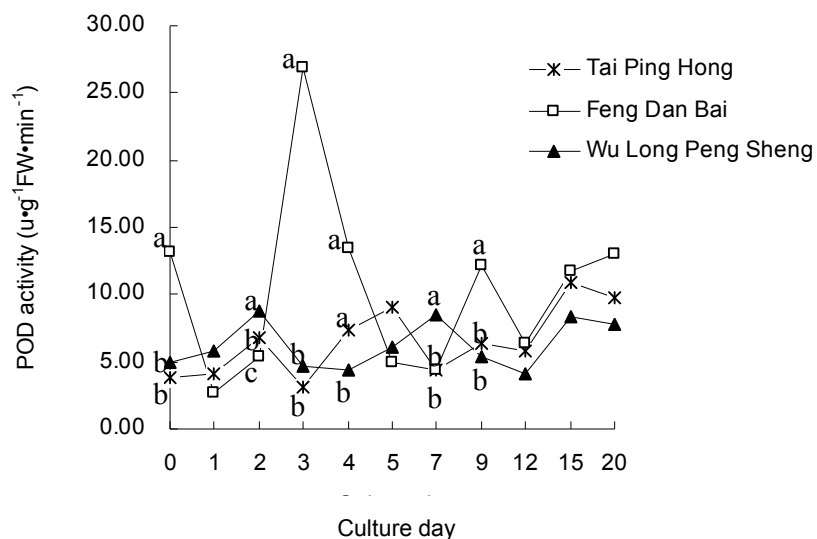


**Figure 1.** Trends in POD activity change in plantlets of different cultivars during the rooting process. Different letters in each column indicate significant difference between the three cultivars on the same day at  $P < 0.05$  using DMRT. Non-significant differences on some days are not indicated by any letters. Each treatment had 10 samples and was repeated in triplicate.

Some studies have shown that there is a close relationship between the activity of POD, PPO and IAAO and the occurrence and growth of adventitious roots in plants and that the changes in these enzymes differ at different periods of rooting [26]. Other studies indicated that the increase in POD activity was a signal of rooting ability in the periods of root induction and expression [7, 27], implying that POD activity would reach two peaks in the induction and expression periods. Pacheco et al. [28] also observed two peaks in the vitro rooting of *Eucalyptus globulus* cuttings, the first on the first day of rooting culture, which might have been related to root induction, and the second peak on the 10<sup>th</sup> day when the root had broken through the epidermis. In our study, the POD activity of easy-to-root ‘Feng Dan Bai’ cultivar had two peaks on the 3<sup>rd</sup> and 9<sup>th</sup> day, corresponding to possible root primordium induction and expression. However, POD activity of ‘Tai Ping Hong’ and ‘Wu Long Peng Sheng’ did not have the same behaviour as that of ‘Feng Dan Bai’. Molassiotis et al. [29] observed that the rooting stems of rootstock GF-677 (*Prunus amygdalus* × *P. persica*) showed a maximum soluble POD activity on the 9<sup>th</sup> day and peaked in ionically-bound POD to cell wall POD activity on the 6<sup>th</sup> and 12<sup>th</sup> days on the rooting medium; a similar behaviour was not observed in non-rooting stems. In the case of the KIBA (potassium salt indole-3-butryic acid) treatment of *A. unedo* genotype D, POD activity showed one peak on day 10, but in the control treatment there was no peak in activity [30].

### PPO Activity

PPO activity changed during the in vitro rooting of the three tree peony cultivars (Figure 2). The activity showed a jagged trend with peaks and troughs similar for all three cultivars. The activity in ‘Feng Dan Bai’ peaked on the 4<sup>th</sup> day and was significantly higher than in ‘Tai Ping Hong’ and

‘Wu Long Peng Sheng’. The activity was also significantly different ( $P < 0.05$ ) among the three tree peony cultivars on the 7<sup>th</sup> and 15<sup>th</sup> day.

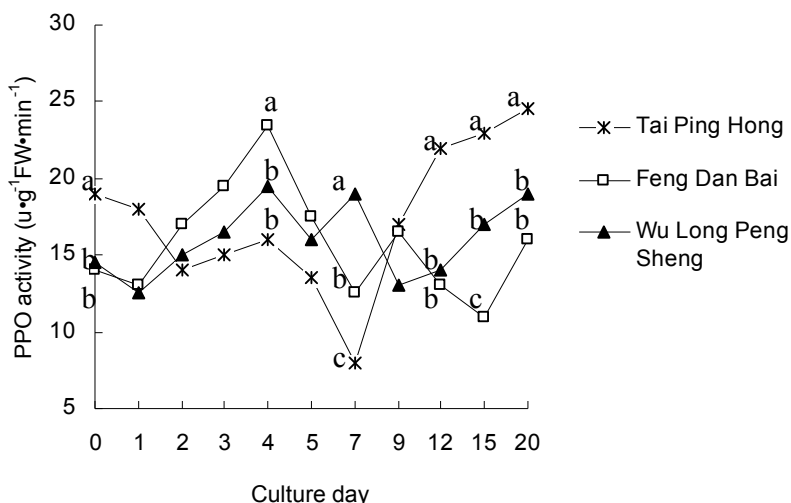


**Figure 2.** Trends in PPO activity change in plantlets of different cultivars during the rooting process. Different letters in each column indicate significant difference between the three cultivars on the same day at  $P < 0.05$  using DMRT. Non-significant differences on some days are not indicated by any letters. Each treatment had 10 samples and was repeated in triplicate.

Bhattacharya [31] proved that PPO can catalyse the metabolism of auxin, promoting the generation and development of adventitious roots. Moreover, PPO can also catalyse phenolic compounds and IAA to form ‘IAA-phenol complexes’, which would be a type of rooting cofactor that can promote the occurrence and development of adventitious roots [27]. In this experiment on tree peony, after 3-4 days of culture, the PPO activity of all three cultivars increased, the increase being significantly greater, however, in easy-to-root ‘Feng Dan Bai’ than in difficult-to-root ‘Tai Ping Hong’ and ‘Wu Long Peng Sheng’, which may be more advantageous to the formation of ‘IAA-phenol complexes’ that promote the induction of root primordia. During days 12-15 of rooting, the PPO activity of ‘Tai Ping Hong’ and ‘Wu Long Peng Sheng’ continued to rise, while that of ‘Feng Dan Bai’ began to drop and became significantly lower than that of the other two cultivars on the 15<sup>th</sup> day. This reduction in PPO activity may have participated in or been responsible for the formation of root primordia. Molnar and Lacroix [32] found that when *Hydrangea macrophylla* formed adventitious roots from stem tissue, PPO activity increased dramatically when the root tip emerged. Habaguchi [33] observed the same result in carrot callus culture: when root tips emerged from callus, PPO activity increased sharply. In this study on tree peony, after rooting for 20 days, the PPO activity of all three cultivars increased, which may be related to the emergence of root tips.

### IAAO Activity

The changes in IAAO activity during rooting of the three tree peony cultivars are shown in Figure 3. Similarly to POD and PPO, IAAO activity was jagged for all three cultivars and was higher in ‘Tai Ping Hong’ and ‘Wu Long Peng Sheng’ than in ‘Feng Dan Bai’ at all times, particularly on

the 2<sup>nd</sup>, 3<sup>rd</sup>, 7<sup>th</sup> and 9<sup>th</sup> days. The activity was similar in ‘Tai Ping Hong’ and ‘Wu Long Peng Sheng’ on the 2<sup>nd</sup>, 3<sup>rd</sup>, 4<sup>th</sup>, 5<sup>th</sup>, 9<sup>th</sup> and 12<sup>th</sup> days. It was significantly different ( $P < 0.05$ ) among the three tree peony cultivars on the 7<sup>th</sup> day.

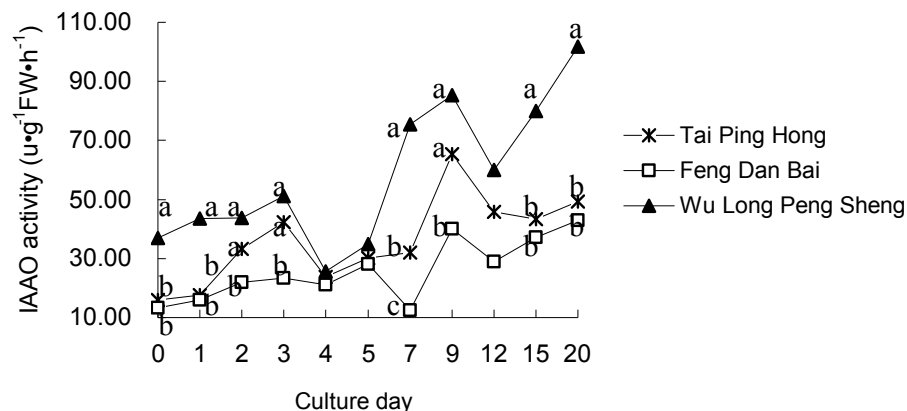


**Figure 3.** Trends in IAAO activity change in plantlets of different cultivars during the rooting process. Different letters in each column indicate significant difference between the three cultivars on the same day at  $P < 0.05$  using DMRT. Non-significant differences on some days are not indicated by any letters. Each treatment had 10 samples and was repeated in triplicate.

IAAO can degrade IAA and modify its level in plants, thereby affecting the rooting of plantlets, and it is theoretically likely that there is a high IAAO activity (in roots, leaves and stems) in difficult-to-root cultivars, which can strongly degrade IAA [34-35]. In this case, more IAA is destroyed and consequently little IAA would be transported downwards to the roots, resulting in few or no roots being induced. Conversely, an easy-to-root cultivar would have a low IAAO activity and hence a lower ability to degrade IAA that facilitates rooting [36]. In this study, IAAO activity of ‘Feng Dan Bai’ was consistently lower than that of ‘Tai Ping Hong’ and ‘Wu Long Peng Sheng’.

Consistent with the results of our study, Hu et al. [26] found that the IAAO activity in *Corylus avellana* cuttings was higher in the control (0% of rooting) than in the plants treated with IBA (60% of rooting). The IAAO activity of *Camellia sinensis* (L.) Kuntze was also higher in the control (0% rooting) cuttings as compared to IBA-treated cuttings (92.6% rooting) [9]. IAAO activity in *Vigna radiata* L. cv. 105 remained higher in controls than in cuttings treated with PUT and IBA [37].

### PAL Activity

The PAL activity followed a pattern similar to that of POD, PPO and IAAO during the in vitro rooting of the three tree peony cultivars (Figure 4). The activity is similar among the three tree peony cultivars on the 0, 1<sup>st</sup>, 2<sup>nd</sup>, 4<sup>th</sup>, 5<sup>th</sup> and 12<sup>th</sup> days, although there were significant differences on the 3<sup>rd</sup> day. PAL activity of ‘Feng Dan Bai’ was also significantly lower than that of ‘Tai Ping Hong’ and ‘Wu Long Peng Sheng’ on the 7<sup>th</sup> and 9<sup>th</sup> days.

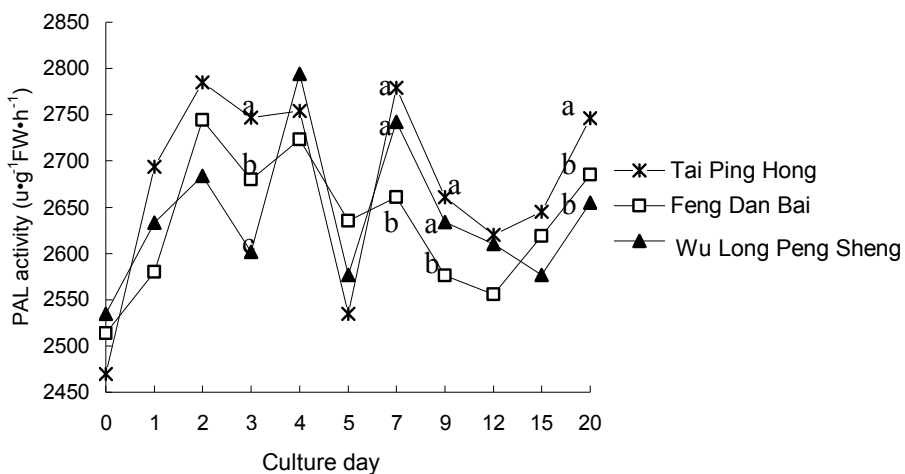


**Figure 4.** Trends in PAL activity change in plantlets of different cultivars during the rooting process. Different letters in each column indicate significant difference between the three cultivars on the same day at  $P < 0.05$  using DMRT. Non-significant differences on some days are not indicated by any letters. Each treatment had 10 samples and was repeated in triplicate.

PAL is a key enzyme in the synthesis of phenolic acids and its activity is affected by external and internal factors in cells [38]. Highly positive correlations were observed between phenolic content and PAL activity or free phenylalanine content in buds and scales in *Lilium davidii* var. *unicolor* bulbs [39]. The total phenolic content of three varieties of *Phalaenopsis* was positively correlated with their PAL activity during tissue culture [40]. Smith-Becker et al. [41] observed that the constitutive activity of PAL in stems and petioles of cucumber was approximately 20-fold higher than in leaves. However, no difference in PAL activity was detected between control and plants inoculated with *Pseudomonas syringae* pv. *syringae* in the leaf directly above the inoculated leaf. In this study, there were changes in PAL activity during the rooting process, implying that PAL participated in the rooting process of tree peony plantlets. However, there was no significant difference in the activity among the three tree peony cultivars, and there was no correlation with the total phenolic content, which seemed to indicate that PAL did not play a leading role in the rooting of tree peony plantlets. Other factors which may be at play would have to be further studied.

### Total Phenolic Content

Figure 5 shows changes in the total phenolic content during the in vitro rooting of the three tree peony cultivars. The jagged patterns of ‘Tai Ping Hong’ and ‘Wu Long Peng Sheng’ were similar to each other, but different from that of ‘Feng Dan Bai’. Except for the 1<sup>st</sup> and 12<sup>th</sup> days of rooting, the phenolic content of ‘Feng Dan Bai’ was significantly higher than that of ‘Tai Ping Hong’ and ‘Wu Long Peng Sheng’ during day 2-7 and day 15-20 of rooting.

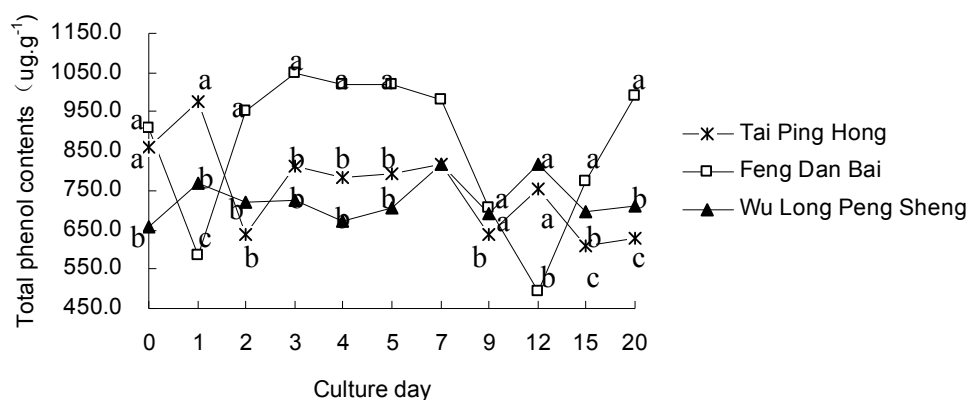


**Figure 5.** Trends in total phenolic content change in plantlets of different cultivars during the rooting process. Different letters in each column indicate significant difference between the three cultivars on the same day at  $P<0.05$  using DMRT. Non-significant differences on some days are not indicated by any letters. Each treatment had 10 samples and was repeated in triplicate.

The function of phenolic compounds in rooting is well established. Hartman et al. [16] proposed one view: differences in the content of phenols indicate differences between easy-to-root and difficult-to-root cuttings, the former having a higher content of phenols than the latter. The content of some flavonoids in *Eucalyptus* seedlings was positively correlated with rooting ability [42]. In a *Rhizobium* isolate of *Vigna mungo* (mung bean), the root nodules contained a higher amount of IAA and phenolic acids than non-nodulated roots [43]. Another study showed that exogenous phenolic compounds and IAA, when used in conjunction, could synergistically promote rooting. Pentahydroxyflavone plus IBA, for example, significantly increased the rooting rate of walnut [44]. In this experiment, the total phenolic content of easy-to-root 'Feng Dan Bai' was also generally higher than that of difficult-to-root 'Wu Long Peng Sheng' and 'Tai Ping Hong', which is in line with the above observations and implies an active role of phenolic compounds in the promotion of rooting.

## CONCLUSIONS

Enzyme-related activities and total phenol content, which were related to the rooting of tree peony, changed in the first 20 days (early phase of in vitro rooting) for all three tree peony cultivars. These changes differed over the rooting period and there were significant differences between easy-to-root 'Feng Dan Bai' and difficult-to-root 'Wu Long Peng Sheng' and 'Tai Ping Hong' cultivars as determined initially by RI values. POD activity and total phenolic content were higher in easy-to-root 'Feng Dan Bai' cultivar than in difficult-to-root 'Tai Ping Hong' and 'Wu Long Peng Sheng' cultivars on the whole, while IAAO activity was lower in 'Feng Dan Bai' than in 'Tai Ping Hong' and 'Wu Long Peng Sheng' throughout the entire experimental period. However, no clear conclusions could be drawn for PPO and PAL activities in relation to the rooting ability of the three tree peony cultivars. The changes in the activity of the POD and IAAO enzymes and phenol content can thus be used as a marker and predictor of rooting ability in tree peony during the early days of in vitro rooting as depicted in Figure 6.

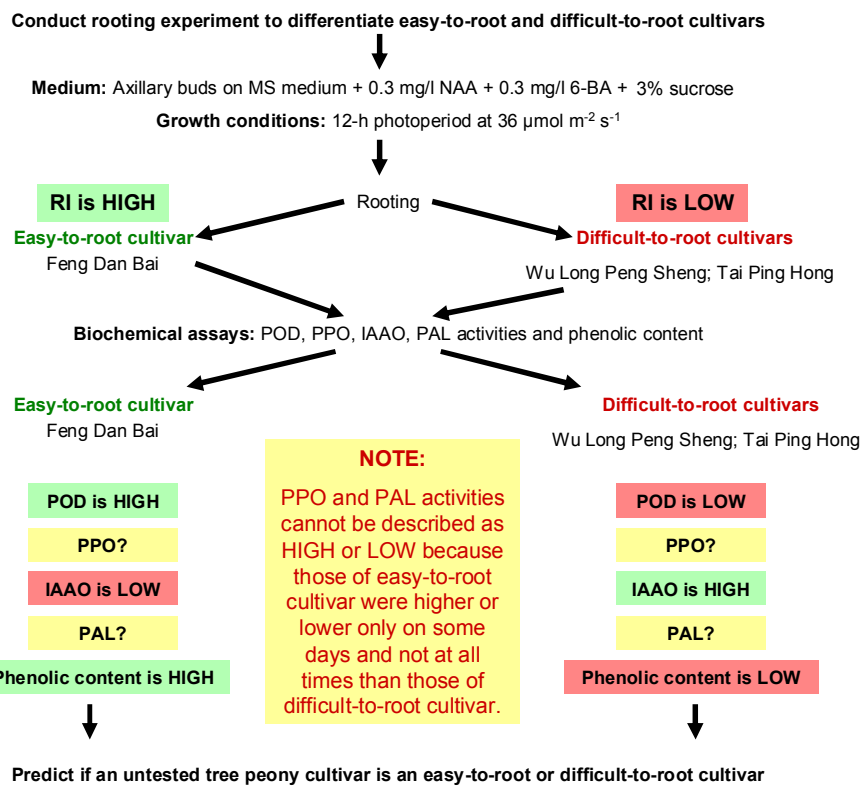


**Figure 6.** Proposed scheme for classifying a tree peony cultivar into easy-to-root or difficult-to-root cultivar based on RI value and other biochemical parameters. Note that RI, POD and IAAO represent ‘stable’ parameters while PPO and PAL are ‘unstable’ parameters for predicting the nature of in vitro rooting of a cultivar.

## REFERENCES

1. D. F. Lu, “Floriculture”, China Agriculture Press, Beijing, **1998**.
2. M. Z. Bao, “Floriculture”, 2<sup>nd</sup> Edn., China Agriculture Press, Beijing, **2003**.
3. Y. L. Li, D. Y. Wu, S. L. Pan and S. L. Xu, “The study on micropropagation technology of tree peony plantlets in vitro”, *Chinese Sci. Bull.*, **1984**, 8, 500-502.
4. L. Bouza, M. Jacques, B. Sotta and E. Miginiac, “The reactivation of tree peony (*Paeonia suffruticosa* Andr.) vitro plants by chilling is correlated with modifications of abscisic acid, auxin and cytokinin levels”, *Plant Sci.*, **1994**, 97, 153-160.
5. M. Murata, M. Nishimura, N. Murai, M. Haruta, S. Homma and Y. Itoh, “A transgenic apple callus showing reduced polyphenol oxidase activity and lower browning potential”, *Biosci. Biotechnol. Biochem.*, **2001**, 65, 383-388.
6. H. Hisamimoto, M. Murata and S. Homma, “Relationship between the enzymatic browning and phenylalanine ammonia-lyase activity of cut lettuce, and the prevention of browning by inhibitors of polyphenol biosynthesis”, *Biosci. Biotechnol. Biochem.*, **2001**, 65, 1016-1021.
7. C. Moncousin and T. H. Gaspar, “Peroxidase as a marker for rooting improvement of *Cynara scolymus* L. cultivated in vitro”, *Biochem. Physiol. Pflanz.*, **1983**, 178, 263-271.

8. A.-C. Nordstrom and L. Eliasson, "Levels of endogenous indole-3-acetic acid and indole-3-acetylaspartic acid during adventitious root formation in pea cuttings", *Physiol. Plant.*, **1991**, 82, 599-605.
9. R. R. Gyana, "Effect of auxins on adventitious root development from single node cuttings of *Camellia sinensis* (L.) Kuntze and associated biochemical changes", *Plant Growth Reg.*, **2006**, 48, 111-117.
10. G. Balakrishnamurthy and V. N. M. Rao, "Changes in phenols during rhizogenesis in rose (*Rosa bourboniana* Desp)", *Curr. Sci.*, **1988**, 17, 960-962.
11. S. Rama Devi and M. N. V. Prasad, "Ferulic acid mediated changes in oxidative enzymes of maize seedlings: Implication in growth", *Biol. Plant.*, **1996**, 38, 387-395.
12. B. Kieliszewska-Rokicha, "Effect of treating Scots pine (*Pinus sylvestris* L.) seedlings with phytohormone on the growth of the root system and on the peroxidase and IAA oxidase enzyme activities in roots", *Arboretum-Kornckie*, **1989**, 32, 207-219.
13. B. Winkel-Shirley, "Evidence for enzyme complexes in the phenylpropanoid and flavonoid pathways", *Physiol. Plant.*, **1999**, 107, 142-149.
14. B. Weisshaar and G. I. Jenkins, "Phenylpropanoid biosynthesis and its regulation", *Curr. Opin. Plant Biol.*, **1998**, 1, 251-257.
15. F. Yin, H. Ge, K. Q. Peng, L. L. Zhao, Y. J. Zhou and Q. X. Li, "Relationship between tissue browning and phenolic acids and related enzymes in *Phalaenopsis*", *Sci. Agric. Sin.*, **2008**, 41, 2197-2203.
16. H. T. Hartman, D. E. Kester, F. T. Davies and R. L. Geneve, "Plant Propagation: Principles and Practices", 6th Edn., Prentice Hall of India, New Delhi, **1996**, pp.280-284.
17. T. Murashige and F. Skoog, "A revised medium for rapid growth and bioassays with tobacco tissue cultures", *Physiol. Plant.*, **1962**, 15, 473-497.
18. D. G. Lloyd and B. H. McCown, "Commercially feasible micropropagation of mountain laurel, *Kalima latifolia* by use of shoot-tip culture", *Proc. Int. Plant Prop. Soc.*, **1980**, 30, 421-427.
19. J. M. Cutler, K. W. Shahan and P. L. Steponkus, "Influence of water deficits and osmotic adjustment on leaf elongation in rice", *Crop Sci.*, **1980**, 20, 314-318.
20. G. L. Zhu, H. W. Zhong and A. Q. Zhang, "Plant Physiology Experiment", Beijing University Press, Beijing, **1990**, pp.37-39.
21. Z. L. Zhang, "Plant Physiology Experiment Guidance", 2nd Edn., Higher Education Press, Beijing, **1990**, pp.210-212.
22. H. S. Li, "Plant Physiology and Biochemistry Experiment Principle and Technology", Higher Education Press, Beijing, **2003**, pp.164-165.
23. S. Gorinstein, R. Haruenkit, Y. S. Park, S. T. Jung, Z. Zachwieja, Z. Jastrzebski, E. Katrich, S. Trakhtenberg and B. O. Martin, "Bioactive compounds and antioxidant potential in fresh and dried Jaffa sweeties, a new kind of citrus fruit", *J. Sci. Food Agric.*, **2004**, 84, 1459-1463.
24. E. Pastrana-Bonilla, C. C. Akoh, S. Sellappan and G. Krewer, "Phenolic content and antioxidant capacity of Muscadine grapes", *J. Agric. Food Chem.*, **2003**, 51, 5497-5503.

25. X. J. Lu, Z. Feng, L. Y. Zhao, L. G. Feng and S. C. Yu, "The effect of polyphenol content and polyphenol oxidase activity on in vitro rooting of Pingyin rose cultivars", *Acta Hortic. Sin.*, **2007**, 34, 695-698.
26. H. J. Hu, B. H. Cao, W. L. Yin, M. P. Zhai, Q. Tang and B. Jia, "Effects of different treatments on hardwood-cutting rooting and related oxidase activity changes during rooting of *Corylus avellana*", *Sci. Silvae Sin.*, **2007**, 43, 70-75.
27. B. E. Haissig, "Influence of auxins and auxin synergists on adventitious root primordium initiation and development", *NZ. J. For. Sci.*, **1974**, 4, 311-323.
28. P. Pacheco, X. Calderon and A. Vega, "Flavonoids as regulators and markers of root formation by shoots of *Eucalyptus globulus* raised in vitro", *Plant Perox. Newslett.*, **1995**, 5, 9-12.
29. A. N. Molassiotis, K. Dimassi, G. Diamantidis and I. Therios, "Changes in peroxidases and catalase activity during in vitro rooting", *Biol. Plant.*, **2004**, 48, 1-5.
30. J. M. Demetrios, D. S. Thomas, Y. Traianos and S. E. Athanasios, "Peroxidases during adventitious rooting in cuttings of *Arbutus unedo* and *Taxus baccata* as affected by plant genotype and growth regulator treatment", *Plant Growth Reg.*, **2004**, 44, 257-266.
31. N. C. Bhattacharya, "Enzyme activities during adventitious rooting", in "Adventitious Root Formation in Cuttings" (Ed. T. D. Davis, B. E. Haissig, and N. Sankhla), Dioscorides Press, Portland, **1988**, pp.88-101.
32. J. M. Molnar and L. J. Lacroix, "Studies of the rooting of cuttings of *Hydrangea macrophylla*: Enzyme changes", *Canadian J. Bot.*, **1972**, 50, 315-322.
33. K. Habaguchi, "Alterations in polyphenol oxidase activity during organ redifferentiation in carrot calluses cultured in vitro", *Plant Cell Physiol.*, **1977**, 18, 181-189.
34. M. B. Jackson, "New Root Formation in Plant and Cuttings", Martinus Nijhoff Publishers, Lancaster, **1986**, pp. 223-253.
35. K. Gebhardt, "Activation of indole-3-acetic acid oxidase from horseradish and *Prunus* by phenols and H<sub>2</sub>O<sub>2</sub>", *Plant Growth Reg.*, **1982**, 1, 73-84.
36. M. Li, Z. L. Huang, S. M. Tan, X. Y. Mao, H. Q. Lin and T. Long, "Comparison on the activities and isoenzymes of polyphenol oxidase and indoleacetic acid oxidase of difficult and easy to root eucalyptus species", *Forest Res.*, **2000**, 13, 493-500.
37. S. Nag, K. Saha and M. A. Choudhuri, "Role of auxin and polyamines in adventitious root formation in relation to changes in compounds involved in rooting", *J. Plant Growth Reg.*, **2001**, 20, 182-194.
38. A. Leyva, J. A. Jarillo, J. Salinas and J. M. Martínez-Zapater, "Low temperature induces the accumulation of phenylalanine ammonia-lyase and chalcone synthase mRNA of *Arabidopsis thaliana* in a light-dependent manner", *Plant Physiol.*, **1995**, 108, 39-46.
39. H. M. Sun, T. L. Li and Y. F. Li, "Changes of phenols content and activity of enzymes related to phenols in Lily bulbs stored at different cold temperatures for breaking dormancy", *Sci. Agric. Sin.*, **2004**, 37, 1777-1782.
40. Y. Zhao, S. H. Yang, W. Y. Ge, Q. X. Li, H. X. Chen and H. Ge, "The metabolism of phenolics and reactive oxygen species in relation to the explant browning differences among the varieties of *Phalaenopsis* during the tissue culture", *Acta Hortic. Sin.*, **2010**, 37, 963-970.

41. J. Smith-Becker, E. Marois, E. J. Huguet, S. L. Midland, J. J. Sims and N. T. Keen, “Accumulation of salicylic acid and 4-hydroxybenzoic acid in phloem fluids of Cucumber during systemic acquired resistance is preceded by a transient increase in phenylalanine ammonia-lyase activity in petioles and stems”, *Plant Physiol.*, **1998**, 116, 231-238.
42. P. Curir, C. F. Van Sumere, A. Termini, P. Barthe, A. Marchesini and M. Dolci, “Flavonoid accumulation is correlated with adventitious roots formation in *Eucalyptus gunnii* Hook micropropagated through axillary bud stimulation”, *Plant Physiol.*, **1992**, 92, 1148-1153.
43. S. M. Mandal, M. Mandal, A. K. Das, B. R. Pati and A. K. Ghosh, “Stimulation of indole-acetic acid production in a *Rhizobium* isolate of *Vigna mungo* by root nodule phenolic acids”, *Arch. Microbiol.*, **2009**, 191, 389-393.
44. W. Chen, “Effects of plant growth regulators, phenolic compounds and polyamines on rooting of walnut shoots in vitro”, *J. Fujian Agric. Univ.*, **1994**, 23, 490-494.

***Maejo International  
Journal of Science and Technology***

ISSN 1905-7873

Available online at [www.mijst.mju.ac.th](http://www.mijst.mju.ac.th)

*Full Paper*

## **A one-mode-for-all predictor for text messaging**

**Vimala Balakrishnan<sup>1,\*</sup>, Sim Foo Guan<sup>2</sup> and Ram Gopal Raj<sup>1</sup>**

<sup>1</sup> Faculty of Computer Science and Information Technology, University of Malaya, 50603 Kuala Lumpur, Malaysia

<sup>2</sup> Faculty of Information Science and Technology, Multimedia University, 75450 Ayer Keroh, Melaka, Malaysia

\* Corresponding author, e-mail: vim.balakrishnan@gmail.com

*Received: 30 September 2010 / Accepted: 8 August 2011 / Published: 9 August 2011*

---

**Abstract:** This paper discusses the enhancements made on the current mobile phone messaging software, namely the predictive text entry. In addition, the application also has a facility to abbreviate any unabbreviated words that exist in the dictionary, so that the message length can be reduced. The application was tested in a computer-simulated mobile environment and the results of the tests are presented here. These additional features will potentially enable users to send messages at a reduced length and thus reduce the cost of sending messages. Moreover, users who are not adept in using the abbreviations can now do so with features made available on their mobile phones. It is believed that these additional features will also encourage more users to use the predictive software as well as further improve users' messaging satisfaction.

**Keywords:** text messaging, predictive text entry, abbreviator, mobile phones

---

### **INTRODUCTION**

Short message service (SMS) is a text messaging technology that has become a huge hit among the mobile phone users, especially the youngsters. It is defined as a digital telecommunications protocol that allows the user to exchange short messages (160 characters or less) via mobile phones and other devices such as the computer and Personal Digital Assistants [1].

The mobile phone text messaging phenomenon found its footing during the design of the global system for mobile communication (GSM) technology. In the 1980s, it was found that sending a short message at the same time as speech is possible, and thus the delivery and receipt of non-voice, or specifically, alphanumeric text-based messages, now popularly known as SMS, began. Today, SMS has become the most widely used mobile application worldwide. It has gained

phenomenal success among its users, especially among the youth [2]. The reason for this has a lot to do with convenience, accessibility, as well as cost. SMS is relatively cheaper compared to all the other types of mobile communications such as voice calls and Multimedia Messaging Service (MMS). The average SMS rate in Malaysia is currently only 0.15 MYR (0.05 USD) per SMS while a typical MMS rate ranges between 0.25-0.5 MYR (0.08-0.16 USD) per MMS [3].

Whilst the popularity of SMS continues to grow, the SMS protocol imposes some serious restrictions and raises flaws in usability, as it was not originally designed for mobile phones. An SMS is entered via a phone keypad using the multi-tap or the predictive method. The main limitation of these methods is due to the standard layout of the keypad that most mobile phones have (Figure 1). The keys are overloaded to accommodate alphabets, numbers and also symbols. Therefore, the task of message composition can be cumbersome and time consuming. Other input devices, such as mini QWERTY keyboards and touch screens are on the rise, although the standard 12-button-keypad-based mobile phones remain vastly common in the current market.

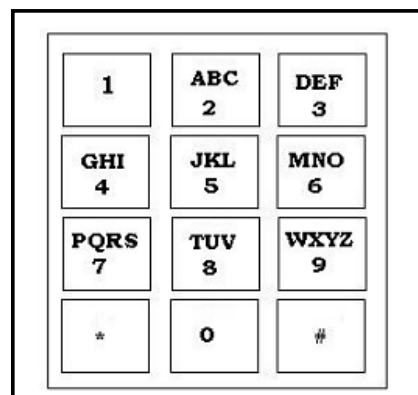


**Figure 1.** Standard ISO 12-key keypad

## SMS TEXT ENTRY

With the limited keys on a standard mobile phone keypad, many vendors have introduced various ways of text input into a mobile phone. However, multi-tap and predictive entry remain the two dominant methods for text entry.

### Multi-tap

Multi-tap is implemented on all mobile phones with SMS capabilities. It disambiguates by requiring the user to press a key once or multiple times to enter the desired character(s). For instance, a user needs to press the key-2 once for 'a', twice for 'b', and thrice for 'c'. Figure 2 below shows the sequence of key presses needed to enter 'The cat is seeing.'

The <!> notation is to signify the timeout interval needed to clear the input buffer, since the character to be entered next resides on the same key. This is called segmentation and can be done either by waiting for the timeout mentioned above or by pressing the timeout kill key [4]. The

8	44	33	0	222	<!>	2	8	0	444	7777	0	7777	33	<!>	33	444	66	4
T	H	E		C		A	T		I	S		S	E		E	I	N	G

0 - spacebar

**Figure 2.** Multi-tap sequence

example clearly shows that a total of 34 key presses are needed to yield only 17 characters (with the space included). Text entry rates for multi-tap are commonly 7-15 words per minute, and with the segmentation issues involving timeout intervals, it is obvious that multi-tap can be slow and tedious [5].

### Predictive Entry

Dictionary or lexicon based methods were introduced to increase the speed of text messaging. There are many variants to these methods, the most popular one being T9® by Tegic Communications [6]. The predictive mechanism works by attempting to anticipate the next string of characters entered by a user based on the existing words in a dictionary. Generally, when the first character is entered, the software will offer the most probable words beginning with the particular character(s). Disambiguating words in this manner is not always perfect as the same key sequence may produce two or more words, a phenomenon known as collision. In this scenario, the software will suggest the most probable words and the user may then traverse through the words using a special key (either Next or the asterisk key). The general steps in the predictive method are given below [7]:

- i. User enters a code sequence of the desired text; for example, ‘lazy’ is entered as ‘5299.’
- ii. The software decodes the code by looking for corresponding targets in the dictionary. The potential words are sorted in a relevant order using linguistic knowledge or according to frequency of most often used words, with the highest frequency word sorted to the top of the list. An example below shows a collision generated by the code sequence ‘5299’:

Jazz  
Lazy  
Lawy

- iii. The user chooses the target word by scrolling with either the asterisk key (e.g. in Nokia) or the up or down navigational key (e.g. in Sony Ericsson).

Figure 3 shows the sequences needed to enter ‘The cat is seeing’ using T9®. A total of only 18 key presses are needed as opposed to 34 key presses on multi-tap, proving that the predictive method is more efficient than the multi-tap. The former usually results in a decreased number of key presses required to write a sentence and hence increases the text entry speed. In addition, the physical effort required to compose a message is also reduced. Unfortunately, this efficiency rate drops very drastically when the user attempts to enter words that are not in the dictionary, be they English words or understandably unlisted non-English words [8]. It is also impossible to enter

8	4	3	0	2	2	8	*	0	4	7	0	7	3	3	4	6	4
T	TH	THE	A	CC	ACT	CAT	I	IS	S	RE	SEE	SEEI	SEEIN	SEEING			

0 – spacebar; \* – end of selection

**Figure 3.** Predictive T9® sequence

numerals, acronyms or any combinations of letters and numerals (e.g. ‘l8r’ for ‘later’). Users are then required to multi-tap the desired word into the original message. Manually switching between the text entry modes will result in a slower text entry rate unless the mobile phone user is skilled in using the predictive method. Instead, providing an automatic switch between multi-tap and the predictive software would enable the users to text at a faster rate.

Another notable flaw of the predictive software is the inability to auto-save words that are created by compounding existing words. For instance, the word ‘roomie’ is not readily available in the T9® dictionary, but the word ‘room’ is. A user would then usually type the word ‘room’ first, and then compound an ‘ie’, thus creating ‘roomie’. However, if the user wishes to type ‘roomie’ again later, he/she would have to retype ‘room’ followed by compounding ‘ie’, as T9® does not auto-save compounded words [9].

## SMS LIMITATIONS

Apart from the improper keypad layouts for text entry, another of the major limitations of SMS is the overall length of messages allowed, which is fewer than 160 characters per message. An addition of a single character would result in a message length of 161 characters, and hence the message will be split into two. This means that the sender will have to pay for two messages instead of one. When the number of characters exceeds 160, users generally will trace back their message and rephrase the message, deleting some words and abbreviating others so as to reduce the message length. This can be quite cumbersome as the users will have to go through their message again and make the necessary modifications. Furthermore, this process results in a higher message composition time. Due to this, the youth created an ingenious way to message by heavily abbreviating the common words. For example, ‘thank you’ is typed as ‘tq’, ‘later’ as ‘l8r’, ‘already’ as ‘dy’ or ‘d’, and ‘please’ as ‘pls’. As there is no de-facto standard for the abbreviations, users who are not familiar with such jargons would shy away from using SMS. This is especially true among the older users [10].

Therefore, the aim of this study is twofold: firstly, to enhance the current implementation of the predictive software to enable users to enter messages at a faster rate and hence improve their messaging satisfaction. Secondly, the aim is to provide a facility to abbreviate the messages, both in English and Bahasa Malaysia, the local and national language of Malaysia. When message length is reduced, it is possible to send a lengthier message at the cost of a single message. Moreover, users who are not very familiar in using abbreviations would benefit from this added feature as well.

## RELATED WORK

### Text Entry

The multi-tap remains to be the prevailing text entry method used on mobile phones, despite being slower than the predictive method [8]. This has led many researchers to explore other techniques to increase text entry speed. For example, many attempted to optimise text entry performance by creating keypad designs that reduce the number of keystrokes needed to enter a word. The one-row keyboard prototype was Nokia's attempt to make the T9® system faster by using more fingers than the normal one or two in typing. The keypad consisted of ten keys, all in one row. The alphabets were similarly distributed among the keys as in T9®. However, tests indicated that the system in fact made the typing of words slower than the T9® system [11].

Sørensen and Springael [12] proposed a new keypad layout to improve text entry when using the predictive method. Called Keymap, it was designed by assigning as many letters as possible on the same key, and then the letters that could cause collisions were distributed on different keys. This keypad works based on Iterated Local Search, an algorithm used to find the best placement of each letter over the keypad keys.

LetterWise [13] is another proposed system to improve text entry using prefix-based disambiguation. It works with a stored database of probabilities of prefixes (letters preceding the current keystroke). For example, if key-3 is pressed with prefix 'th', the most likely next letter is 'e' because 'the' in English is far more probable than either 'thd' or 'thf'.

Some efforts have also been made to move away from text entry optimisation, exploring gestural interactions such as the use of joysticks [14], tilting [15], motion [16] and also the possibility of using speech to text [17].

### Message Abbreviation

It is important to note that message abbreviation differs from message compression. A compression method generally reduces the message length by encoding the message in fuzzy characters, and hence it requires the receiver to decode the characters to its original form. Although this technique successfully reduces the message length, both communicating parties need to have the compressor/decompressor at their ends. Currently, there are very few implementations of SMS compression, one of which worth mentioning is KirimSMS [18]. This program uses the traditional fixed Huffman coding that reduces the code length of frequently used characters while increasing the code length of those that are less frequently used. Messages that are generally split into two are sent as one message based on the compression software. However, as mentioned before, the sender and receiver must have the same software installed on their mobile phones; otherwise the recipient could only view unintelligible characters [18].

Instead of compressing a message, abbreviation of the common words to reduce the overall length of the message is used in this study. The technique used is similar to the abbreviation technique employed in the computer-based MobiSMS for Outlook which was developed by MobiMarketing [19]. This application abbreviates a message based on a dictionary located in the computer hard drive. An unabridged word is paired with its abbreviated partner and kept in this

dictionary, which the user can easily modify to add more abbreviations, words, or to edit existing ones. For example, the sentence ‘Please phone me if you can meet for lunch at one today’ will be abbreviated to ‘Pls phone me if u can meet 4 lunch @ 1 2day.’ However, this program is only available for Outlook, and thus can only be used on a computer [19].

The main aim of this study is to design an application that abbreviates common words in a text message to make the whole message significantly shorter yet understandable, without requiring the users to have the exact application in their mobile phones. Moreover, a lossless abbreviation technique is implemented whereby punctuations, spaces, etc. remain intact even after the abbreviation takes place.

## METHOD

For the enhancement of the predictive text system, some of the existing ideas in T9® were retained. These include the dynamic search for words from the dictionary on-the-go as the user types, ability to learn new words (though this is not done automatically), the use of the asterisk key to scroll through the list of possible words, and the use of word frequency to determine the most probable word that the user intends to type. The current study aims to enhance T9® by including the ability to automatically (i) save new words into the dictionary, (ii) learn words by compounding, (iii) insert a question mark when words such as ‘how, where and when,’ are encountered, and (iv) enter numerals. In short, the system works on a one-mode-for-all concept, whereby users get to perform all the functions above without having to switch to multi-tap, or from multi-tap to predictive mode.

For the abbreviation mechanism, an algorithm that is very close to MobiSMS’s was used, whereby unabbreviated words were matched with their abbreviated partners in the word list or stored dictionary. If a particular word has no abbreviated partner in the dictionary or if the entry is already an abbreviated word, then the original word will be displayed as it is.

The general algorithm used in the current system can be presented in four main steps, beginning with the enhancement of the predictive text entry. Figure 4 shows the steps for both the enhancement and the abbreviation. Note that the abbreviator can be used regardless of the text entry mechanism employed.

The four main steps as indicated in Figure 4 can be elaborated as follows:

Step 1: Get the code sequence, e.g. ‘5299’, entered by the user, breaking only if the ‘right’, ‘send’, ‘delete’, ‘hash’ or ‘asterisk’ key is detected.

Step 2: Constantly update the list of possible words with words corresponding with the code sequence by checking with the dictionary. Sort the list according to the frequency of each word, with the highest frequency word sorted to the top. For example, ‘5299’ would produce the list of words as depicted in Table 1. To cycle through the list of possible words, the user would have to press the asterisk key. If the intended word did not exist in the used word list or the dictionary, an automatic switch to multitap mode would occur, and the list as well as the word would be cleared to allow a multitap entry of the word (first time entry).

Step 3: Once a right directional key is detected, the word that was previously entered would be saved to the dictionary. If the word already existed in the dictionary, then its frequency (prediction rate) would be increased.

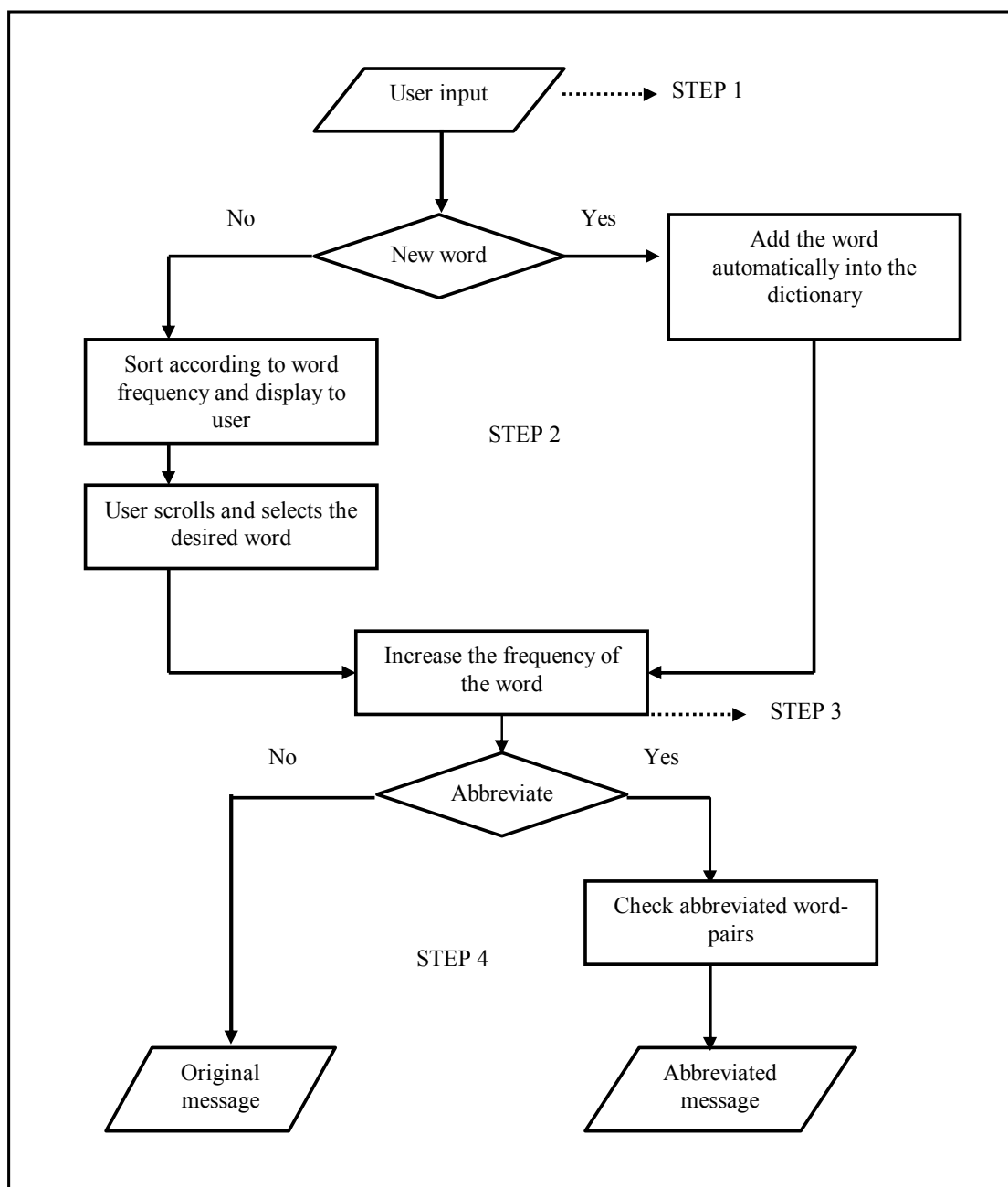


**Figure 4.** General algorithm for the predictive system and abbreviator

Step 4: Once the user has finished typing the desired message, he/she would be prompted to choose to abbreviate the message. If selected, the abbreviator would iterate through all the words in the original message, find their abbreviations if any, and copy the abbreviation, or if no abbreviation is found, the original word is retained.

**Table 1.** The list of possible words generated and the code sequence

Code sequence	5	52	529	5299
List of possible words	K, L, J	La, Lb, Ka, Ja, Kb	Jay, Law, Lay, Jaw, Lax, Kay, Laz, Jaz, Kaz	Jazz, Lazy, Lawy

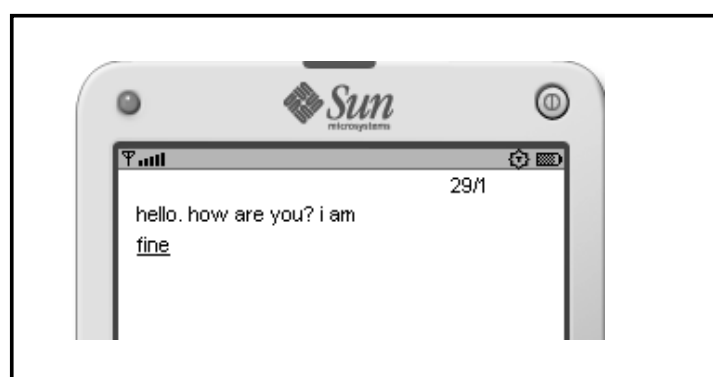
In step 4 above, the abbreviation takes place only when the message is completed and not after the completion of each word in the message. Having a process where the words are abbreviated automatically as they are entered may interrupt the flow of messaging or perhaps even confuse the user.

The system was developed using Java and was simulated on a mobile phone environment using the SERIES 40 SDK Version 0.9 in conjunction with JRE 6.0.

## RESULTS AND DISCUSSION

### Enhancement of the Predictive Software

Figure 5 shows a simple example involving a question. The number '29/1' at the top right-hand corner means there are 29 characters in the message and the total message is one. The underlined word refers to the current word being entered, which is 'fine'. In this example, the system automatically inserts a question mark when a sentence involving 'how, where and where, etc.' is detected rather than the period character '.'. The question mark will be automatically inserted when the user presses the hash key for punctuation. The current predictive software does not have this ability and users are required to enter the question mark manually.

**Figure 5.** Automatic insertion of the question mark

The system is also capable of automatically adding new words into the dictionary, including compounded words. Users need not switch to the multi-tap mode manually. In other words, the users can enter any new words and they will be saved automatically without the user's intervention. Figure 6 shows an entry example for a new compounded word, 'roomie.' The system will predict 'room' (Figure 6a) and then the user can automatically insert 'ie' (Figure 6b) without any manual mode switching. The word 'roomie' is automatically added to the dictionary, and hence it will be predicted when another attempt to enter 'roomie' is encountered (Figure 6c).

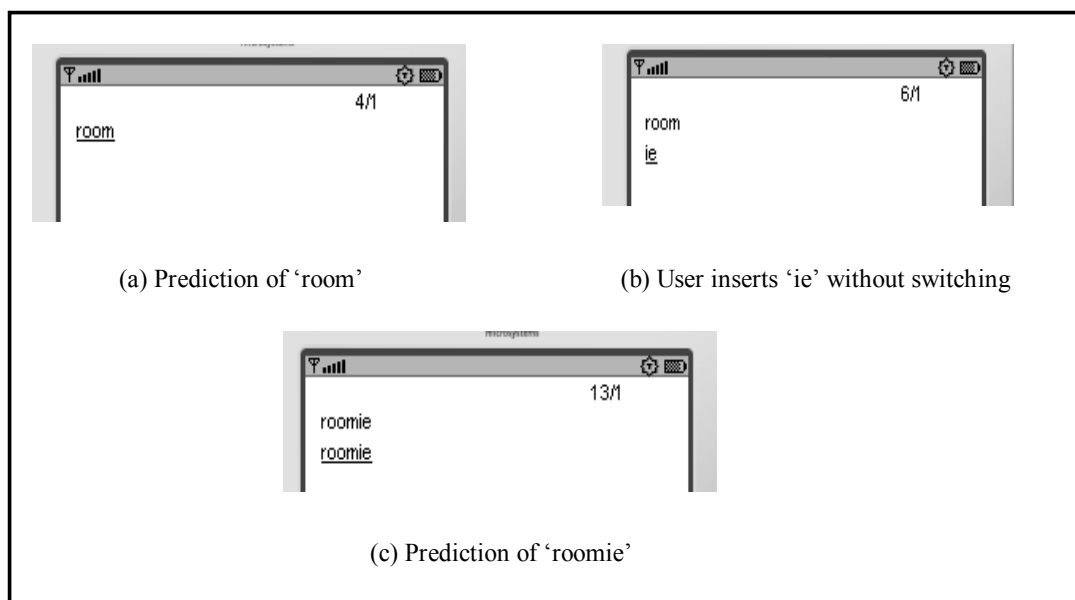


**Figure 6.** Automatic learning of a new compounded word

Similarly, the system also allows the user to easily enter numerals without the need to switch to the number mode, hence making messaging simpler and faster (Figure 7).



**Figure 7.** Automatic numeral entry

### Abbreviator

This section shows the displays for the abbreviator which can be used regardless of the text entry methods. Figure 8(a) shows the original message as entered by the user. This particular message consists of 178 characters, and hence would be split into two messages, as indicated on the screen. Figure 8(b) shows the message after the abbreviation. Words that are already abbreviated and those that do not have an abbreviation partner are left in their original forms. Note that the message length now is reduced to 157 characters and the number of message is one instead of two. Apart from saving cost, this feature would be beneficial to users who are not so adept in using abbreviations.

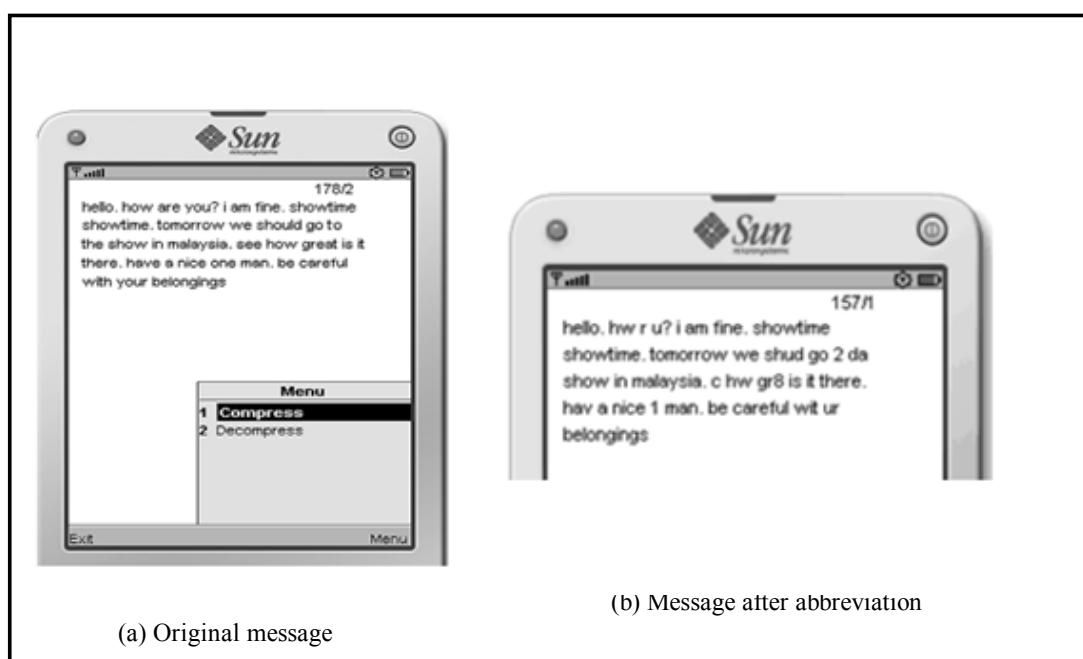


**Figure 8.** Example of abbreviations

Another advantage of this system is that the recipient can choose to expand the abbreviated word/message to its original form by choosing decompression from the menu (Figure 9a). Figure 9(b) shows how the originally abbreviated word ‘l8r’ is expanded to ‘later’. This feature would be very useful especially if users are unsure about the meaning of an abbreviated word.

Finally, a dictionary to support messages in the national language, i.e. Bahasa Malaysia, was also added into the system. The original message in Figure 10(a) can be translated (non-verbatim) as ‘I will not be able to report to work today, I would like to apply for leave for today and tomorrow.’ Figure 10(b) depicts the abbreviated message consisting of only 91 characters, shorter than the original message with 109 characters.

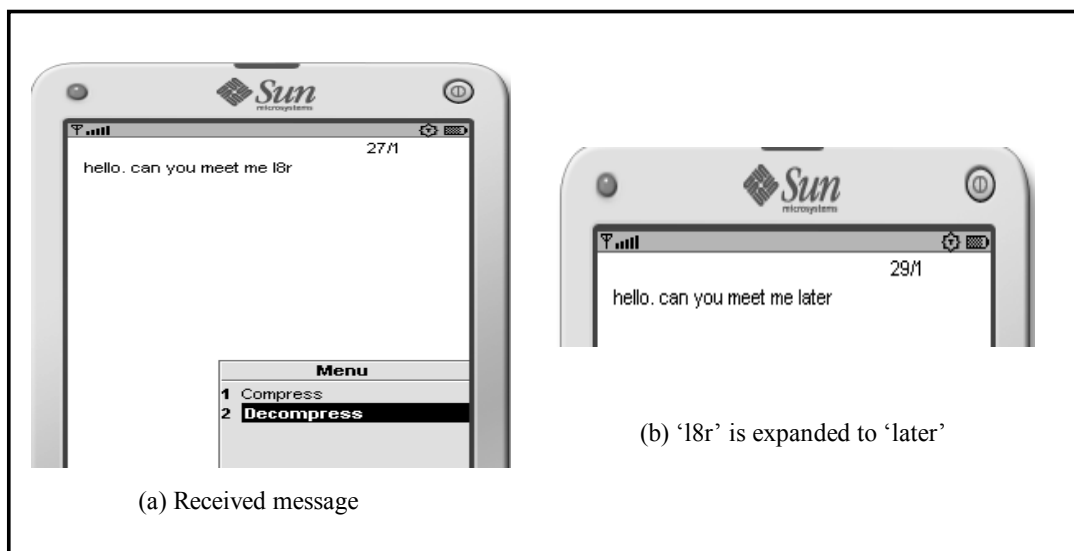


**Figure 9.** Example of expanding abbreviated words to their original forms

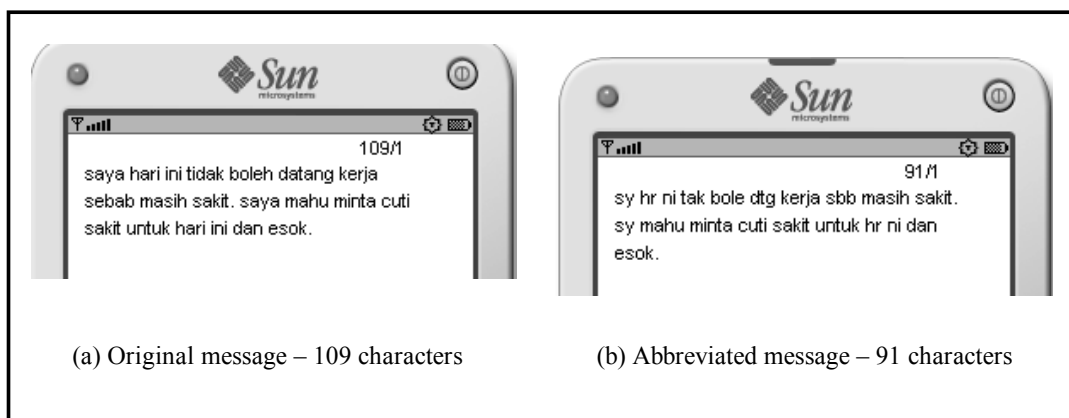


**Figure 10.** Example of abbreviations in Bahasa Malaysia

### Limitations and Future Work

The implemented system is not without its limitations. First of all, the system does not support insertion. For example, if the user wanted to enter ‘March’ but accidentally keyed in ‘Marh’, he/she needs to delete the letter ‘h’ to enter ‘ch’. Instead, it would be simpler if the user could just move to the intended location and insert the missing character(s). Currently this can only be done on mobile phones with QWERTY keyboard.

As for the abbreviator, new word-pairs currently cannot be added into the dictionary, meaning users only depend on the existing pairs to abbreviate their messages. Future work would provide the flexibility for users to add their own word-pairs. Another important feature that will be included is the support for emoticons (for mobile phones that support these icons), since users, especially the youngsters, have a high tendency to use emoticons in their messages.

It should be noted that the system was tested in a mobile simulated environment. Therefore, though it is inferred that the system should work successfully when implemented in the actual mobile phones, further study is required to conclusively confirm the efficacy of the system. The implementation will be ported to real mobile phones for further testing in future work.

Finally, the future work will also include a usability study. This is necessary to assess mobile phone users' messaging satisfaction when using the implemented system. One of the features that will be tested is the option given to the users for abbreviation. Currently, it is assumed that automatic abbreviations (as user types the message) would confuse the users; therefore, an option to abbreviate or not is provided. User testing with (and without) the option needs to be conducted to address this assumption in the future.

## CONCLUSIONS

In this study, a one-mode-for-all application for the predictive text entry software on mobile phones was developed. The existing predictor software was enhanced by enabling automatic word saving (both new and compounded words), insertion of question marks and automatic entry of numerals. All of these features can be done without having to switch to multi-tap, thus saving message composition time. In addition, an abbreviator that abbreviates and expands messages both in English and Bahasa Malaysia was also implemented. This would be useful as users who are not adept in using abbreviations can now do so. Moreover, message lengths will be reduced and hence users can compose and send longer messages at the cost of a single message (as long as the total characters are less than 160).

## REFERENCES

1. J. Sciallo, "Short message service (SMS) support in Sun Java System Messaging Server 6.3", [http://www.sun.com/bigadmin/features/hub\\_articles/sms\\_support\\_msg\\_server.jsp](http://www.sun.com/bigadmin/features/hub_articles/sms_support_msg_server.jsp), **2007** (accessed: November 30 2008).
2. S. N. Audrey and L. Srivastava, "Mobile phones and youth: A look at the U.S. student market", ITU/MIC Workshop on Shaping the Future Mobile Information Society and Policy Unit, **2004**, Seoul, South Korea.
3. Maxis Co., "Value Plus 50", [http://www.maxis.com.my/personal/mobile/plan\\_pricing/value\\_plan\\_50.asp?iStruct=0:2:1](http://www.maxis.com.my/personal/mobile/plan_pricing/value_plan_50.asp?iStruct=0:2:1), **2009** (accessed: February 11, 2010).
4. T. Igarashi, J. Takai and T. Yoshida, "Gender differences in social network development via mobile phone text messages: A longitudinal study", *J. Social Person. Relations.*, **2005**, 22, 691–713.
5. L. Leung, "Unwillingness-to-communicate and college students' motives in SMS mobile messaging", *Telemat. Informatics*, **2007**, 24, 115–129.
6. D. L. Grover, M. T. King and C. A. Kuschler, "Reduced keyboard disambiguating computer", Tegic Communications, Inc., *US5818437* (**1998**).

7. I. S. MacKenzie and K. Tanaka-Ishii, "Text entry using a small number of buttons", in "Text Entry Systems: Mobility, Accessibility, Universality" (Ed. I. S. Mackenzie and K. Tanaka-Ishii), Morgan Kaufmann, San Francisco, **2007**, pp.105–121.
8. M. Silfverberg, I. S. MacKenzie and P. Korhonen, "Predicting text entry speed on mobile phones", Proceedings of the ACM Conference on Human Factors in Computing Systems, **2000**, New York, USA, pp.9–16.
9. S. Rajeev, S. Ghosh, G. N. Kumar and S. N. Sivanandam, "A simple algorithm for text entry in mobile communication devices", *Acad. Open Internet J.*, **2003**, 10, <http://www.acadjournal.com/2003/v10/part1/p1/>, (accessed: December 11, 2008).
10. H. Du and F. Crestani, "Spoken versus written queries for mobile information access", in "Mobile and Ubiquitous Information Access - Mobile HCI 2003 International Workshop", (Ed. F. Crestani, M. Dunlop and S. Mizzaro), Springer-Varlag, Udine, **2004**, pp.67–78.
11. M. Silfverberg, 'The one-row keyboard: A case study in mobile text input', in "Mobile Usability: How Nokia Changed the Face of the Mobile Phone" (Ed. C. Lindholm, T. Keinonen and H. Kiljander), McGraw Hill, New York, **2003**, pp. 157–168.
12. K. Sørensen and J. Springael, "Optimization of SMS keyboards with a dictionary using local search", Workshop on Real Life Applications of Metaheuristics, **2003**, Antwerp, Belgium.
13. I. S. MacKenzie, H. Kober, D. Smith, T. Jones and E. Skepner, "LetterWise: Prefix-based disambiguation for mobile text input", Proceedings of the ACM Symposium on User Interface Software and Technology, **2001**, New York, USA, pp. 111–120.
14. J. O. Wobbrock, B. A. Myers and H. H. Aung, "Writing with a joystick: A comparison of Date Stamp, Selection Keyboard and EdgeWrite", Proceedings of Graphics Interface Conference, **2004**, London, UK, pp.1-8.
15. D. Wigdor and R. Balakrishnan, "Tilttext: Using tilt for text input to mobile phones", *Comp. Inform. Sci.*, **2003**, 5, 81-90.
16. J. Wang, S. Zhai and J. Canny, "Camera phone based motion sensing: Interaction techniques, applications and performance study", Proceedings of the ACM Symposium on User Interface Software and Technology, **2006**, Montreux, Switzerland, pp.101– 110.
17. A. L. Cox, P. A. Cairns, A. Walton and S. Lee, "Tlk or txt? Using voice input for SMS composition", *Person.Ubiquit. Comput.*, **2008**, 12, 567–588.
18. Y. Sugianto, "SMS text compression", <http://www.kejut.com/kompressionsm>, **2007** (accessed: April 10, 2010).
19. T. D. Susanto and R. D. Goodwin, "Content presentation and SMS-based e-government", Proceedings of the International Conference on Electrical Engineering and Informatics, **2007**, Jakarta, Indonesia, pp.1082–1085.

***Maejo International  
Journal of Science and Technology***

ISSN 1905-7873

Available online at [www.mijst.mju.ac.th](http://www.mijst.mju.ac.th)

*Full Paper*

**The production and shelf life of high-iron, pre-cooked rice porridge with ferrous sulphate and other high-iron materials**

**Chowladda Teangpook\*** and **Urai Paosangtong**

Institute of Food Research and Product Development, Kasetsart University, P.O. Box 1043  
Kasetsart, Bangkok 10903, Thailand

\* Corresponding author, e-mail: [ifrcdt@ku.ac.th](mailto:ifrcdt@ku.ac.th)

*Received: 11 June 2010 / Accepted: 20 August 2011 / Published: 22 August 2011*

---

**Abstract:** The production and shelf life of high-iron, dried, pre-cooked rice porridge with ferrous sulphate and other high-iron materials was studied. Broken brown rice was soaked in water and ferrous sulphate was added at 0.05, 0.1 and 0.15% of the dried brown rice. The mixture was steamed for 20 min and dried in a double drum dryer. Green shallot, young ginger and cooked chicken fillet were dried in an electric cabinet dryer. Chicken blood and edible fern were dried in a double drum dryer and vacuum freezer respectively. The optimum ferrous sulphate added to the rice was 0.05% and the developed formulation of dried porridge consisted of ferrous sulphate rice (67.80%), chicken fillet (20%), chicken blood (3%), green shallot (0.7%), young ginger (1%), edible fern (0.5%), pepper powder (0.5%), sucrose (3%), salt (3%) and monosodium glutamate (0.5%). The dried porridge had a high iron content of 10.18 mg/50 g and the shelf life was three months at room temperature when stored in either aluminum foil laminated bag or metalite bag.

**Keywords:** pre-cooked rice porridge, ferrous sulphate, iron fortification

---

## INTRODUCTION

Iron deficiency anemia is still considered the number one nutritional deficiency worldwide [1-2]. A survey by the Department of Health, Thailand revealed that from 1995 to 2003, iron-deficiency anemia had increased by 50% in infants aged 6-11 months, and in a second group consisting of elders, school-age children, preschool-age children and pregnant women, it had increased by over 20%. Iron-fortified foods have been a generally used strategy to combat iron deficiency throughout the world, especially cereal flour (wheat and maize), which is currently the most common vehicle for

iron fortification [3-6]. Condiments and sauces have also been widely consumed as a means of iron fortification where central processing of staple foods is absent. The following examples can be mentioned: curry powder fortified with NaFeEDTA [7]; sugar with NaFeEDTA [8]; salt fortified with ferric orthophosphate, ferrous fumarate, sulphate or bisglycine chelate [9-10]; and soya sauce and fish sauce fortified with NaFeEDTA [11-12].

Porridge is a dish made by boiling oats (rolled, crushed or steel cut) or other grains or legumes in water or milk (or both). It is usually served hot in a bowl or dish. Porridge is a simple and staple dish, especially for breakfast in Thailand. Dried porridge in Thailand is a semi-instant food and a specially controlled product with its quality set according to the Ministry of Public Health [13]. Nowadays, it is a popular food item for every age group, especially children; there are many brands available in Thailand.

Rice is a staple food for half of the world's population including those in Thailand. Thailand's paddy rice output was 31.65 million tonnes in 2008/9 and the country was the world's biggest rice exporter when sales reached 13.09 million tonnes [14]. Rice in Thailand is therefore cheap and suitable for processing. In particular, porridge from brown rice has become popular because it has a high mineral and vitamin content, especially of iron and phytate, which are about 5 and 2.5 times higher respectively than that in white rice [15]. Phytic acid, however, shows a very marked inhibitory effect on the absorption of non-heme Fe in humans [16].

The objective of the current study is to investigate the production, quality and shelf life of high-iron, pre-cooked rice porridge from brown rice fortified with ferrous sulphate and other high-iron materials. Ferrous sulphate containing 32% iron (w/w) has been used in several cases of iron supplementation in such products as parboiled glutinous rice [17], cereal porridge [18], iron supplemented product for schoolchildren [19] and ferrous sulphate tablets used by the Department of Health [20].

## MATERIALS AND METHODS

### Raw Materials

Supanburi-1 brown rice was sourced from the Department of Agriculture, Thailand. Green shallot, young ginger, chicken fillet, chicken blood, edible fern and other flavouring agents (sugar, salt, soya sauce, white blended pepper powder and monosodium glutamate) were purchased from local markets. Ferrous sulphate powder (food grade) was sourced from Asia Drug & Chemical Ltd. Metalite bags (OPP30u and MCPP25u), 10.8×18.8 cm (water vapour transmission rate of 0.10 g/m<sup>2</sup>/day), were purchased from a local market. Aluminum foil laminate bags (OPP20/ALU9/LLDPE71), 11×18 cm and 100±10 µm in thickness, were purchased from B.T.T. Thailand Co. Ltd.

### Preparation of Dried Ingredients

Fresh green shallot and fresh young ginger were cut into small pieces of about 0.3 cm and 2×0.2×0.2 cm respectively. They were then dried in an electric cabinet dryer at 50°C. Chicken fillets were blended with a blender for about 2 min and 1% salt, 5% soya sauce and 50% water by weight

were there added. The mixture was cooked on a gas stove and dried in an electric cabinet dryer at 60°C. Chicken blood was blended with a blender and dried in a double drum dryer at 140°C and 8 rpm, with a 0.20-mm nip gap. Fresh edible fern was cut into small pieces (about 1 cm), kept at -20°C and dried in a vacuum freeze drier (LyoLab 3000). The dried ingredients were weighed and stored in a refrigerator at 10°C until use. The rate of rehydration (RHD) of the dried ingredients was determined in triplicate by adding 50 parts by weight of hot water (80°C), soaking for 20 min and filtering with a 40-mesh screen for 5 min. The RHD value was taken as weight of rehydrated material/weight of dried material (method modified from Champagne et al. [21]). All dried ingredients were blended in a blender for about 2 min and analysed in triplicate for water activity ( $a_w$ ) with a water-activity measuring system (Novasina, type  $a_w$  -box, Model Ubersicht, No. 861168, Switzerland), and for colour with a spectrophotometer (Spectraflash 600 plus, Data-color International, USA). The CIE colour values recorded were: L\* = lightness (0 = black, 100 = white);  $a^*(-a^* =$  greenness,  $+a^* =$  redness); and  $b^*(-b^* =$  blueness,  $+b^* =$  yellowness). The iron content in the chicken fillet and dried chicken blood was determined by AOAC method [22].

### **Fortification of Rice with Ferrous Sulphate**

A completely randomised experimental design with two replications was used. Broken brown rice (200 g) was soaked in water 2.5 times its weight for 3 h and dried ferrous sulphate was added at 0.05, 0.1 and 0.15% (w/w) of the dried brown rice. The samples were steamed for 20 min and placed in a double drum dryer at 140°C and 4 rpm, with 0.20 mm nip gap. The dried iron fortified rice was analysed by the same procedure detailed above. It was then mixed with other dried ingredients to afford the following composition: dried iron fortified rice (67.83%), seasoned chicken fillet (20%), chicken blood (3%), green shallot (0.7%), young ginger (1%), edible fern (0.5%), white blended pepper powder (0.5%), sugar (3%), salt (3%) and monosodium glutamate (0.5%). The mixture was added to 8 parts by weight of hot water (80°C) and boiled for 1 min. A panel of 20 people (24-55 years old) carried out a sensory evaluation which involved appraisal for colour, aroma, flavour, texture and overall preference, using a 7-point hedonic scale (1 = dislike very much, through to 7 = like very much). The data were analysed using analysis of variance and Duncan's new multiple range test for mean comparisons at the 0.05 level of significance, using the SPSS statistical software version 12. The optimum dried iron fortified porridge was analysed for iron, moisture, fat, protein (Kjeldahl method with 6.25 as conversion factor), crude fibre, ash, and carbohydrate according to AOAC methods [22].

### **Shelf Life of Dried Iron Fortified Porridge**

The dried porridge samples produced were packed in aluminum foil laminate (A) bags and metalite (M) bags (30 g/bag) and kept in a darkened drawer at room temperature for 6 months (April–September 2007). Each month, the samples were subjected to tests for colour,  $a_w$ , thiobarbituric acid [TBA] [23], microbiological total plate count [24], yeast and mould [25], *Escherichia coli* [26], *Staphylococcus aureus* [27], *Clostridium perfringens* [28], *Bacillus cereus*

[29] and *Salmonella sp* [30], and also to a sensory test of the rehydrated product as detailed above. Analysis of the data for both packaged products followed the process described above.

## RESULTS AND DISCUSSION

### Preparation of Dried Ingredients

The yields of the dried products were 9.40, 8.80, 9.62, 28.68 and 6.22% of the fresh materials for green shallot, young ginger, edible fern, chicken fillet and chicken blood respectively. Some qualities observed for of the dried ingredients are shown in Figure 1. The product colours were: rice - white; young ginger - light yellow; chicken fillet - light brown; green shallot and edible fern - green; and chicken blood - dark brown. The water activity in the samples ranged between 0.22 and 0.40. Since no microorganisms can proliferate if the water activity is less than 0.50 [31], the dried products could be classified as shelf stable. The RHD of edible fern was highest (about 22.10) and that of chicken fillet lowest (4.48) because its texture was lumpy and very hard.

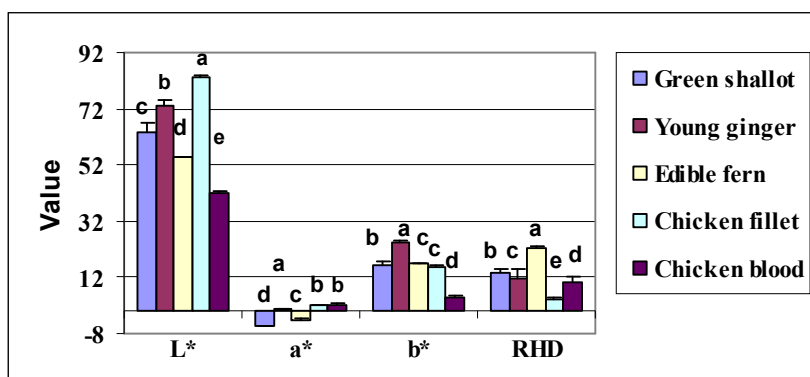


**Figure 1.** Colour values ( $L^*$ ,  $a^*$ ,  $b^*$ ) and RHD (average  $\pm$  standard deviation) of dried ingredients. Means of ingredients with the same letter in each attribute were not significantly different ( $p > 0.05$ ). ( $\bar{T}$  indicates the upper range of the mean plus standard deviation.)

### Fortification of Rice with Ferrous Sulphate

The results of the colour analysis of the dried ferrous sulphate fortified rice are shown in Figure 2. Addition of ferrous sulphate, which is brown in colour, caused a reduction in  $L^*$ , but increased  $b^*$  while  $a^*$  (0.39-0.49) was not changed significantly. The results agreed with those of Theuer [18], who found that iron added as ferrous sulphate at 500 mg/kg to rice, oat, whole grain wheat or proanthocyanidin-free barley porridges caused significant changes in the  $L^*$ ,  $a^*$  and  $b^*$  values, but the visual appearance of these porridges remained satisfactory.

The results of the sensory evaluation of the rehydrated porridge (mixed with the other ingredients) are shown in Figure 3. The scores were not significantly different except for odour, which was reduced when the level of ferrous sulphate was increased, with 0.05% level registering the highest score. Most attributes had scores from 'like a little' to 'like moderately', especially texture since the porridge was made from brown rice with a high crude fibre content (approximately twice that in polished rice) [15] and so its texture was rather rough. The results of iron analysis of the

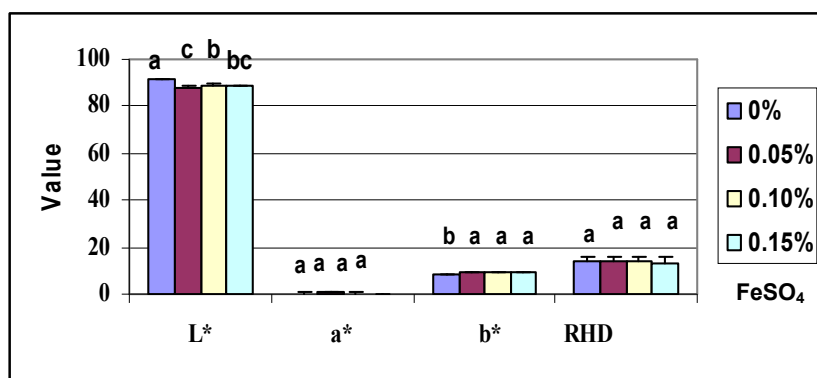


**Figure 2.** Colour values ( $L^*$ ,  $a^*$ ,  $b^*$ ) and RHD (average  $\pm$  standard deviation) of rice with different percentages of ferrous sulphate. Means of each treatment with the same letter were not significantly different ( $p > 0.05$ ). (T indicates the upper range of the mean plus standard deviation.)

dried porridge were 10.18, 20.10 and 30.16 mg/50-g bag for the three treatments of 0.05, 0.1 and 0.15% fortification respectively. The main iron component in the porridge came from the ferrous sulphate, although this was supplemented by other high heme-iron ingredients, namely dried chicken blood and dried chicken fillet with 1,499 and 122 mg/kg respectively. Also, the porridge had non-heme iron from edible fern (36.3 mg/kg fresh weight) and brown rice itself (7.71 mg/kg) [32]. Non-heme iron, however, is poorly absorbed compared with heme iron [33].

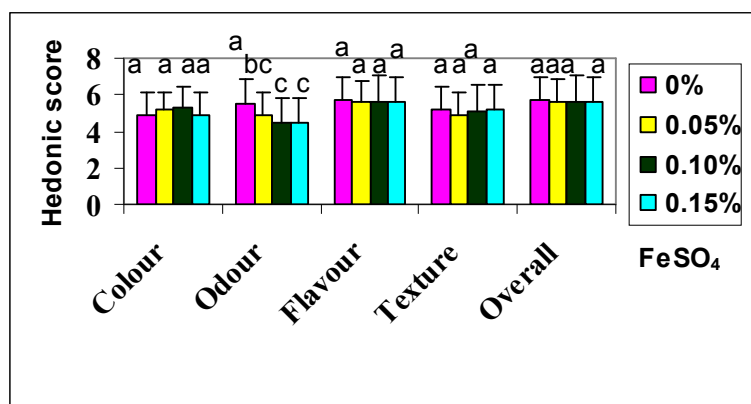


**Figure 3.** Sensory evaluation (average  $\pm$  standard deviation) of the quality of rehydrated porridge. Means of each treatment for each attribute with different letters were significantly different at  $p \leq 0.05$ .

In general, the Thai people should receive iron at a rate of 10-15 mg/day [34]. Thus, the amount of iron (10.18 mg/50-g dried porridge) supplied by the 0.05% fortification treatment should be sufficient since people may receive additional iron from other foods consumed in other meals during the day. Among the elderly, intake of highly bioavailable forms of iron (supplementary iron and red meat), fruits and non-heme iron absorption enhancer (vitamin C) can promote high iron stores. The risk of high iron stores is significantly higher in subjects who take in more than 30 mg of

supplementary iron per day than in nonusers, whereas foods containing phytate (whole grains) decrease these stores [35]. High iron stores may be associated with many chronic diseases such as heart disease [36–37] and cancer [38]. The demand for iron, however, differs according to sex and age, e.g. 8.1 mg/day for 6-8 year-olds, 11.8 mg/day for 9-12 year-olds and 28.2 mg/day for girls 13-15 years old [34]. Thus, having the highest score of sensory evaluation for odour and optimum amount of iron, the 0.05% ferrous sulphate fortification treatment was selected for the study of shelf life. The correlations between colour, odour, flavour, texture and overall impression are shown in Table 1 with all attributes correlated, especially texture and overall impression.

**Table 1.** Pearson correlation coefficients of sensory evaluation at probability levels of  $p \leq 0.05$  (\*) and  $p \leq 0.01$  (\*\*)

	Colour	Odour	Flavour	Texture	Overall
Colour	1				
Odour	0.380**	1			
Flavour	0.383**	0.581**	1		
Texture	0.389**	0.442**	0.556**	1	
Overall	0.375**	0.463**	0.692**	0.745**	1

The chemical composition (% dry weight) of the optimally iron fortified dried porridge was  $6.34 \pm 1.10$ ,  $65.85 \pm 2.56$ ,  $19.16 \pm 0.88$ ,  $2.30 \pm 0.81$ ,  $5.10 \pm 0.33$  and  $6.35 \pm 0.2$  % for moisture, carbohydrate (including crude fibre), protein (factor 6.25), fat, dietary fibre and ash respectively. The moisture content of the product was lower than 10% while also having a high protein content of more than 8%, the minimum value set out by the Ministry of Public Health [13]. The main protein source of the porridge was chicken fillet, which was also effective at enhancing iron absorption [39]. The product therefore could be claimed to be an iron source as well as a protein source.

### Shelf Life of Iron Fortified Porridge

Based on the analysis during the months of storage, the only feature of the dried porridge in the two packaging systems that was significantly different was the water activity,. The product's water activity in the lower-quality M-type packages registered higher values than those from the A-type packages. However, all samples had a water activity of less than 0.51, although the value increased with storage time (Figure 4).

The colours of the dried porridge from the two types of packaging were not significantly different, with L\* ranging from 79.80 to 81.23, a\* from 0.11 to 0.33 and b\* from 8.46 to 10.05 (Figures 5-7).

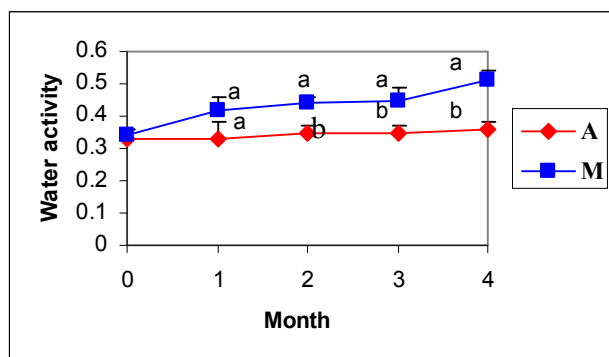


**Figure 4.** Water activity (average  $\pm$  standard deviation) of dried porridge in two types of packaging (A and M bags) plotted against storage month. Means for each type of packaging for each month of storage with the same letter were not significantly different ( $p > 0.05$ ). ( $\text{T}$  indicates the upper range of the mean plus standard deviation.)

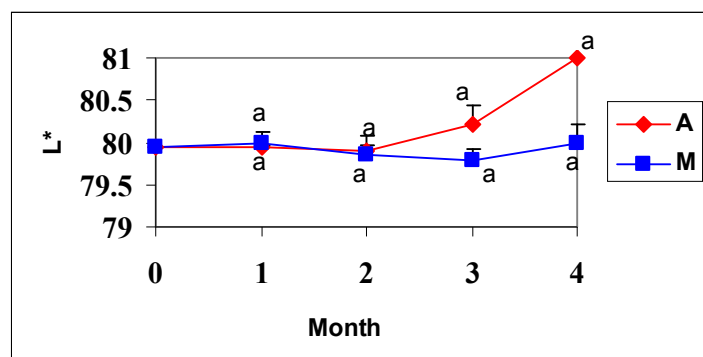


**Figure 5.** Colour ( $L^*$ ) values (average  $\pm$  standard deviation) of dried porridge in two types of packaging (A and M bags) plotted against storage month. Means for each type of packaging for each month with the same letter were not significantly different ( $p > 0.05$ ). ( $\text{T}$  indicates the upper range of the mean plus standard deviation.)

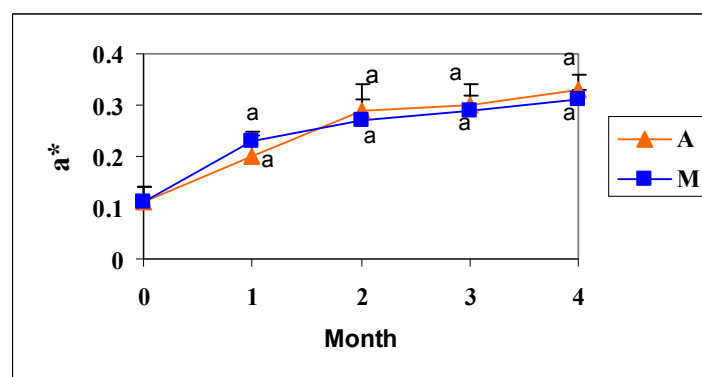


**Figure 6.** Colour ( $a^*$ ) values (average  $\pm$  standard deviation) of dried porridge in two types of packaging (A and M bags) plotted against storage month. Means for each type of packaging for each month with the same letter were not significantly different ( $p > 0.05$ ). ( $\text{T}$  indicates the upper range of the mean plus standard deviation.)

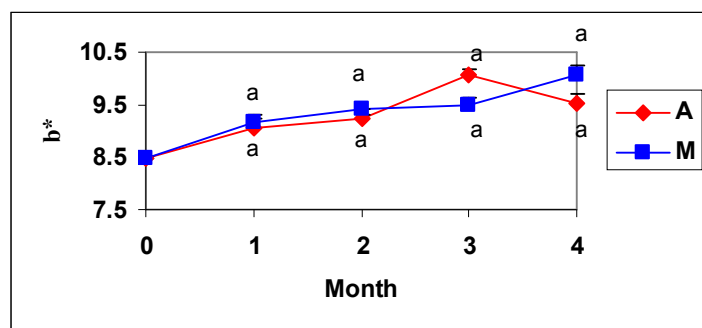


**Figure 7.** Colour ( $b^*$ ) values (average $\pm$ standard deviation) of dried porridge in two types of packaging (A and M bags) plotted against storage month. Means for each type of packaging for each month with the same letter were not significantly different ( $p > 0.05$ ). ( $\text{T}$  indicates the upper range of the mean plus standard deviation.)

Figure 8 shows results of TBA test used for the measurement of fat oxidation [40] in the porridge samples contained in the two types of packaging. Malonaldehyde, an end-product in the autoxidation process, was observed to increase with storage time, with samples in the A-type packages having lower values than those obtained from the M-type packages, although the levels were not significantly different.

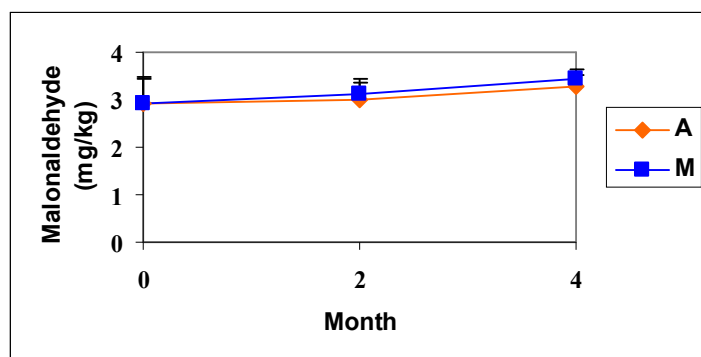


**Figure 8.** Results of TBA test: malonaldehyde (average  $\pm$  standard deviation) in of dried porridge from two types of packaging (A and M bags) plotted against storage month. ( $\text{T}$  indicates the upper range of the mean plus standard deviation.)

Results of the monthly sensory evaluation of the rehydrated porridge from the A- and M-type packagings by the panelists are shown in Figure 9. Most scores were not significantly different except those for colour and flavour, especially for the porridge from M-type packaging at the fourth month of storage, which were less than those from A-type packaging. The porridge from the lower-quality, translucent M-type packaging showed some rancidity. Furthermore, in this month, the overall score for the two packaging types reduced markedly, with scores of only ‘dislike a little’, which suggested that the product could not be kept for more than three months. This is also apparent from the TBA levels (Figure 8) after three months at about 3.3 and 3.1 mg/kg for samples in the M- and A-type packagings respectively. As for the microorganism levels, even though they were still

within the safe ranges in both types of package, there was a clear trend of increasing microbial activity with time (Table 2).

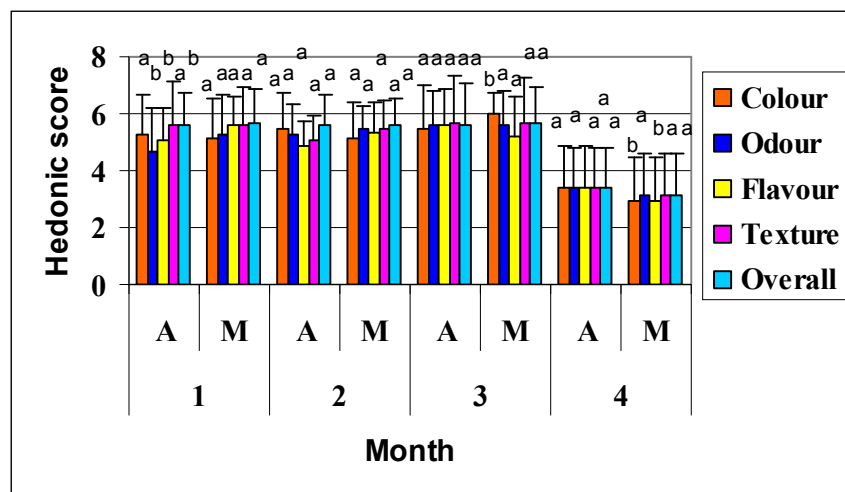


**Figure 9.** Sensory evaluation (average  $\pm$  standard deviation) of the quality of rehydrated porridge from two types of packaging (A and M bags). Means for each type of packaging for each month with the same letters were not significantly different ( $p > 0.05$ ). (T indicates the upper range of the mean plus standard deviation.)

**Table 2.** Microbial sampling of dried porridge samples from the shelf life study

Month	Sample	Microorganism	Result
0	A and M	Total plate count (cfu/g)	$6.7 \times 10^4$
		Yeast and mould (cfu/g)	< 10
		<i>Escherichia coli</i> (MPN/g)	< 3
		<i>Staphylococcus aureus</i> (cfu/g)	< 10
		<i>Clostridium perfringens</i> /0.1 g	Not detected
		<i>Salmonella</i> sp./25 g	Not detected
		<i>Bacillus cereus</i> (cfu/g)	10
	A	Total plate count (cfu/g)	$7.7 \times 10^4$
		Yeast and mould (cfu/g)	< 10
		Total plate count (cfu/g)	$1.0 \times 10^4$
		Yeast (cfu/g)	< 10
		Mould (cfu/g)	20
2	A	Total plate count (cfu/g)	$3.2 \times 10^4$
		Yeast and mould (cfu/g)	< 10
		Total plate count (cfu/g)	$1.8 \times 10^5$
	M	Yeast (cfu/g)	< 10
		Mould (cfu/g)	20

**Table 2.** (Continued)

<b>Month</b>	<b>Sample</b>	<b>Microorganism</b>	<b>Result</b>
3	A	Total plate count (cfu/g)	$1.5 \times 10^5$
		Yeast (cfu/g)	< 10
		Mould (cfu/g)	30
	M	Total plate count (cfu/g)	$5.9 \times 10^4$
		Yeast (cfu/g)	< 10
		Mould (cfu/g)	20
4	A	Total plate count (cfu/g)	$8.1 \times 10^4$
		Yeast (cfu/g)	< 10
		Mould (cfu/g)	20
	M	Total plate count (cfu/g)	$8.4 \times 10^4$
		Yeast (cfu/g)	< 10
		Mould (cfu/g)	40

## CONCLUSIONS

Fortification of rice with ferrous sulphate was found to be optimum at 0.05% of dried brown rice. The dried, seasoned porridge had a high iron content (10.18 mg/50 g) supplied by the ferrous sulphate as well as other high-iron materials (chicken blood, chicken fillet and edible fern), meeting the requirements for a high-iron food product. The shelf life of this product was three months at room temperature in an aluminum foil laminate bag or a metalite bag.

## ACKNOWLEDGEMENT

Financial support for this research from the Kasetsart University Research and Development Institute (KURDI) is acknowledged.

## REFERENCES

1. S. Denic and M. M. Agarwal, "Nutritional iron deficiency: An evolutionary perspective", *Nutr.*, **2007**, 23, 603-614.
2. R. J. Stoltzfus, "Defining iron-deficiency anemia in public health terms: A time for reflection", *J. Nutr.*, **2001**, 131, 565S-567S.
3. UNICEF, "Preventing Iron Deficiency in Women and Children: Technical Consensus on Key Issues", UNICEF/UNU/WHO/MI Technical Workshop, **1998**, New York, USA, pp.29-32.
4. R. Hurrell, T. Bothwell, J. D. Cook, O. Dary, L. Davidsson, S. Fairweather-Tait, L. Hallberg, S. Lynch, J. Rosado, T. Walter and P. Whittaker, "The usefulness of elemental iron for cereal flour fortification: a SUSTAIN Task Force report. Sharing United States Technology to aid in the improvement of nutrition", *Nutr. Rev.*, **2002**, 60, 391-406.

5. R. F. Hurrell, D. E. Furniss, J. Burri, P. Whittaker, S. R. Lynch and J. D. Cook, “Iron fortification of infant cereals: A proposal for the use of ferrous fumarate or ferrous succinate”, *Am. J. Clin. Nutr.*, **1989**, 49, 1274-1282.
6. M. B. Zimmermann, P. Winichagoon, S. Gowachirapant, S. Y. Hess, M. Harrington, V. Chavasit, S. R. Lynch and R. F. Hurrell, “Comparison of the efficacy of wheat-based snacks fortified with ferrous sulphate, electrolytic iron, or hydrogen-reduced elemental iron: Randomized, double-blind, controlled trial in Thai women”, *Am. J. Clin. Nutr.*, **2005**, 82, 1276-1282.
7. D. E. Ballot, A. P. MacPhail, T. H. Bothwell, M. Gillooly and F. G. Mayet, “Fortification of curry powder with NaFe(III)EDTA in an iron-deficient population: Report of a controlled iron-fortification trial”, *Am. J. Clin. Nutr.*, **1989**, 49, 162-169.
8. F. E. Viteri, E. Alvarez, R. Batres, B. Torun, O. Pineda, L. A. Mejía and J. Sylui, “Fortification of sugar with iron sodium ethylenediaminetetraacetate (FeNaEDTA) improves iron status in semirural Guatemalan populations”, *Am. J. Clin. Nutr.*, **1995**, 61, 1153-1163.
9. Working Group on Fortification of Salt with Iron, “Use of common salt fortified with iron in the control and prevention of anemia: A collaborative study”, *Am. J. Clin. Nutr.*, **1982**, 35, 1442-1451.
10. H. Foy, “Fortification of salt with iron”, *Am. J. Clin. Nutr.*, **1976**, 29, 935-936.
11. X. Yang, Y. Tian, J. Huo and J. Piao, “Iron absorption of NaFeEDTA in soy sauce in Chinese female”, Proceedings of Conference on Forging Effective Strategies to Combat Iron Deficiency, **2001**, Atlanta, USA, Abstract M8.
12. P. V. Thuy, J. Berger, L. Davidsson, N. C. Khan, T. T. Nga, N. T. Lam, T. T. Mai, C. Flowers, Y. Nakanishi, J. D. Cook, R. F. Hurrell and H. H. Khoi, “Regular consumption of NaFeEDTA fortified fish sauce improves iron status of anemic Vietnamese women”, Proceedings of Conference on Forging Effective Strategies to Combat Iron Deficiency, **2001**, Atlanta, USA, Abstract M10.
13. Ministry of Public Health, “Announcement No 210”, <http://www.fda.moph.go.th/fda-net/html/product/food/ntfmoph/ntf210.htm>, **2000** (Accessed: May 23, 2010).
14. C. Damrongkiat, “Thai rice research, crisis and opportunity”, <http://www.thairice.org/news/TRFnews/doc/TRresearch1.ppt#366,6>, **2010** (Accessed: May 23, 2010).
15. N. Boontaveeyuwat and D. Keawsiri, “Does brown rice decrease iron availability of rice based meals?”, *J. Nutr. Assoc. Thailand*, **2004**, 39, 10-16.
16. A.-S. Sandberg and U. Svanberg, “Phytate hydrolysis by phytase in cereals; Effects on in vitro estimation of iron availability”, *J. Food Sci.*, **1991**, 56, 1330-1333.
17. P. Wiriyacharee, C. Techapun, S. Pruenglampoo, W. S. Wattanutchariya, S. Jongkaewwattana and R. Techapun, “Increasing nutritive value of parboiled glutinous rice”, *J. Nation. Res. Coun. Thailand (Soc.)*, **2007**, 39, 65-75 (in Thai).
18. R. Theuer, “Effect of iron on the color of barley and other cereal porridges”, *J. Food Sci.*, **2002**, 67, 1208-1211.
19. R. Sunghong, L. Mo-Suwan, V. Chongsuvivatwong and A. F. Geater, “Once weekly is superior to daily iron supplementation on height gain but not on hematological improvement among schoolchildren in Thailand”, *J. Nutr.*, **2002**, 132, 418-422.

20. Bureau of Drug Control, “Ferrous sulphate, nourishing blood tablets”, [http://www2.fda.moph.go.th/drug/zone\\_drug/dru001.asp?title=3&display=a16b1603](http://www2.fda.moph.go.th/drug/zone_drug/dru001.asp?title=3&display=a16b1603) (Accessed: May 23, 2010).
21. D. A. Smith, R. M. Rao, J. A. Liuzzo and E. Champagne, “Chemical treatment and process modification for producing improved quick-cooking rice”, *J. Food Sci.*, **1985**, *50*, 926-931.
22. W. Horwitz (Ed.), “Official Methods of Analysis”, 17<sup>th</sup> Edn., Association of Official Analytical Chemists, Gaithersburg, **2000**.
23. B. G. Tarladgis, B. M. Watts and M. Yonathan, “Distillation method for the determination of malonaldehyde in rancid foods”, *J. Am. Oil Chem. Soc.*, **1960**, *37*, 44-48.
24. L. Maturin and J. T. Peeler, “Bacteriological analytical manual: Aerobic plate count”, <http://www.fda.gov/Food/ScienceResearch/LaboratoryMethods/BacteriologicalAnalyticalManualBAM/ucm063346.htm>, **2001** (Accessed: June 20, 2010).
25. V. Tournas, M. E. Stack, P. B. Mislicvec, H. A. Koch and R. Bandler, “Bacteriological analytical manual: Yeasts, molds and mycotoxins”, <http://www.fda.gov/Food/ScienceResearch/LaboratoryMethods/BacteriologicalAnalyticalManualBAM/ucm071435.htm>, **2001**, (Accessed: June 20, 2010).
26. P. Feng, S. D. Weagant and M. A. Grant, “Bacteriological analytical manual: Enumeration of *Escherichia coli* and the coliform bacteria”, <http://www.fda.gov/Food/ScienceResearch/LaboratoryMethods/BacteriologicalAnalyticalManualBAM/ucm064948.htm>, **2002** (Accessed: June 20, 2010).
27. R. W. Bennett and G. A. Lancette, “Bacteriological analytical manual: *Staphylococcus aureus*”, <http://www.fda.gov/Food/ScienceResearch/LaboratoryMethods/BacteriologicalAnalyticalManualBAM/ucm071429.htm>, **2001** (Accessed: June 20, 2010).
28. E. J. Rhodehamel and S. M. Harmon, “Bacteriological analytical manual: *Clostridium perfringens*”, <http://www.fda.gov/Food/ScienceResearch/LaboratoryMethods/BacteriologicalAnalyticalManualBAM/ucm070878.htm>, **2001** (Accessed: June 20, 2010).
29. E. J. Rhodehamel and S. M. Harmon, “Bacteriological analytical manual: *Bacillus cereus*”, <http://www.fda.gov/Food/ScienceResearch/LaboratoryMethods/BacteriologicalAnalyticalManualBAM/ucm070875.htm>, **2001** (Accessed: June 20, 2010).
30. “ISO 6579:2002 - Microbiology of food and animal feeding stuffs: Horizontal method for the detection of *Salmonella spp.*”, 4<sup>th</sup> Edn., International Organization for Standardization, Switzerland, **2002**.
31. L. R. Beuchat, “Microbial stability as affected by water activity”, *Cereal Foods World.*, **1981**, *26*, 345-349.
32. Department of Health, “Nutritive Values of Thai Foods”, Nutrition Division, Ministry of Public Health, Bangkok, **2001** (in Thai).
33. L. Hallberg and L. Hulthen, “Prediction of dietary iron absorption: An algorithm for calculating absorption and bioavailability of dietary iron”, *Am. J. Clin. Nutr.*, **2000**, *71*, 1147-1160.
34. The Committee on Recommended Daily Dietary Allowances, “Dietary Reference Intake for Thais 2003”, Ministry of Public Health, Bangkok, **2003**, p.345.

35. D. J. Fleming, K. L. Tucker, P. F. Jacques, G. E. Dallal, P. W. Wilson and R. J. Wood, "Dietary factors associated with the risk of high iron stores in the elderly Framingham Heart Study cohort", *Am. J. Clin. Nutr.*, **2002**, 76, 1375-1384.
36. J. T. Salonen, K. Nyssonen, H. Korpela, J. Tuomilehto, R. Seppanen and R. Salonen, "High stored iron levels are associated with excess risk of myocardial infarction in eastern Finnish men", *Circulation*, **1992**, 86, 803-811.
37. T. Tuomainen, K. Punnonen, K. Nyssonen and J. T. Salonen, "Association between body iron stores and the risk of acute myocardial infarction in men", *Circulation*, **1998**, 97, 1461-1466.
38. R. G. Stevens, D. Y. Jones, M. S. Micozzi and P. R. Taylor, "Body iron stores and the risk of cancer", *N. Engl. J. Med.*, **1988**, 319, 1047-1052.
39. M. B. Reddy, R. F. Hurrell, M. A. Juillerat and J. D. Cook, "The influence of different protein sources on phytate inhibition of nonheme-iron absorption in humans", *Am. J. Clin. Nutr.*, **1996**, 63, 203-207.
40. C. G. Sidwell, H. Salwin, M. Benca and J. H. Mitchell Jr., "The use of thiobarbituric acid as a measure of fat oxidation", *J. Am. Oil Chem. Soc.*, **1954**, 31, 603-606.